Increasing distributed generation penetration when limited by voltage regulation

by
Jonathan Mark Nye

Thesis presented in fulfilment of the requirements for the degree of Master of Engineering (Research) in the Faculty of Engineering at Stellenbosch University

Supervisor: Dr Hendrik Johannes Beukes
Co-supervisor: Mobolaji Bello

April 2014

Declaration

By submitting this thesis electronically, I declare that the entirety of the work contained therein is my own, original work, that I am the sole author thereof (save to the extent explicitly otherwise stated), that reproduction and publication thereof by Stellenbosch University will not infringe any third party rights and that I have not previously in its entirety or in part submitted it for obtaining any qualification.

April 2014

Abstract

This work investigated the influence of photo-voltaic generators on the voltage control of distribution feeders and the methods that can be used to increase the maximum penetration levels of these feeders. Initially, a brief overview of the reasons why it is necessary to increase the generation penetration levels on distribution feeders was provided. A review of various issues associated with connecting generation to the distribution network; methods and technologies that can be used to increase penetration levels; and ways to improve voltage regulation on MV feeders was given. The grid code for renewable power plants and the voltage apportionment standard were reviewed to determine what limits penetration levels and what can be done to increase them.

The operation and control of a typical distribution network, without any connected generation, was initially investigated. A control strategy was implemented that provided suitable voltage regulation on the feeder during both high and low load. The influence of connecting generation to this typical distribution network, without making any modifications to the control of the feeder, was investigated. Base penetration levels, for various generation connection cases, were found. It was shown that the penetration is limited by the rapid voltage change or voltage rise. The base penetration levels were compared to the optimal amount of generation that provides the lowest losses. It was shown that the penetration needs to be increased by between 100% and 200% for the feeder's losses to be minimised. Voltage regulator and capacitor control was influenced by the generation and they could not function as expected. It was shown that flicker will not be an issue, even with penetration limits well above the current allowable limits.

Various methods that can be used to increase the amount of generation that is connected to the typical network were investigated. On-load tap changer setpoint reduction, reactive power control and electronic voltage regulators are some of the methods or technologies that can be used to increase penetration levels. It was shown that each of the technologies can assist, depending on the circumstance, in increasing penetration. The individual modifications can increase penetration up to 100% at the cost of increased tap changes and in some cases losses. Two proposed control strategies were assessed, that combine the investigated technologies. The results showed that it is possible to increase penetration levels by 50-80%, while improving power quality and reducing losses when compared to the base generation connection case.

Opsomming

Hierdie werk ondersoek die invloed van die foto- voltaïes kragopwekkers op die spanning beheer van die verspreiding voerder asook die metodes wat gebruik kan word om die maksimum penetrasie vlakke van hierdie voerders te verhoog. Aanvanklik is 'n kort oorsig van die redes waarom dit nodig is om die opwekking penetrasie vlakke op die verspreiding voerders, te verhoog voorsien . Eerstens word 'n hersiening van verskeie kwessies wat verband hou met die koppeling van generasie na die verspreidingsnetwerk gegee. Tweedens word metodes en tegnologie wat gebruik kan word om penetrasie te verhoog gegee en laastens word maniere om spanning regulasie op medium spanning voerders te verbeter, gegee. Die rooster kode "grid code => probeer liewer netwerk regulasies" vir hernubare krag aanlegte en die spanning toedeling standaard is hersien om te bepaal wat beperk die penetrasie vlakke en wat gedoen kan word om dit te verhoog.

Die werking en beheer van 'n tipiese verspreiding netwerk, sonder enige verbonde generasie, is aanvanklik ondersoek. 'n Beheer-strategie is toe geïmplementeer wat geskikte spanning regulasie op die voerder tydens beide hoë en lae belasting verskaf. Die invloed van die koppeling van opwekking tot hierdie tipiese verspreiding netwerk, sonder om enige veranderinge aan die beheer van die voerder, is ondersoek. Basis penetrasie vlakke, vir verskeie generasie verband gevalle, is gevind. Daar is bewys dat die penetrasie word beperk deur die vinnige spanning verandering of spanning styging. Die basis penetrasie vlakke word vergelyking met die optimale aantal generasie wat die laagste verliese bied. Daar is bewys dat die penetrasie moet met tussen 100% en 200% verhoog word sodat die voerder se verliese beperk kan word. Die spanning reguleerder en kapasitor beheer is beïnvloed deur die opwekking en hulle kon nie reageer soos verwag nie. Daar is getoon dat flikker nie 'n probleem sal wees nie; selfs al is die penetrasie vlakke ver bo die huidige toelaatbare grense.

Verskillende metodes wat gebruik kan word om die aantal generasie wat gekoppel is aan die tipiese netwerk te verhoog is ondersoek. Aan-las tap wisselaar vermindering, reaktiewe krag beheer en elektroniese spanning reguleerders is 'n paar van die tegnieke wat gebruik kan word om penetrasie te verhoog. Daar is bewys dat elkeen van die tegnologieë kan help, afhangende van die omstandighede, vir toenemende penetrasie. Die individuele veranderinge kan penetrasie verhoog tot 100% by die koste van 'n verhoogde tap veranderinge en in sommige gevalle verliese. Twee voorgestelde beheer strategieë is beoordeel, wat die ondersoek tegnologie kombineer. Die resultate het getoon dat dit moontlik is om penetrasie te verhoog met 50% tot 80%, terwyl die verbetering van gehalte en die vermindering van krag verliese in vergelyking met die basis generasie verband hou.

Acknowledgements

I would like to thank the following:

My supervisor Dr Johan Beukes, for his excellent guidance and support during my research. Without his knowledge and experience I would not have been able to focus my distractions and complete the tasks at hand. The discussions about mountain biking also contributed to my enjoyment of the project.

Eskom and the EPPEI program, for funding my studies and giving me the opportunity to study full time, while still receiving my salary. I hope many more people can benefit from the EPPEI program in the future.

My industrial mentor Mobolaji Bello, for the advice and knowledge of renewable power plant grid integration.

My friends for their encouragement and distraction that made the period more enjoyable.

My parents Pierre and Michele for their love, support and guidance. They opened the doors, to the opportunities, that allowed me to reach where I am today.

Table of Contents

List of Figures

List of Tables

Abbreviations

AAAC	–	All aluminium alloy conductor
AC	–	Alternating current
ACSR	–	Aluminium conductor steel reinforced
APC	–	Active power curtailment
CEVR	–	Continuously regulating electronic voltage regulator
CPF	–	Constant power factor
CT	–	Current transformer
DC	–	Direct current
DEVR	–	Discrete electronic voltage regulator
DG	–	Distributed generation/generator
EPRI	–	Electric power research institute
EVR	–	Electronic voltage regulator
GMR	–	Geometric mean radius
HV	–	High voltage
LB	–	Lower bound
LDC	–	Line drop compensator
LV	–	Low Voltage
MV	–	Medium voltage
OLTC	–	On load tap changer
POC	–	Point of connection
PV	–	Photo-voltaic
RPC	–	Reactive power control
RPP	–	Renewable power plant
RVC	–	Rapid voltage change
SO	–	System operator
STATCOM	–	Static synchronous compensator
SVC	–	Static VAR compensator
TZ	–	Tap zone
UB	–	Upper bound
VR	–	Voltage regulator
VT	–	Voltage transformer

Variables

α	–	Vertical angle
a	–	Per unit change in voltage per tap
A	–	Area
β	–	Horizontal angle
Δt	–	Change in time
ΔV	–	Change in voltage
DT	–	Tap changes by a device
E	–	Energy
f	–	Frequency
G	–	Irradiance
I	–	Current
J	–	Objective function
k	–	Bus number
K	–	Gain
λ	–	Distance from substation (between 0 and 1)
L	–	Inductance
LF	–	Load factor
m	–	Droop coefficient
n	–	Number of parallel feeders or number of busses
N	–	Number of simulations/Number of plants/Turns ratio
pf	–	Power factor
P	–	Power or flicker level
PL	–	Penetration level
ϕ	–	Power factor angle
Q	–	Reactive power
R	–	Resistance
S	–	Apparent power
td	–	Time delay
T	–	Temperature
TAP	–	Tap position
TT	–	Total tap changes
V	–	Voltage
X	–	Reactance
Z	–	Impedance

1. Introduction

1.1 Background

The introduction of distributed generation (DG) from renewable resources onto an electricity grid can have profound impact on its reliability, power quality and operation [1]. In South Africa, most of the DG will be connected to the medium voltage (MV) distribution network at voltage levels of 11 kV, 22 kV and 33 kV. Large plants will be connected to the high voltage (HV) network at 66 kV to 400 kV. The DG penetration levels are limited due to the long, weak MV distribution networks that service most of the areas that renewable power plants (RPPs) can be installed [2]. Currently there have not been many studies on the impact of connecting DG to the South African network, mainly due to the limited installed capacity. Recently there has been a major drive to encourage individual power producers to build RPPs and feed power into the national grid. By 2030 South Africa aims to add an additional 20 GW of renewable energy to the national grid [3]. 8.4 GW of this renewable generation will consist of photo-voltaic (PV) plants. PV generation will be the focus of this work and forms one of the potential energy sources for DG. Any new large scale developments (>1 MW) will either be connected directly to the sub-transmission system, via a dedicated feeder or via an existing feeder close to the MV substation [2].

The electricity grid has been designed to operate from the top down, with generation typically being connected to a meshed transmission network as shown in Figure 1.1. Distribution substations connect radially to the network and power flows in a single direction [4].

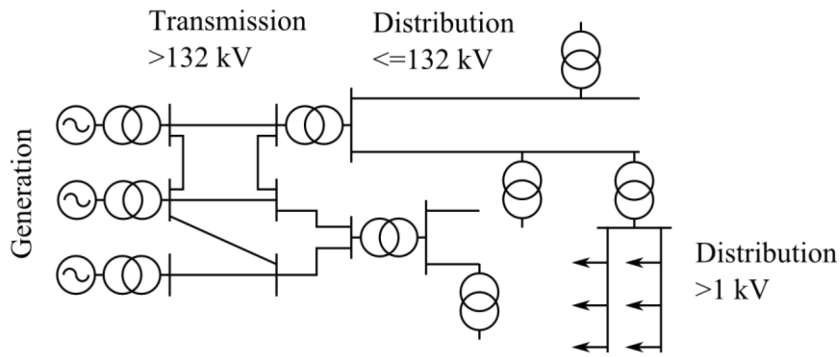

Figure 1.1: Conventional power system overview

The introduction of DG onto the network will alter the network topology by connecting generators to the HV and MV distribution networks as shown in Figure 1.2. The addition of DG onto a feeder causes a change in power flow on the network and the distribution system will no longer have unidirectional power flow [5], [6]. Small DGs such as rooftop PV systems will be connected to low voltage (LV) networks. DG with power greater than about 20 MW will be connected to the 66/132 kV network and DG greater than 100 MW will be connected to the transmission system at 132-400 kV.

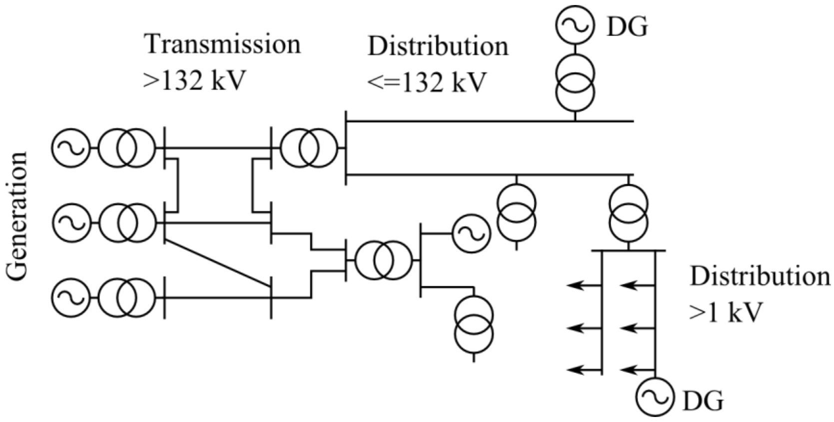

Figure 1.2: Future power system overview

Over the next few years most of the potential DG sites, with a strong connection to the grid, will have been used. Most of the open land and renewable resources lie where no existing infrastructure exists [7]. In many cases DG will have to be connected to weak feeders far away from substations and load centres. It becomes economically infeasible if long dedicated power lines need to be built to access these resources.

Currently distribution systems are passively controlled, designed for one way power flow and control problems are solved during the network planning stage using simple load flow tools. Many of the issues associated with the connection of DG will only be apparent if more complex planning methods are used [8]. To connect the amount of DG to the South African network, as stipulated by the integrated resource plan of 2010, there are many technical challenges that must be overcome [3]. Some of the technical problems of connecting DG to a distribution feeder are [5], [9]:

- Power quality: Voltage regulation, harmonic distortion, rapid voltage changes, flicker and voltage unbalance
- Protection: Relay co-ordination, anti-islanding, relay blinding, DG protection from fault currents
- Stability: Transient stability, long term dynamic stability and voltage collapse

Currently it is undetermined how much generation can be connected to various parts of the Eskom MV network. There are basic guidelines to determine if detailed studies need to be performed. From the above list, there are four main criteria that need to be investigated when assessing the integration of a new RPP [10]:

1. Voltage regulation or voltage rise
2. Rapid voltage changes
3. Thermal limits
4. Protection limits

These criteria ensure that voltages and currents will never exceed the defined limits during worst case loading scenarios. Protection issues are more of a concern when integrating synchronous and induction generators into the distribution network. Fault current from generation, with power electronic converters, is limited to about double the rated power of the inverter. They do not cause as many problems with protection coordination as synchronous generators [6], [11]. In [11] it was found that with inverter based DG, voltage regulation problems and RVC are substantially more limiting to DG penetration levels than protection co-ordination issues. The protection must function as expected with and without the DG's contribution to the fault current. Some of the protection modifications that might need to be performed include:

- Modifying the time current setting
- Adding directional overcurrent relay
- Reconfiguring autoreclosers with an increased time delay before reclosing
- Installing additional circuit breakers along the feeder
- Differential protection

Current penetration guidelines have been specified based upon European standards. The suitability of these guidelines needs to be investigated for their use on the Eskom network. Network planners ensure that any future load growth can be accommodated with very little change to the network. The amount of DG, connected at a point, is often limited by the maximum generation, minimum load scenario. During these worst case scenarios, the voltage rise must be kept within a suitable level. The voltage rise, caused by a DG, is dependent on the amount of power that the DG generates and the short circuit power level at the point of connection (POC) [8]. Presently, the utility will have very little control of the DG plants and considers the generation as negative load [5].

DG, from renewable resources, has a relatively predictable average daily generation profile, but large changes in power output can occur over a short period of time. For example, the power output of a PV plant varies throughout the day. It increases from zero to a peak at around midday and then reduces to zero in the evening. On a partly cloudy day, the clouds will cause changes in output power each time they pass over the panels. The effect of clouds can have a large impact on voltage levels due to the rapid power swings that can be experienced [12]. The rapid voltage swings are caused by the high resistance and low reactance of distribution lines. Therefore, the active power generated has a large influence on the voltage. Repetitive large rapid power swings are undesirable, because they can be noticed as flicker and impact customer equipment [13].

The Electric Power Research Institute (EPRI) [10] found that steady state voltage limits provide a much greater installation capacity than can realistically be integrated without causing power quality concerns. The power quality issues that they expect includes flicker and is one of the more severe power quality problems. Therefore, they concluded that the change in voltage that is caused by DG is more of a concern. The limitation to the change in voltage, caused by the connection or disconnection of DG, needs to be determined. The values specified by different organisations vary substantially. The EPRI planning guideline [10], specifies a 1% voltage change limit for renewable generation and a 5% voltage change limit for fixed generation. Rapid voltage change limits are defined in the grid code and NRS48-2-2008 [14]. The NRS specifies a maximum rapid voltage change of 10% on MV and 15% on LV, while the grid code [15] specifies a 3% limit for switching events of DG plants.

On feeders that have a large amount of connected generation, the voltage can be supported along the length of the feeder, depending on where the generators are placed. If there is a sudden disconnection of the generation, there will be a voltage drop that causes an increase in current. The voltage drop and increased current could cause an under-voltage condition along the feeder [8]. The under-voltage condition can cause damage to customer equipment and cause motor contactors to release that will have to be manually closed.

A distribution feeder's voltage is regulated using the on load tap changer (OLTC) at the transformer and voltage regulators (VRs) down the line [16]. In certain cases shunt capacitor banks are used to 'boost' the voltage and reduce reactive power flow [17]. These devices are configured to regulate the local voltage or make use of line drop compensators (LDCs) to regulate the voltage at a remote point. These devices are typically slow to respond and are well suited to the passive nature of a standard distribution line with slowly changing loads [18]. In [19], [20] an overview of the voltage control strategies for a MV network that has DG was provided. The documents highlight methods that can be used to ensure voltages remain within the limits set by the network operator. In the case of a radial distribution feeder, bidirectional power flow can cause over voltages, because the control philosophy assumes that the power is flowing in a single direction [19]. VR control can be affected if not configured correctly and might not operate as intended.

There are various methods proposed in the literature, on how to regulate the voltage of the MV network when distributed generation has been installed. DG can be connected passively or actively to the distribution network. A passively connected generator aims to maximise the supply of active power. It relies on the distribution equipment to ensure that the voltage and current remains within the system specifications. Actively controlled generation can play a role in voltage and frequency control and could increase DG penetration and grid stability. Many sources [9], [20]–[24] recommend the transformation of the distribution system from a passive network to an actively controlled, intelligent network. To create an actively controlled network, it is necessary to install new control and plant equipment. Many countries do not allow active voltage control by DG to prevent the risk of islanding; however unintentional islanding can be prevented by keeping the voltage control sufficiently slow [25].

1.2 Objectives

There is a lot of uncertainty about the influence of distributed generation on the South African network voltage. This work aims to address some of the issues including:

1. Assess the impact of PV distributed generation on MV distribution feeders voltage and voltage control devices
2. Determine the maximum renewable power generation penetration levels on distribution feeders, using voltage rise and rapid voltage change limitations, without modifying network voltage control or operation
3. Investigate various methods that can be used to increase penetration levels
4. Provide solutions to combine the various voltage control techniques to increase penetration levels

further, without negatively impacting power quality

5. Provide guidelines and tools for network planners to assess the impact of DG on the network voltage

1.3 Structure

The document is broken down into various sections, each considering a specific aspect of the problem. A breakdown of the structure is provided below:

Chapter 1 provides an introduction to the work. It gives an overview of DG integration and the issues that can be encountered on the network.

Chapter 2 covers the various standards and design philosophies that are relevant for DG connection to the network. The grid code for renewable power plants is assessed and the minimum requirements for the different categories of generation are given. The concept of network classes and tap zones is covered and the maximum voltage rise limitation of the network with DG is presented.

Chapter 3 covers the theory of the network equipment typically used on distribution networks to control the voltage. A test network that can be used for simulations, to assess different control scenarios, is developed. The operation of the test network is covered and a method to control the voltage of the network is developed by following the Eskom guidelines for equipment placement and control.

Chapter 4 introduces DG to the test network. The base penetration limits are determined, providing there are no control modifications to the existing network equipment and the DG is controlled to operate at unity power factor. Various connection cases are tested and it is shown what limits the penetration level for each case. An analysis shows how the DG penetration is limited by different factors, such as the rapid voltage change or voltage rise. The influence of PV plant size and geographical dispersion, on the expected maximum power changes for a period of time, is investigated. It is shown that multiple smaller plants have reduced power changes, when compared to a single larger plant of the same size. The DG penetration level that provides the minimum amount of losses on the network is determined. The base penetration level is shown, in most connection cases, to be lower than the penetration level that causes minimum losses. Flicker caused by PV plants is investigated and the worst case scenario, that would cause the most flicker, is initially assessed by turning the PV plant on and off repetitively. It is shown that the continuous tripping of a plant will exceed the recommended flicker levels. It is unlikely that the PV plant will operate in such a manner, so more realistic worse case scenarios were investigated. The investigation shows that it is unlikely that PV will cause flicker except at penetration levels greater than three times the currently allowed maximum levels.

Chapter 5 investigates the various technologies that can be used to increase the DG penetration level. An analysis of each technology is provided and a comparison is made to the base penetration level defined in *Chapter 4*. The technologies are independently assessed, to show how each technology influences the maximum penetration level. The technologies that are assessed include: modification of OLTC and VR setpoint voltages; various reactive power control strategies; and changing the voltage regulators to electronic voltage regulators. It is shown that penetration levels can be increased substantially by implementing a single technology to increase penetration levels; however a combined strategy provides even greater increases. Two combined control strategies were shown to increase penetration levels up to 80%, while reducing voltage variations on the test network.

Chapter 6 provides the conclusions and recommendations that are made for the work in this document.

2 Standards and design philosophies

2.1 Assessment of the grid code for renewable energy power plants in South Africa

The South African renewable grid code [15] has been developed to provide the minimum technical requirements, for renewable energy power producers, to connect generation to the Transmission System (TS) or Distribution System (DS). This set of minimum technical requirements must be met by the renewable energy power plants (RPPs) so that they can be connected to the grid. Some of the requirements will be used only once an agreement has been made between the RPPs and the system operator (SO). Renewable energy power generation is the focus of this work, so the grid code requirements for various RPPs will be discussed in this section. The RPP grid code is investigated to determine the operating conditions that the RPPs must be able to operate in and which of the technical requirements can be used to increase the penetration levels. Some of the concepts covered will be discussed in more detail in later sections. This section only aims to provide an overview of certain technology requirements by the grid code.

The RPPs are classified into three categories; Category A, B and C, with category A being sub divided into a further three categories; A1, A2 and A3. Category A includes any RPP connected to the LV network up to 1 MVA; category B includes any RPP connected to the MV network up to 20 MVA; and category C includes any RPP connected to the MV/HV network greater than 20 MVA. The regulations require that the RPPs meet the requirements at their POC. The categories are defined by the rated active power at the POC. Table 2.1 shows the requirements for grid connection and as can be seen they become stricter for each subsequent category.

Table 2.1: Grid code requirements for each category [15]

Category	**A1**	**A2**	**A3**	**B**	**C**
Power output [kVA]	0-13.8	13.8-100	100-1000	>1000-20000	>20000
Voltage Level	LV	LV	LV	MV	MV/HV
Operating frequency	49 - 51Hz				
Operating voltage range	-15 to +10%			±10%	
Operating power range	20-100%				
Low voltage ride through	60% for 0.15 s			0% for 0.15 s	
High voltage ride through	N/A			120% for 2s	
Power factor operating range (leading and lagging)	0.95			0.975	0.95

The operating requirements, for the different categories of DG, are covered in the grid code for normal operating conditions and disturbances. These requirements include: voltage ride through, reactive power support, frequency operating ranges and frequency control. These requirements are illustrated by figures to show the operating ranges and limits graphically.

Figure 2.1 and Figure 2.2 show a range of frequencies that the RPPs must be able to operate in and the length of time required to remain connected at the specific frequencies. If the RPPs are disconnected due to a frequency disturbance, category A units can reconnect after 60 s and category B/C can reconnect after 3 s; once the frequency has returned within the range of 49 and 50.2 Hz. Both of these figures illustrate that the RPPs are relatively immune to minor frequency disturbances. The ride through prevents sudden disconnection of a large amount of generation when the system is already under strain [11].

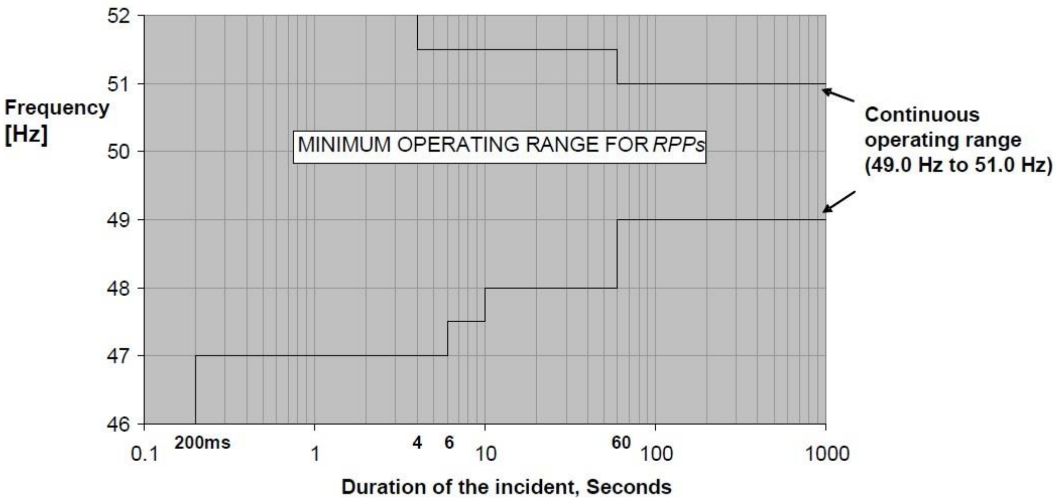

Figure 2.1: Frequency operating range during a disturbance [15]

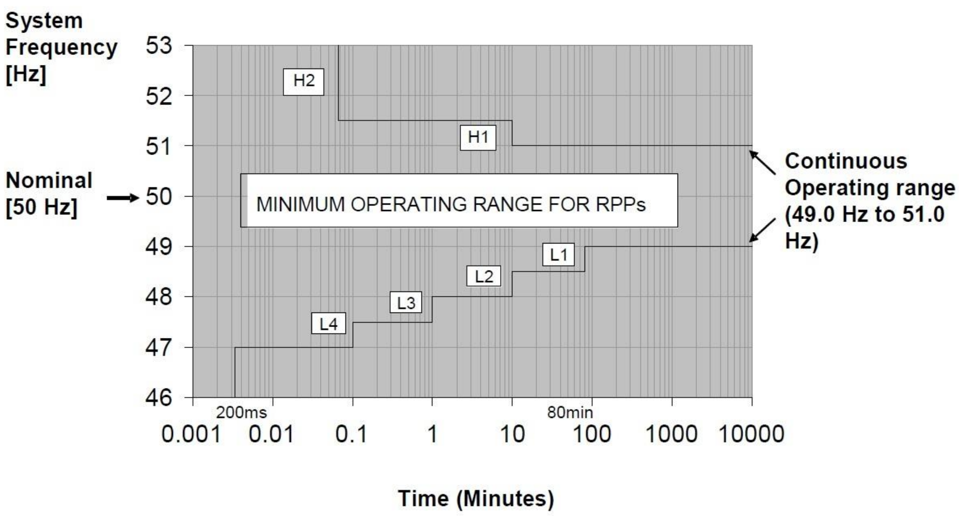

Figure 2.2: Frequency operating range over the lifetime of the plant [15]

The system operator can request that the RPP helps to support the frequency of the system during disturbances or periods of low and high demand. The operating requirements for frequency support are shown in Figure 2.3.

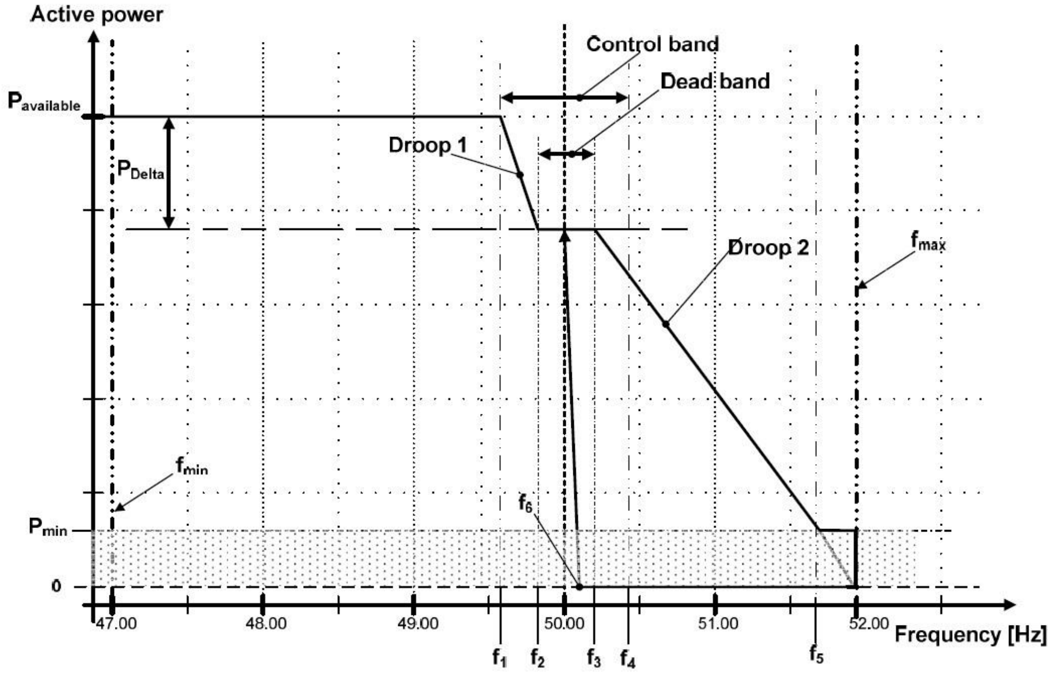

Figure 2.3: Frequency control requirements for category B and C [15]

Category A RPPs must be able to reduce their active power along a linear line from 100% at 50.5 Hz to 20% at 52 Hz. If the frequency has been above 52 Hz for 4 s then the RPP must disconnect. Category B and C RPPs must be able to follow a curve as shown in Figure 2.3. The frequency points f_1 to f_4 can be specified by the network operator. Their purpose is to form a dead band and control band for primary frequency response control. The RPPs can switch off individual units to meet the reduced power command required by the frequency control. It should be noted that it is only compulsory for an RPP to respond to the high frequency part of the curve, as P_{Delta} will be set to zero unless there is an agreement between Eskom and the RPP. While this is not compulsory, any RPPs except for PV, should be capable of operating with a P_{Delta} of 3%.

The voltage ride though requirements of a RPP depends on its category. Figure 2.4 and Figure 2.5 define various regions that the RPP must be able to operate in. Category A1 and A2 have to only ride through minor grid disturbances, because their effect on voltage support and grid stability are small. Categories A3, B and C have considerably stricter requirements and must be able to operate for the specified amount of time in each of the regions.

Each area in Figure 2.5 is defined in [15] as:

- Area A: The RPP must remain connected to the grid and uphold normal production
- Area B: The RPP must remain connected to the grid and provide voltage support by supplying a controlled amount of reactive power. The supply of reactive power is first priority but active power production should be maintained if possible.
- Area C: Disconnecting the RPP is allowed
- Area D: The RPP must remain connected to the grid and provide voltage support by absorbing a controlled amount of reactive power

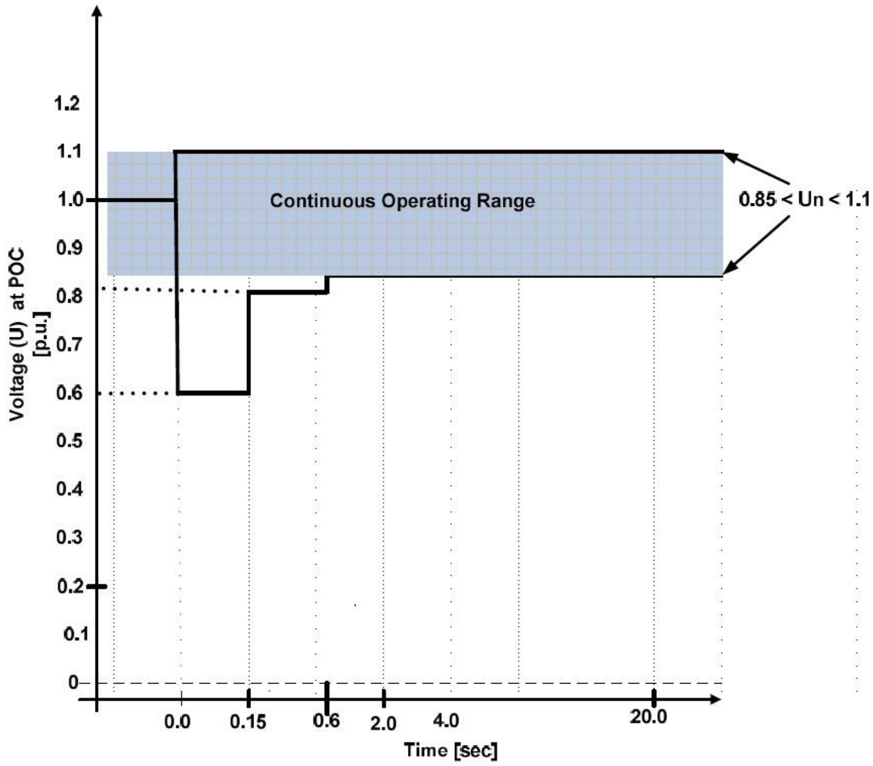

Figure 2.4: Voltage ride through for category A1 and A2 [15]

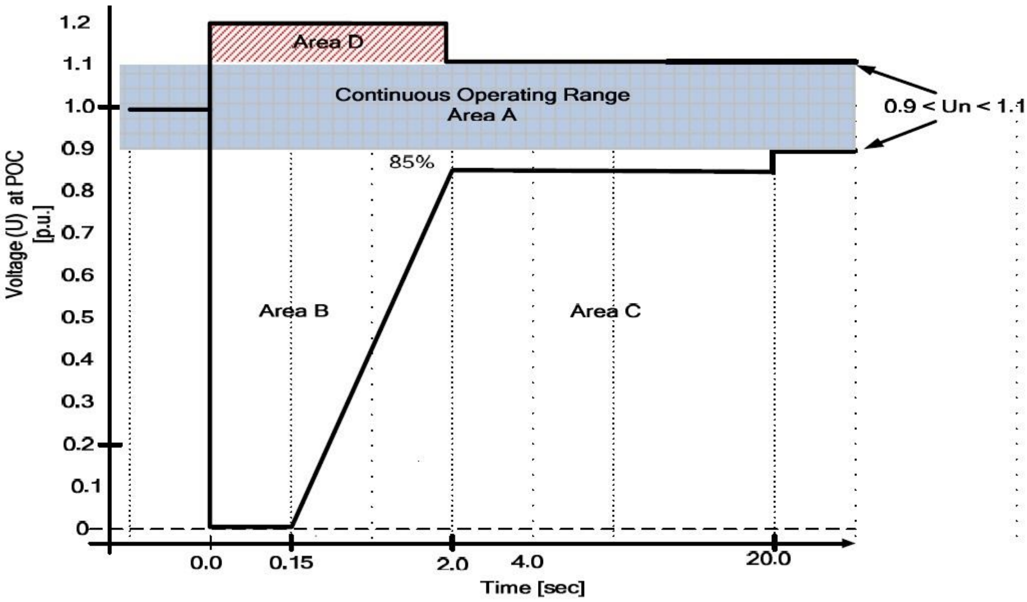

Figure 2.5: Voltage ride through for category A3, B and C [15]

The RPPs must be able to operate beyond the range of normal network operating conditions. There is however the possibility of them disconnecting due to a remote fault that will cause a decrease in local network voltage. This is undesirable as short term under voltages are considerably less dangerous to network equipment than short term over voltage [11].

Figure 2.6 show the reactive power support requirements during fault or abnormal operating conditions. If the RPPs are disconnected due to a voltage disturbance, they can reconnect after 60 s for category A and 3 s for category B & C, after the voltage has returned to be within the required limits. The limits are -15 to +10% for category A and +-10% for Category B & C on the DS and +-5% on the TS. If the voltage returns to Area A after a fault, then each subsequent drop is regarded as a new fault situation. Figure 2.6 shows what reactive power support must be provided by the RPP during voltage dips and overvoltage. In area B the supply of reactive power takes preference over active power.

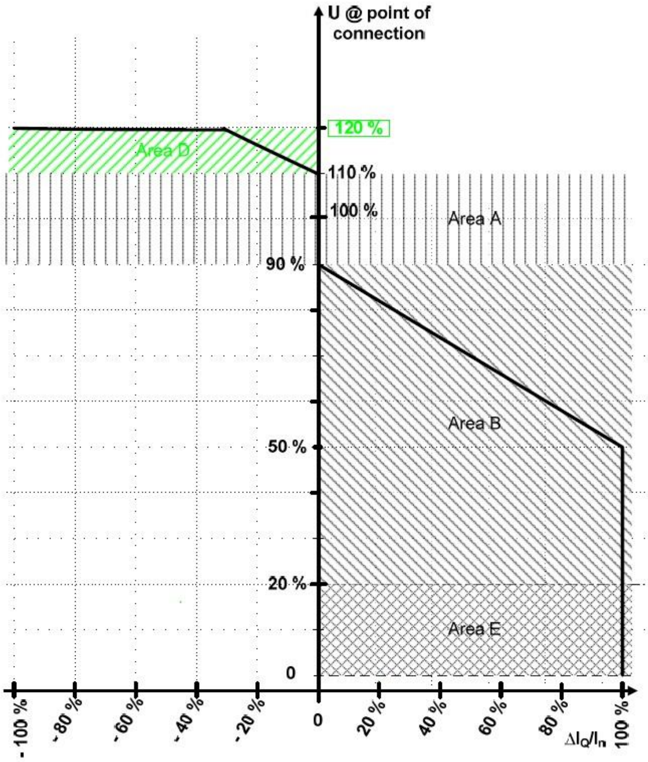

Figure 2.6: Reactive power support requirements [15]

RPPs are required to supply or absorb reactive power during normal operating conditions depending on the type of control used and reactive power agreement with the system operator. They must be able to supply reactive power according to Figure 2.7. All RPPs must be able to operate at rated reactive power from 20% of rated power. RPPs with power electronic interfaces would be able to supply reactive power equivalent to the rating of the converter from 0% of rated power, but this is not a requirement in the grid code. RPPs will by default be operated at unity power factor, unless specified by the system operator. The sign convention of loads, leading and lagging power factor and generation are discussed in Appendix 0.

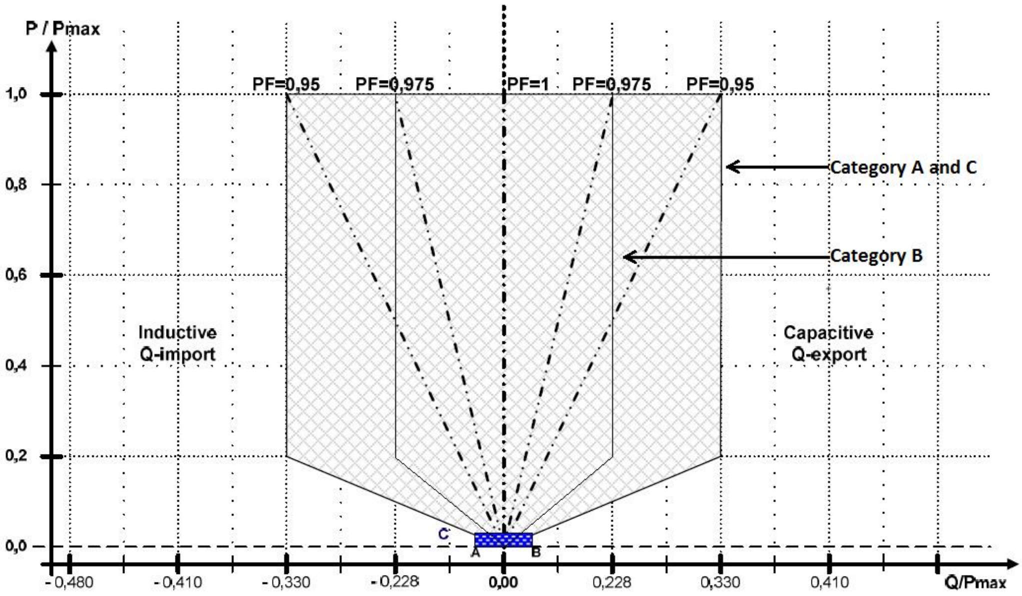

Figure 2.7 Reactive power requirements for categories A and C (power factor=0.95) and category B (power factor=0.975) [15]

Category A3, B and C RPPs must be able to operate in power factor control mode as shown in Figure 2.8. Category B and C must also be able to operate in constant reactive power mode as shown in Figure 2.8 and voltage control mode as shown in Figure 2.9.

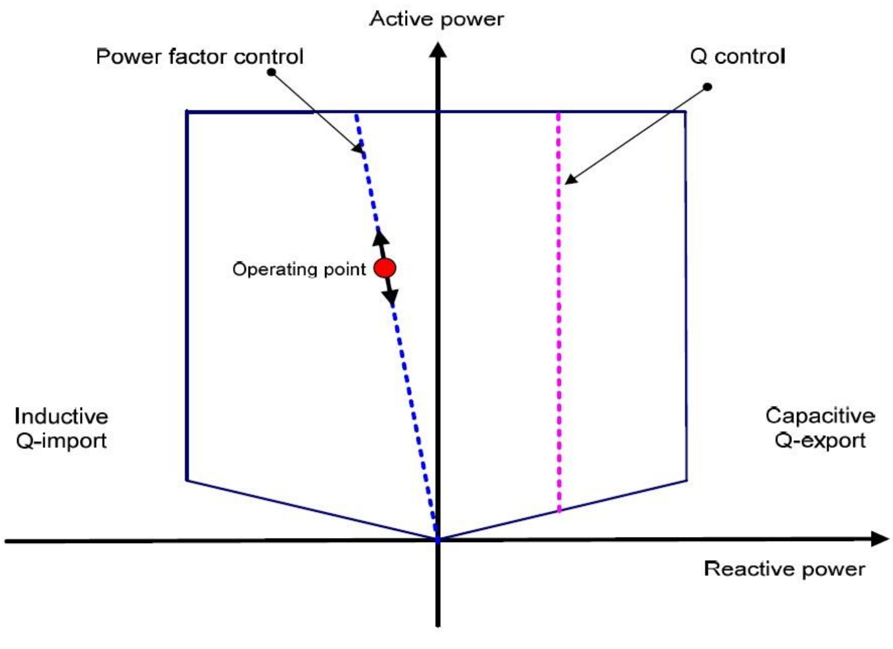

Figure 2.8: Power factor and constant reactive power control [15]

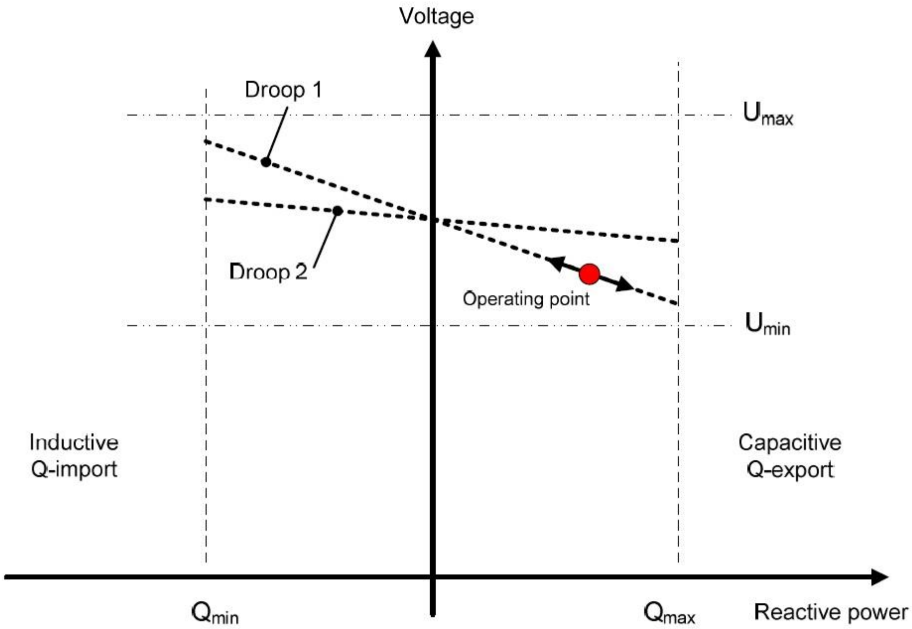

Figure 2.9: Droop voltage control [15]

If the operator requests voltage control, the RPP must be able to either absorb or supply reactive power depending on whether it must lower or raise the voltage. It is necessary for the RPP to be able to operate at maximum active power while still being able to operate at its rated power factor. The voltage control will be regulated by a droop function that will be determined by the utility. Once the RPP has reached its design limit for voltage control, it will wait for further control action by the tap changer or other methods of voltage control on the network. Droop voltage control is used to share the reactive power burden among multiple generators and has the potential to reduce voltage variations if properly configured [26].

The power quality of the RPP will meet the requirements set out by the NRS 048-2 or relevant parts of the IEC 61000. Eskom will ensure that the RPP does not cause excessive voltage fluctuations, flicker, harmonics and voltage unbalance. This is partly achieved by limiting the RVC caused by a switching event of a non-synchronous RPP to below 3% and a synchronous RPP to below 5%.

The RPPs of categories A3, B and C must have various active power constraint functions if an active power limit is set by the system operator. The constraint functions are an absolute production constraint, a delta production constraint and a power gradient constraint. These constraint functions aim to prevent the system from overloading, enable a control reserve for frequency control and to improve the system stability by preventing rapid power changes. Table 2.2 provides an overview of the various control functions each category RPP is required to support. Category A1 and A2 are not required to have their control settings changed remotely.

Table 2.2: Control functions required for RPPs [15]

Control function	**Category A3**	**Category B**	**Category C**
Freqency control	X	X	X
Absolute production constraint	X	X	X
Delta production constraint	-	X	X
Power gradient constraint	-	X	X
Q control	-	X	X
Power factor control	X	X	X
Voltage control	-	X	X

This section has covered the various rules, regulations, constraints and other factors associated with a RPP's connection to the South African grid. This research will aim to test and verify the various control solutions, limits and functions specified in the grid code.

2.2 Voltage Apportionment limits

In this section the voltage apportionment limits are covered. Eskom has defined the various voltage limits depending on the type of network and voltage control employed [27]. It is necessary to understand the voltage apportionment limits to ensure that voltages on the LV network are adequate when assessing the voltage on the MV network. The LV voltage must fall within the +- 10% limits defined by the quality of supply standard, the NRS-048-2-2008 [14].

2.2.1 Network class and tap zones

Each distribution network can be classified into a specific class and tap zone (TZ). The network class is defined by the ratio of voltage drop between the MV and LV network. The tap zone is defined by the maximum voltage experienced by a specific portion of network during minimum load. A distribution feeder can be subdivided into different network classes and tap zones depending on the voltages experienced at different locations on the network. There are four network classes: C1, C2, C3 and C4. The various network classes are defined as follows:

1. C1- Most commonly an urban cable network with the maximum MV voltage drop about a third of the LV voltage drop. The load density after diversity is greater than 200 kVA/km^2.
2. C2- The maximum MV voltage drop is about equal to the LV voltage drop. The network is typically a rural network that supplies urban loads. The load density after diversity is less than 200 kVA/km^2.
3. C3- The maximum MV voltage drop is about double the LV voltage drop. The network is typically rural and supplies little urban load. The load density after diversity is usually less than 100 kVA/km^2. C3 would be the network class for a farmer's feeder where motors and other equipment are supplied, but some urban load may be connected.

4. C4-The maximum MV voltage drop is triple the LV voltage drop. This network class is seldom used, but would be used on rural feeders that do not supply any urban load.

Figure 2.10 shows the difference between the different classes graphically.

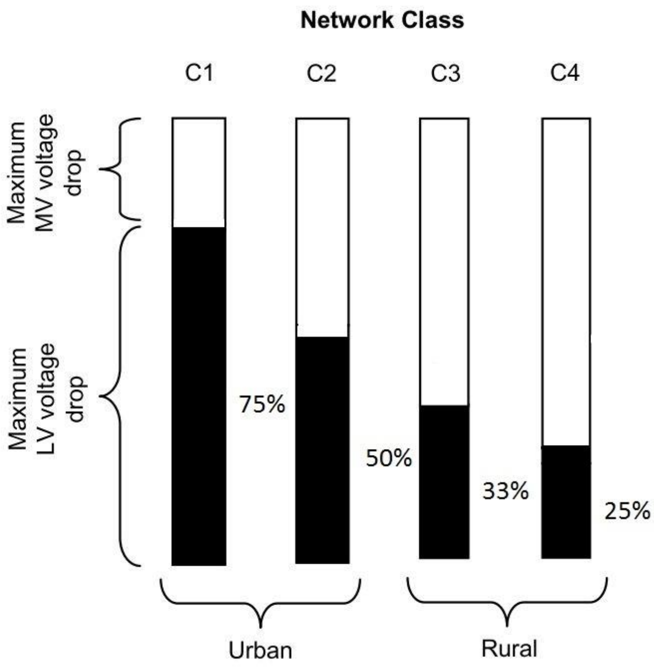

Figure 2.10: Apportionment of maximum voltage drops in the MV and LV network for the four network classes [27]

Portions of the network are also classified into regions called tap zones. A TZ specifies the tap setting for the MV/LV transformers connected within the zone. There are three levels of tap zone: TZ1, TZ2 and TZ3. Each TZ has an upper and lower voltage range that defines it. The maximum voltage must fall within the limits to be classified into a particular zone. The minimum voltage limit is dependent on the network class. The voltage limits ensure that the range of voltage experienced on the LV network falls within the LV voltage limits of ±10% of nominal voltage. The MV/LV transformer taps are configured based upon the expected tap zone at that point in the network. Table 2.3 shows the MV voltage limits for each network class and tap zone. The tap zone and network class is defined for a portion of network by determining the maximum voltage during minimum load and the minimum voltage during maximum load. The abnormal limits are used when evaluating network contingencies such as temporary network reconfiguration.

Table 2.3: MV Voltage limits per tap zone for each network class [27]

Network Class		Maximum Voltage			Minimum Voltage		
		TZ1	**TZ2**	**TZ3**	**TZ1**	**TZ2**	**TZ3**
C1	Normal	105%	103%	100%	101.5%	99.5%	97%
	Abnormal	106%	105%	102%	99.5%	97%	94.5%
C2	Normal	105%	103%	100%	98%	95.5%	93.5%
	Abnormal	106%	105%	102%	95.5%	93.5%	91%
C3	Normal	105%	103%	100%	95.5%	93%	91%
	Abnormal	106%	105%	102%	93%	91%	88.5%

A portion of MV network can be classified as C2 and TZ3. If a voltage regulator is installed, the portion of the network after the voltage regulator could be classified as C1 and TZ1 because the voltages and expected MV/LV voltage drop ratio will be restricted between the limits of the respective class and tap zone. In the steady state a voltage regulator can effectively be regarded as a controlled voltage source. Figure 2.11 shows how a the network class after a voltage regulator can change. Eskom uses TZ2 as the standard tap zone however the Western Cape has standardised on using TZ1.

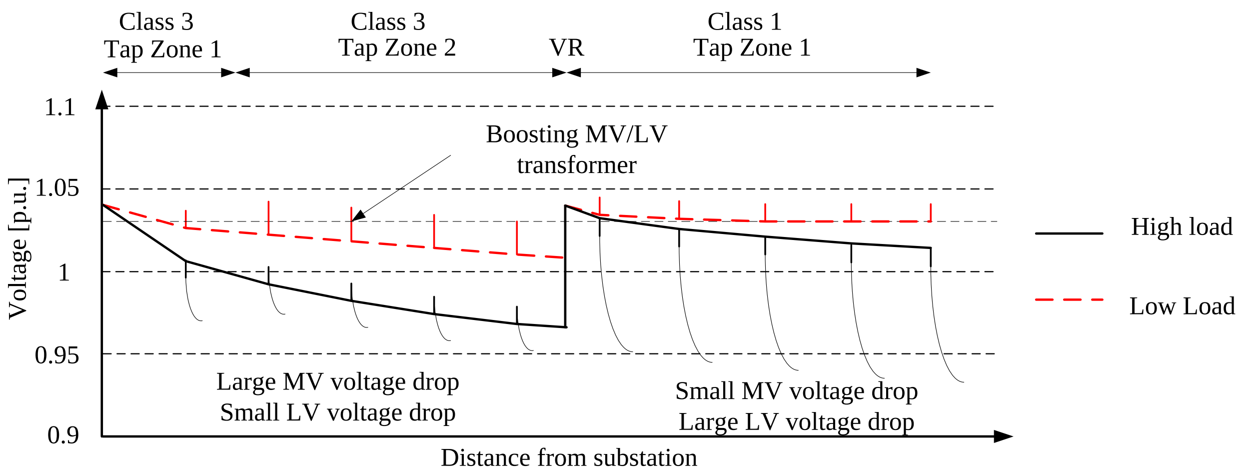

Figure 2.11: Example of multiple network classes on a distribution network

2.2.2 DG voltage limits

If DG is connected to a feeder, it could cause the voltage to rise during maximum generation and minimum load operating conditions. If this operating condition occurs for less than 5% of the year, the generator can be sized such that it would cause a voltage rise of 2% above the maximum TZ voltage during minimum load. If the generator will generate its maximum power at minimum load, for a time period greater than 5% of the year, then the voltage rise is limited to 1% above the maximum TZ voltage during minimum load [27].

The voltage limits defined by the network tap zone provide an additional limitation to the amount of DG that can be connected to a feeder. The addition of intermittent DG will not modify the tap zone as the generation cannot be guaranteed. When installing DG at a particular point, the voltage of the entire feeder should be assessed to ensure that the installed generation does not cause the voltage to exceed the limits defined by the TZ. PV generation reaches its peak during the day when the load is usually not at its minimum. Therefore the feeder voltage profile and voltage change should be assessed using the 2% voltage rise limitation specified above.

In this document it is assumed that if the MV network voltages fall within the limits for the specific tap zone and network class, the LV network voltages will be acceptable.

2.3 Conclusions

In this chapter, a summary of the grid code for renewable power plants in South Africa was provided and the relevant sections for DG connection to the grid were discussed. The minimum technical requirements for the different categories of DG were summarised and analysed. One of the limiting requirements relevant for this study is the 3% RVC limitation for non-synchronous generators.

The voltage apportionment limits and the concept of a network class and tap zone were covered. The network class and TZ provide a simple method of determining whether or not a customer on the LV network will experience adequate voltage levels. The voltage rise limits during minimum load and maximum generation operating conditions was provided. It was concluded that PV can be sized such that it would cause a 2% voltage rise during minimum load conditions.

3 Modelling and control of existing distribution systems

To accurately simulate a distribution network, the various components that have an effect on the overall accuracy of the model must be understood. The components of a typical distribution network include lines, transformers, voltage regulators and capacitor banks. The models for each of these devices are developed in the following sections and any assumptions made are stated. There are many more devices and components used on distribution networks such as protection, metering and telecommunications but they are not the focus of this work.

3.1 Voltage drop

3.1.1 Line model

The line model has been developed using a combination of the models developed in [28]–[31]. The majority of Eskom distribution lines are three phase and are connected in delta at the substation transformer. The various types of lines encountered on a distribution network include three phase delta, star with neutral wire, single wire earth return and dual phase. A distribution line can be modelled as a series impedance and the equivalent model is shown in Figure 3.1.

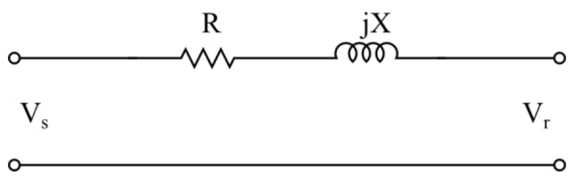

Figure 3.1: Equivalent circuit of a short transmission line

A three phase delta line can be represented by three individual equivalent impedances as shown in Figure 3.2.

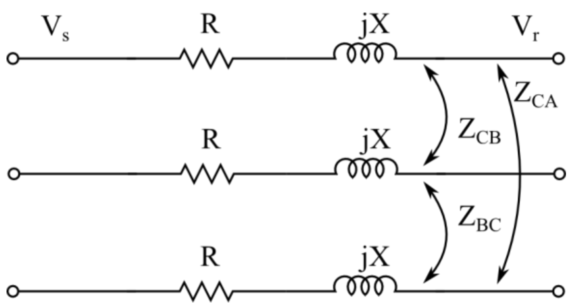

Figure 3.2: Three phase equivalent line

The resistance of a line is dependent on the type of conductor used and is often specified for a temperature of 20°C. The manufacturers supply the DC resistance of a conductor. The DC resistance can be considered to be similar to the AC resistance on MV networks. The resistance of a conductor at a new temperature can be calculated using (3.1).

$$R_2 = R_1\left(\frac{T_2 + T}{T_1 + T}\right) \tag{3.1}$$

R_1 and R_2 are the resistances at temperatures T_1 and T_2 respectively. T is the temperature constant for a particular conductor and for hard drawn aluminium it is 228.1°C.

The impedance matrix of the three phase line is shown in (3.2).

$$Z = \begin{bmatrix} Z_A & Z_{AB} & Z_{AC} \\ Z_{BA} & Z_B & Z_{BC} \\ Z_{CA} & Z_{CB} & Z_C \end{bmatrix} \tag{3.2}$$

The resistance value of Z can be found in the data sheets for the various types of conductors. The reactance has to be calculated as it varies between tower types and phase spacing. For equal phase spacing, with each of the lines connected in delta (physically 120° apart), the inductance can be calculated using (3.3), with D being the phase spacing and D_S the geometric mean radius (GMR) of the conductor. The inductance is equal for each phase in an equally spaced or completely transposed three phase line.

$$L_{phase} = 2\times10^{-7}\ln\frac{D_{eq}}{D_S} \quad [\mathrm{H/m}] \tag{3.3}$$

D_{eq} is calculated using (3.4).

$$D_{eq} = \sqrt[3]{D_{12}D_{23}D_{31}} \quad [\mathrm{m}] \tag{3.4}$$

The reactance can then be calculated using (3.5).

$$X = 2\pi fL \quad [\Omega] \tag{3.5}$$

Table 3.1 shows the typical parameters for distribution lines commonly used by Eskom. Eskom generally uses aluminium conductor steel reinforced (ACSR) or all aluminium alloy conductor (AAAC) lines, with the main drive to use ACSR over AAAC lines. AAAC lines are only used in areas where corrosion is a concern.

Each of the lines in Table 3.1 has an equivalent all aluminium alloy conductor that is used near coastal areas. AAAC conductors are used near the coast because the steel in ACSR conductors might have corrosion problems. An Oak AAAC conductor can be used to directly replace a Hare ACSR conductor as the current carrying capacity is similar. For simplicity the ACSR conductors will be used in this document.

Table 3.1: Typical ACSR line parameters [29]

Conductor	**Current at 50°C [A]**	**Size [mm^2]**	**DC resistance at 20°C [Ω/km]**	**X/R ratio (Typical)**	**Max 11 kV thermal loading [MVA]**
Squirrel	104	20	1.3677	0.25-0.29	2
Fox	148	37	0.7822	0.43-0.52	2.8
Mink	206	63	0.4546	0.71-0.88	3.9
Hare	280	105	0.2733	1.1-1.28	5.3
Chicadee	419	201	0.1427	2.5-2.78	8

The low X/R ratio on weak networks implies that the real current has a much greater effect on the voltage than the reactive current does. The lines used by Eskom all have a name that refers to a very specific conductor. A complete list of conductors that are used in Eskom distribution networks can be found in [29] and a complete list of almost any conductor can be found in [32]. Commonly, a combination of Hare and Mink lines are used for the main backbone of a distribution feeder. Such a feeder has a combined X/R ratio of around 1 and all distribution lines can be assumed to have an X/R ratio below 1.5.

The maximum current that a line can carry is determined by the templating temperature that the line was designed for. Lines are designed with a templating temperature of between 50°C and 80°C, with the more common rating being 70ºC. This limit can be exceeded for short periods of time during emergencies, but should not be used in calculations for maximum power transfer. It can be assumed that the higher templating temperature does not affect the impedance. The X/R ratio of each line varies based upon the phase spacing used. It is typical to have between 1-2 m of phase spacing. The apparent power each line can carry at 22 kV is approximately double the apparent power at 11 kV because $S = \sqrt{3} V_{LL} I$.

While the majority of problems at the distribution voltage level can be adequately modelled using just the resistance and reactance of the line, lines of greater length (>50 km) and higher voltage (22 kV - 33 kV) can experience the Ferranti effect under low loads. The Ferranti effect can become a problem when the voltage rise, caused by the capacitive charging of the line, exceeds the voltage drop due to real and reactive current along the line [17]. The lines under study in this work have a length of around 30 - 60 km and therefore are short enough to neglect shunt capacitance for the estimations [29]; however DIgSILENT PowerFactory incorporates this into the line model.

3.1.2 Voltage drop along a radial feeder

A basic substation, line and load model is shown in Figure 3.3. All of the calculations assume that the values are converted to per unit and the results are specified in per unit unless otherwise stated. They can easily be converted to their percentage values by multiplying the per unit value by 100. Certain results are referred to as a percentage in the analysis to conform to the standard representation as used in the literature.

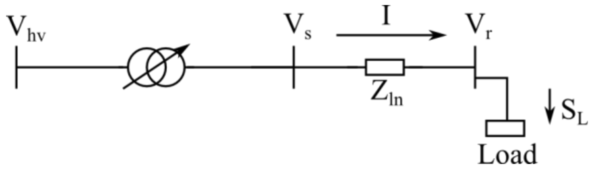

Figure 3.3: Basic line model

If it is assumed that the voltage at the sending end has an angle of zero in Figure 3.3, then the voltage can be calculated by solving (3.6) for $\boldsymbol{V_r}$.

$$S_L = P_L + jQ_L = \boldsymbol{V_r}\left(\frac{\boldsymbol{V_r} - V_s}{R_{\ln} + jX_{\ln}}\right) \tag{3.6}$$

The solution to the quadratic equation is provided in [33] and is shown in (3.7). A solution is only valid if (3.9) is positive with a constant P_L and Q_L. This method of calculating the voltage is known as the exact voltage calculation and the solution will be referred to as the actual voltage.

$$\boldsymbol{V_r} = 0.5\left[V_s \pm \sqrt{V_s^2 - 4\left(\left(\frac{P_L X_{\ln} - Q_L R_{\ln}}{V_s}\right)^2 - \left(P_L R_{\ln} + Q_L X_{\ln}\right)\right)}\right] + j\frac{P_L X_{\ln} - Q_L R_{\ln}}{V_s} \tag{3.7}$$

The voltage sensitivities to a change in active or reactive power can be found by taking the partial derivative of (3.7) with respect to P_L and Q_L to get (3.8) and (3.9).

$$\frac{\partial \boldsymbol{V_r}}{\partial P_L} = \pm\frac{R_{\ln} - 2\dfrac{\left(P_L X_{\ln} - Q_L R_{\ln}\right)X_{\ln}}{V_s^2}}{\sqrt{V_s^2 - 4\left(\left(\dfrac{P_L X_{\ln} - Q_L R_{\ln}}{V_s}\right)^2 - \left(P_L R_{\ln} + Q_L X_{\ln}\right)\right)}} + j\frac{X_{\ln}}{V_s} \tag{3.8}$$

$$\frac{\partial \boldsymbol{V_r}}{\partial Q_L} = \pm\frac{X_{\ln} + 2\dfrac{\left(P_L X_{\ln} - Q_L R_{\ln}\right)R_{\ln}}{V_s^2}}{\sqrt{V_s^2 - 4\left(\left(\dfrac{P_L X_{\ln} - Q_L R_{\ln}}{V_s}\right)^2 - \left(P_L R_{\ln} + Q_L X_{\ln}\right)\right)}} - j\frac{R_{\ln}}{V_s} \tag{3.9}$$

The sensitivity of the voltage magnitude is only affected by the part which is parallel to $\boldsymbol{V_r}$ and can be calculated using (3.10) [33].

$$\begin{aligned} \frac{\partial|\boldsymbol{V_r}|}{\partial P_L} &= \Re\left(\frac{\partial \boldsymbol{V_r}}{\partial P_L}\frac{\boldsymbol{V_r}^*}{|\boldsymbol{V_r}|}\right) \\ \frac{\partial|\boldsymbol{V_r}|}{\partial Q_L} &= \Re\left(\frac{\partial \boldsymbol{V_r}}{\partial Q_L}\frac{\boldsymbol{V_r}^*}{|\boldsymbol{V_r}|}\right) \end{aligned} \tag{3.10}$$

If the load power is low compared to the short circuit power, then the voltage drop can be approximated by the first order Taylor expansion of (3.8) and (3.9), by setting P_L and Q_L to zero to get (3.11).

$$\boldsymbol{V_r} \approx V_s + \frac{R_{\ln}P_L + X_{\ln}Q_L + j\left(X_{\ln}P_L - R_{\ln}Q_L\right)}{V_s} \tag{3.11}$$

If the power transfer is small, then the voltage angle is small and the change in voltage from the source to receiving end can be approximated using (3.12) [6], [34]. When the complex part of the numerator in (3.11) is less than 10% of the nominal voltage, (3.12) provides similar results and the error is shown to be less than 0.5% between the two equations [35].

$$\Delta V \approx \frac{R_{\ln}P_L + X_{\ln}Q_L}{V_r} \tag{3.12}$$

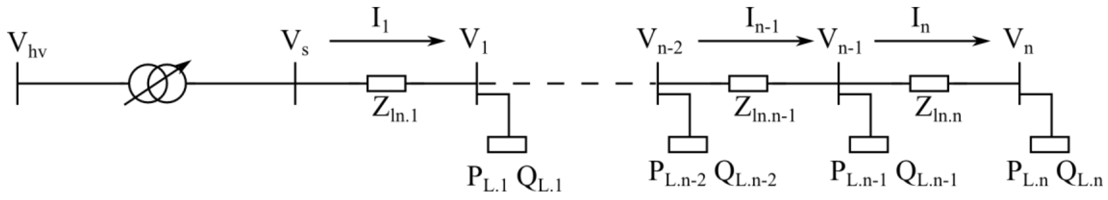

Figure 3.4: Line model with multiple nodes

On a more realistic feeder with multiple nodes, as shown in Figure 3.4, the individual voltage drops between nodes can be calculated using (3.13).

$$\Delta V_k \approx \frac{R_{\ln.k}P_k + X_{\ln.k}Q_k}{V_k} \tag{3.13}$$

Where P_k and Q_k are the active and reactive power flowing through the segment k of a feeder. They can be calculated using (3.14) and (3.15).

$$P_k = \sum_{i=k}^{n} P_{L.i} + \sum_{i=k+1}^{n} I_i^2 R_{\ln.i} \tag{3.14}$$

$$Q_k = \sum_{i=k}^{n} Q_{L.i} + \sum_{i=k+1}^{n} I_i^2 X_{\ln.i} \tag{3.15}$$

Where $P_{L.i}$ and $Q_{L.i}$ are the real and reactive power of the load at node i. The current in (3.14) and (3.15) can be calculated using (3.16).

$$I_i = \sum_{j=i}^{n} \frac{\sqrt{P_j^2 + Q_j^2}}{V_j} \tag{3.16}$$

Equations (3.7) to (3.12) can be used to determine the voltage change along a feeder. The change in voltage at a specific location can be approximated by adding the series impedance of the transmission line and transformer to find the total impedance of the point under investigation. The shunt impedance of the network can be neglected. The following figures compare the exact voltage change calculated using (3.7), the first approximation calculated using (3.11) and the second approximation calculated using (3.12) to the results obtained using DIgSILENT PowerFactory. The exact voltage calculation would provide more accurate results if the network was reduced to a Thevenin equivalent impedance. The effort required to obtain the Thevenin parameters negates the simplifications made, as multiple load flows are required to find the parameters. These results show that if the shunt impedance is neglected for the approximate calculations, that the results provide suitable accuracy for analysis. The simulations are performed on the test network developed later in this document and the results can be used without knowing the reference parameters of the network.

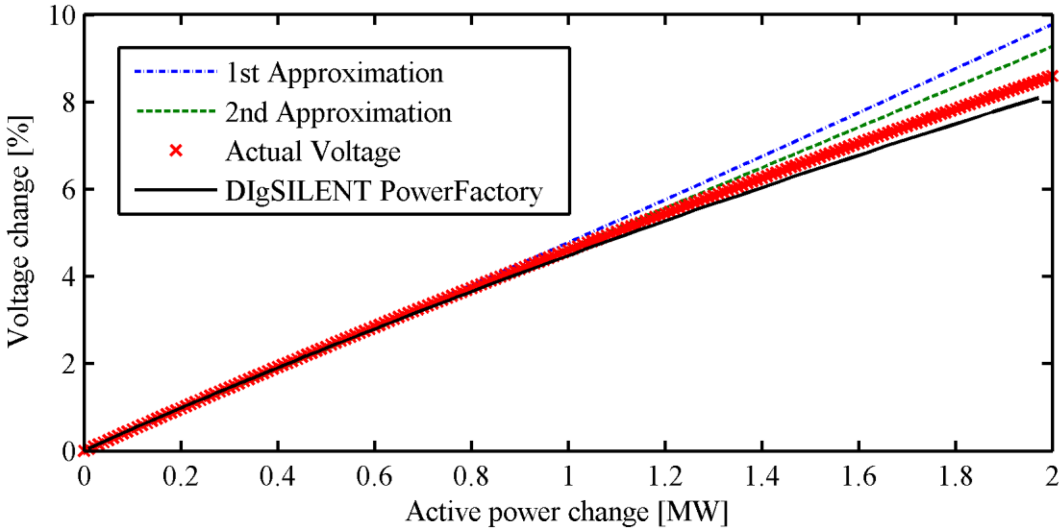

Figure 3.5: Voltage change comparison for the three methods at a power factor of 1

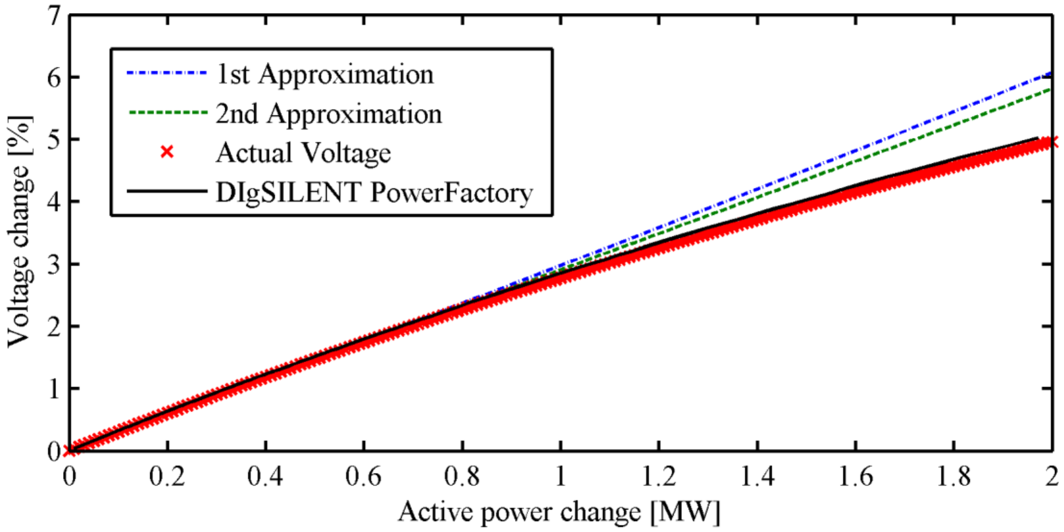

Figure 3.6: Voltage change comparison for the three methods at a power factor of 0.95

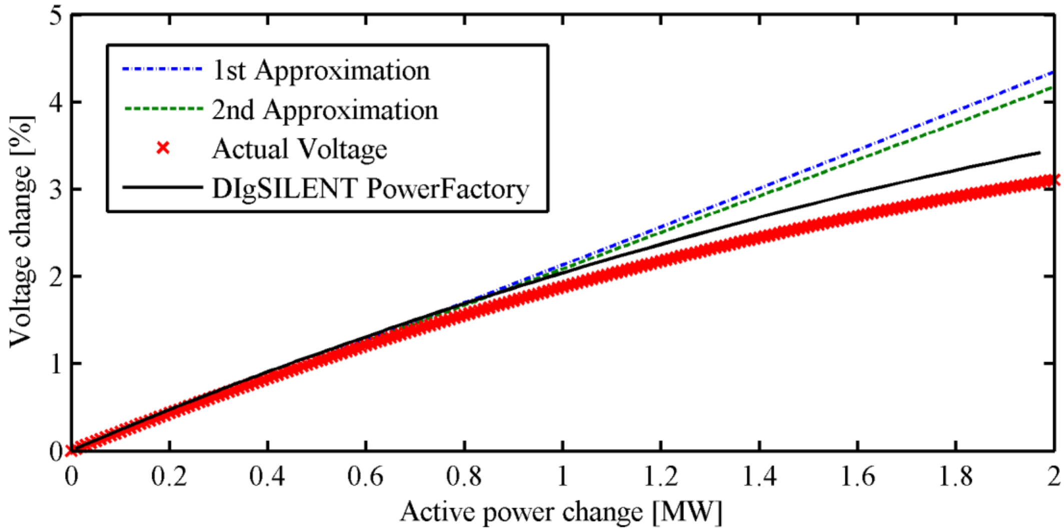

Figure 3.7: Voltage change comparison for the three methods at a power factor of 0.9

Figure 3.5 to Figure 3.7 show that the approximations made in (3.12) provide good accuracy when compared to the DIgSILENT simulation. The method used to calculate the feeder voltage in equations (3.12) to (3.16) is known as the approximate method [6]. The approximate method is simple and allows for basic hand calculations to be performed. The accuracy of the approximate method declines when feeders become too complex, the load is high or the power factor is low. The figures show that the approximations overestimate the voltage change and therefore can be considered suitable for the worst case estimations. The actual change in voltage as calculated by DIgSILENT can be up to 25% less for large changes in power at a low power factor. The estimations are much more accurate for smaller changes in power and at a power factor closer to unity where the error is within a few percent. The figures confirm the findings in [6] where it was shown that the approximate method provided good analytical results. In [6] it was determined that the loss summation method provided more accurate results when confirmed against a load flow program. In this document all results and simulations are verified using DIgSILENT PowerFactory.

A method of calculating the voltage drop of a feeder, with evenly distributed loads, is shown in (3.17). λ is the distance away from the substation, where $\lambda = 0$ represents the beginning of the feeder and $\lambda = 1$ represents the end of the feeder [11]. For example, on a 30 km feeder the 12 km point would be represented as $\lambda = 0.4$.

$$\Delta V \approx \frac{R_{\text{ln.tot}} P_L + X_{\text{ln.tot}} Q_L}{V_{\text{nom}}} \left(\lambda - 0.5\lambda^2 \right) \tag{3.17}$$

Where V_{nom} is the per unit nominal feeder voltage and in most cases it will be equal to 1. $R_{\text{ln.tot}}$ and $X_{\text{ln.tot}}$ are the total resistance and reactance of the feeder.

On a practical feeder there are multiple conductors with different series impedances. The different conductors can be accounted for by using the series impedance to point λ instead of the total feeder impedance. Therefore (3.17) can be modified and the voltage change from V_s can be calculated using (3.18).

$$\Delta V \approx \frac{R_{\text{ln}.\lambda} P_L + X_{\text{ln}.\lambda} Q_L}{V_{\text{nom}}} (1 - 0.5\lambda) \tag{3.18}$$

Where $R_{\text{ln}.\lambda}$ and $X_{\text{ln}.\lambda}$ are the series resistance and reactance of a line from the source to a point λ.

Figure 3.8 illustrates the effect of varying the X/R ratio of a line. The reactance remains relatively constant for different conductors and only the resistance varies substantially. As can be seen, the voltage magnitude at the receiving end of a line can be improved by reducing the resistance. The figures also illustrate how neglecting the voltage angle, during high load at a poor power factor, on lines with a large X/R ratio, could result in voltage magnitude errors; however this angle is small when the X/R ratio is below one.

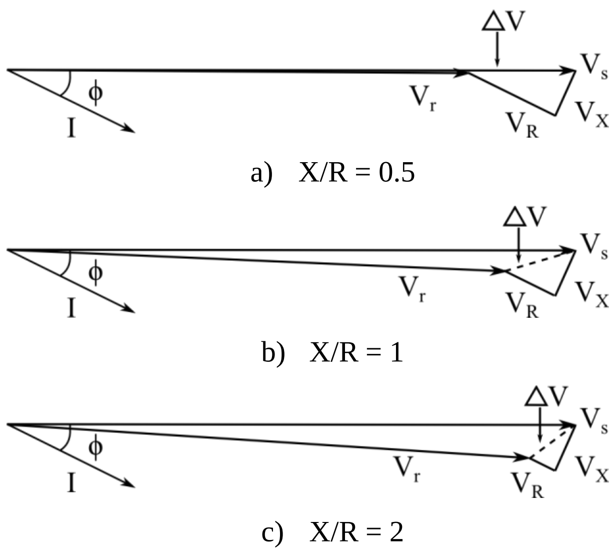

Figure 3.8: Effect on voltage regulation, of a line, for different X/R ratios with a constant reactance

This section has illustrated that the voltage decreases along a radial line when power flows in a single direction. Using the assumption that power flows in a single direction is how networks have been designed and operated up until now.

3.2 Classical voltage regulation equipment on a radial feeder

3.2.1 On-load tap changer

Eskom HV/MV transformers are equipped with on-load tap changers (OLTCs) that are configured to regulate the secondary voltage within the maximum voltage range defined by the tap zone. The upper and lower bound voltages of the controller are defined as V_{UB} and V_{LB} respectively. The controller dead band of the OLTC should be at least 1.5 times greater than the individual tap step size to prevent hunting. OLTCs typically have 16 steps with a 1.25% step size [36].

An OLTC should be the first unit to regulate the voltage of a feeder, unless there is a switched capacitor installed on the feeder. It should operate after a time delay if the voltage at the substation busbar falls outside of the upper and lower bound voltage setting. The typical time delay for an OLTC is in the range of 30 to 45 seconds. The time delay prevents the transformer initiating a tap change for voltage fluctuations that occur for a short time period, such as motor starting [6]. An OLTC only compensates for the voltage drop or rise over the impedance of the transformer and the HV line. If proper reactive power control is performed on the feeders or MV busbar, the number of OLTC operations will be minimised. The OLTC should only operate when large changes in load occur. The basic control loop of an OLTC is shown in Figure 3.9.

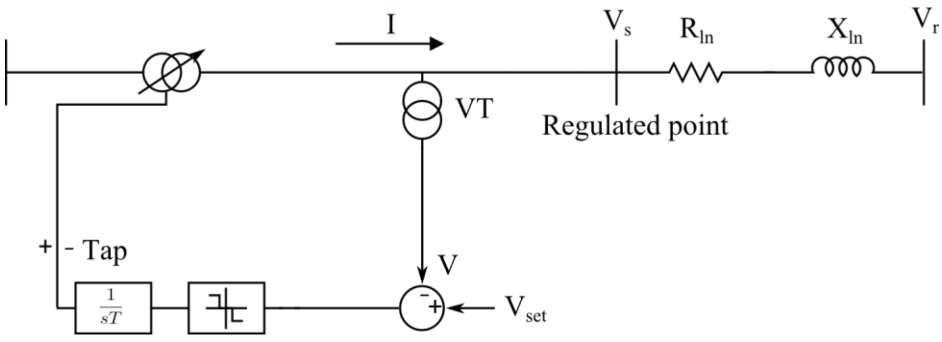

Figure 3.9: OLTC control diagram

3.2.2 Voltage regulator

The model for a voltage regulator (VR) is developed using [16], [28], [31]. A combination of VRs and OLTCs are the main equipment that Eskom uses to regulate voltage on MV feeders. VRs are installed when the voltage along a feeder needs to be boosted because the line is long, or the feeder load increases and low voltage limits are not met [27]. VRs are easy to install and are a much cheaper option than upgrading the conductors along a line to improve the steady state voltage regulation. A voltage regulator consists of a single phase auto transformer with a tap changer, as shown in Figure 3.10.

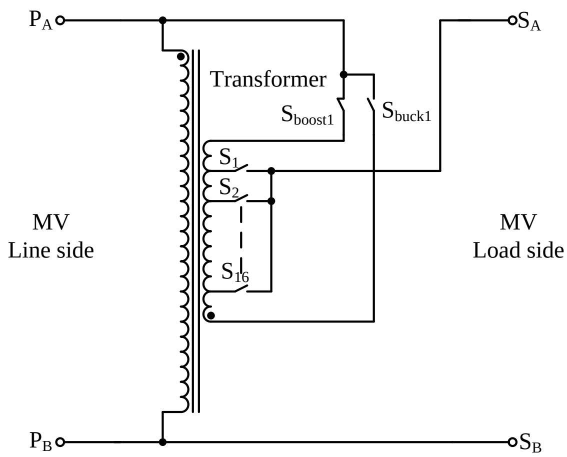

Figure 3.10: VR transformer and tap changer configuration

They typically have a total of 16 steps, with a reversing tap to buck or boost the voltage, which gives +-10% single phase regulation at 0.625% per step. Their time delay is typically 15 to 30 seconds longer than that of any upstream tap changing devices. VRs are designed to provide rated voltage regulation, at rated current, with a power factor of 0.8 lagging. The VRs used on the distribution network are single phase units connected in either open or closed delta as shown in Figure 3.11 and Figure 3.12. Open delta results in a voltage regulation capability of ±10% and closed delta ±15% with a step size of 0.9375%.

Regulators connected in open delta cause a neutral voltage shift, at the secondary side, as shown in Figure 3.11. The result of the neutral voltage shift is a regulated line to line voltage, but an unbalanced line to ground voltage. Unbalanced line to ground voltage can cause problems in certain scenarios, such as when SWER systems are used, because the phase c voltage is not regulated with respect to ground. If the network is paralleled with another feeder, the regulators are set to stay in the neutral position because circulating currents could cause the source’s earth fault protection to trip [16]. Regulators connected in closed delta cause a phase shift of 30° that can be configured to lead or lag the primary side voltage. When simulating a network with open delta connected voltage regulators, it is necessary to use unbalanced calculations because of the neutral voltage shift.

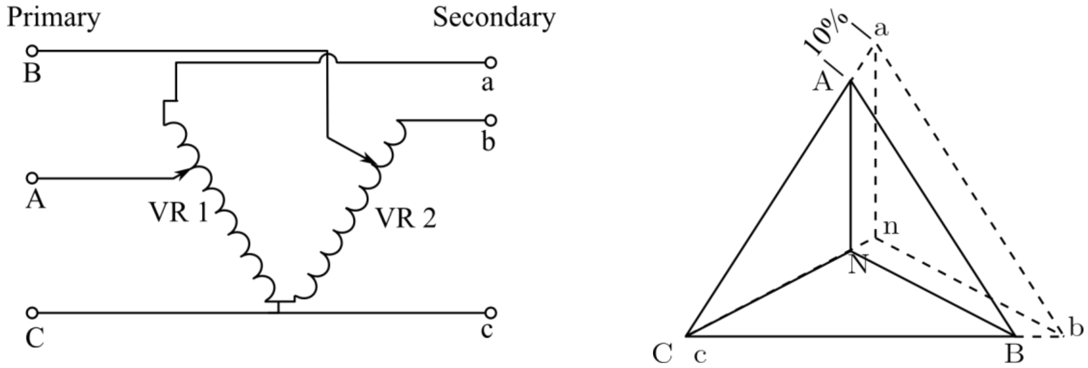

(a) (b)

Figure 3.11: a) Open delta connection for a voltage regulator and b) neutral voltage shift

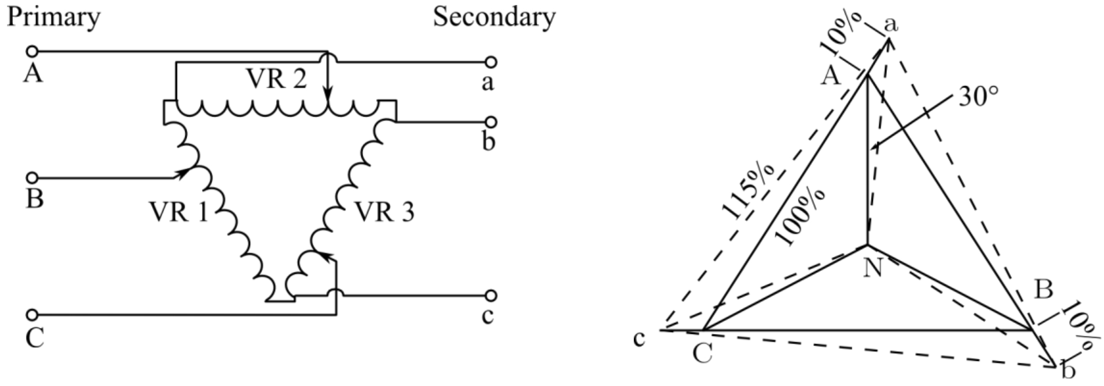

(a) (b)

Figure 3.12: a) Closed delta connection for a voltage regulator and b) voltage phase shift

VRs come in two main types: A and B. Type-A regulators contain the series winding on the load side and have higher losses when bucking the voltage. Type-B regulators have the shunt winding on the load side and have lower losses when bucking the voltage. A dedicated potential transformer is not needed to sense the load side voltage on a Type-B regulator, as the tertiary winding can be used for that purpose. The most commonly used voltage regulators on the Eskom network are type B Cooper voltage regulators. There are seven different control modes for a Cooper voltage regulator [37]. They are:

1. Locked forward
2. Locked reverse
3. Reverse idle
4. Bi-directional
5. Neutral idle
6. Co-generation
7. Reactive bi-directional

The controller always measures the real component of the current except for when using mode 7. For the following descriptions, it is assumed that the 'source side' is the side towards the substation and the 'load side' is the side towards the end of the feeder during standard network operation. For modes 1 to 3, the power flow should not reverse as the VR will lock the current tap position until power flow returns to normal, but mode 3 allows for reverse power flow metering. Mode 4 will always regulate in the direction that the current is flowing. In the case of reverse power flow, due to a DG, the controller will respond by trying to regulate the source side and will cause the load side voltage to increase. Mode 5 causes the VR to regulate to the neutral tap position if reverse power flow is detected for 10 continuous seconds. Mode 6 is the setting that has to be used if generation is connected downstream of the regulator. In this mode the regulator will always regulate the load side irrespective of the power flow. The control can also be configured to have two line drop compensator settings, so that during periods of reverse power flow the voltage can be regulated at the load side terminals. In mode 7 the reactive current is used to determine the power flow direction. [37]

The series impedance and shunt admittance of a VR can be considered negligible and can therefore be ignored in the calculations. The equations used for VRs are shown below. The secondary voltage can be calculated using (3.19).

$$V_{\mathrm{sec}} = V_{\mathrm{pri}}(1 + aTAP) \tag{3.19}$$

V_{sec} is the secondary voltage, V_{pri} is the primary voltage, a is the per unit change in voltage per tap change and TAP is the tap position. Similarly the current can be calculated using (3.20).

$$I_{\mathrm{sec}} = \frac{I_{\mathrm{pri}}}{aTAP} \tag{3.20}$$

The controller will ensure the voltage remains within a certain range such that $V_{LB}<V<V_{UB}$. V_{LB} and V_{UB} are the lower and upper bound voltages. When the voltage falls outside of this limit for a period of time as defined in the control settings, the controller will initiate a tap change.

The regulators that Eskom use are either 100 A or 200 A units. They are installed based upon the line current rather than apparent power. The rating of a voltage regulator is usually specified in regulation apparent power as opposed to system apparent power. The rating refers to the power capability of the series winding and is shown in (3.21).

$$S = \frac{V \times I \times \text{Reg}}{1000} \quad [\text{kVA}] \tag{3.21}$$

Reg is the maximum voltage boost of the regulator in per unit. The percentage voltage regulation along a line is defined by (3.22). Using this equation one can determine the percentage of voltage variation between two load conditions.

$$\%VR = \frac{V_{L.\min} - V_{L.\max}}{V_{L.\max}} \times 100 \quad [\%] \tag{3.22}$$

$V_{L.\min}$ and $V_{L.\max}$ are the voltages at minimum load and maximum load at the point that the voltage is measured.

If a voltage regulator is installed at a point λ_{vr}, the change in voltage from the substation voltage can be approximated using (3.23).

$$\begin{aligned} \Delta V &\approx \frac{R_{\text{ln}.\lambda} P_L + X_{\text{ln}.\lambda} Q_L}{V_{\text{nom}}} (1 - 0.5\lambda) \quad \lambda \leq \lambda_{vr} \\ \Delta V &\approx \frac{R_{\text{ln}.\lambda} P_L + X_{\text{ln}.\lambda} Q_L}{V_{\text{nom}}} (1 - 0.5\lambda) - aTAP \quad \lambda > \lambda_{vr} \end{aligned} \tag{3.23}$$

The lifetime of a VR is typically expected to be over 20 years. Manufacturers recommend services every 5 to 7 years or after a certain number of tap changes. Eskom do not have any fixed maintenance programs for VRs and therefore their reliability is quite poor [16]. The devices can operate up to 500 000 tap changes before a major overhaul which equates to an average of 68 tap changes per day over the 20 year period [38]. This is the total number of tap changes that the regulator can perform, assuming all of the taps are used equally. It is unlikely that all of the taps will be used equally and therefore a limitation of about 4 tap changes per day can be specified for each tap position. It is expected that about 8-10 of the taps will be regularly used and therefore the total limitation for daily tap changes is in the region of 32-40, to prevent degradation at an accelerated rate.

3.2.3 Line drop compensator

Most OLTC and VR controllers are equipped with a line drop compensator (LDC). LDCs are seldom used on the South African network due to the increased complexity when a single LDC regulates several feeders [2]. The use of a LDC requires the settings to be updated every time there is a significant change to the network. The constant need to update the LDC settings can be costly and time consuming.

LDCs are employed in cases where a regular OLTC does not provide adequate regulation along a feeder. In these cases, a LDC can be used to regulate the voltage at a point further down the line [6]. The basic LDC regulation is accomplished by setting the resistance and reactance controls of the regulator based upon the CT and VT ratio. VRs equipped with a LDC must be able to sense the direction of current flow.

The model for a LDC is developed using [16], [28], [31]. The layout of an OLTC with LDC is shown in Figure 3.13.

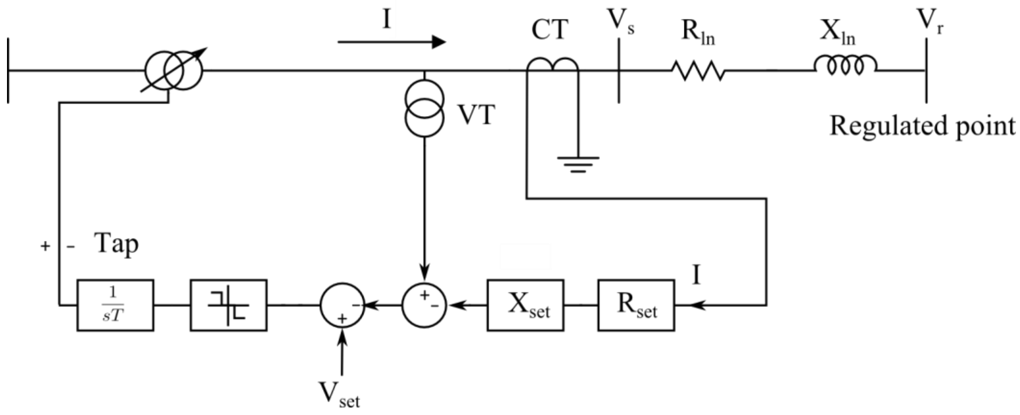

Figure 3.13: OLTC with LDC

A LDC estimates the voltage drop along the line to the regulation point based upon the impedance of the line and current flow through the transformer. The corrected voltage is sent to the tap changer controller that regulates to the remote point rather than the local voltage. The LDC must ensure that the voltages fall within the maximum and minimum limits defined by the network operator. The voltage at the control point will be controlled within a band defined by the tap zone. The equations for LDC control and settings are covered in [6] and the theory is covered here.

The voltage at the regulation point is calculated using (3.24).

$$V_r = V_s - I(R_{\ln}\cos\phi + X_{\ln}\sin\phi) \tag{3.24}$$

The voltage at the regulation point for maximum and minimum load can be estimated using (3.25) and (3.26) respectively.

$$V_{r.L.\max} = V_{s.\max} - I_{L.\max}(R_{\ln}\sin\phi + X_{\ln}\cos\phi) \tag{3.25}$$

$$V_{r.L.\min} = V_{s.\min} - I_{L.\min}(R_{\ln}\cos\phi + X_{\ln}\sin\phi) \tag{3.26}$$

$V_{s.\max}$ and $V_{s.\min}$ are the maximum and minimum sending end voltages. $I_{L.\max}$ and $I_{L.\min}$ are the line current at maximum and minimum load. $\cos\phi$ is the power factor at the tap changer's location.

The LDC is configured with the line parameters adjusted for the voltage transformer (VT) and current transformer (CT) ratio. The method to calculate the value for the LDC settings R_{set} and X_{set} is shown in (3.27) and (3.28).

$$R_{\text{set}} = \frac{N_{CT}}{N_{VT}} R_{\ln} \tag{3.27}$$

$$X_{\text{set}} = \frac{N_{CT}}{N_{VT}} X_{\ln} \tag{3.28}$$

Where R_{set} and X_{set} are the LDC resistance and reactance settings, N_{CT} is the turns ratio of the CT and N_{VT} is the turns ratio of the VT.

There can be voltage errors at the regulation point depending on how accurately R_{set} and X_{set} match the real line parameters and can be calculated using (3.29). From the equation it can be seen that the voltage error will increase as the power factor decreases or the load increases. The configuration settings also need to be reviewed regularly as the network configuration and loading could change over the years that can lead to greater inaccuracies.

$$V_r - V_{set} = IR_{ln}\sin\phi\left(\frac{X_{set}}{R_{set}} - \frac{X_{ln}}{R_{ln}}\right) \tag{3.29}$$

The voltage variation at the substation busbar can be calculated using (3.30).

$$V_{s.L.max} - V_{s.L.min} = I_{L.max}(R_{ln}\cos\phi + X_{ln}\sin\phi) - I_{L.min}(R_{ln}\cos\phi + X_{ln}\sin\phi) \tag{3.30}$$

The setpoint voltage of the LDC can be derived from (3.30) and is shown in (3.31).

$$V_{set} = V_{s.L.min} - \frac{V_{s.L.max} - V_{s.L.min}}{I_{L.max} - I_{L.min}} \tag{3.31}$$

The LDC controls the source voltage to be high during high load and low during low load. It accounts for the voltage drop to the regulation point so that the voltage at the regulation point remains within the control band. The voltage profile of a feeder when the OLTC is equipped with a LDC can be estimated using (3.32).

$$V(\lambda) \approx V_{set} + \frac{R_{set}P_L + X_{set}Q_L}{V_{nom}} - \frac{R_{ln.\lambda}P_L + X_{ln.\lambda}Q_L}{V_{nom}}(1 - 0.5\lambda) \tag{3.32}$$

Figure 3.14 shows the voltage profile of a feeder with an OLTC equipped with a LDC. The voltage profile is generated using (3.32). It shows how the source voltage varies with changing feeder loads. It can be seen that the voltage remains constant at the regulation point.

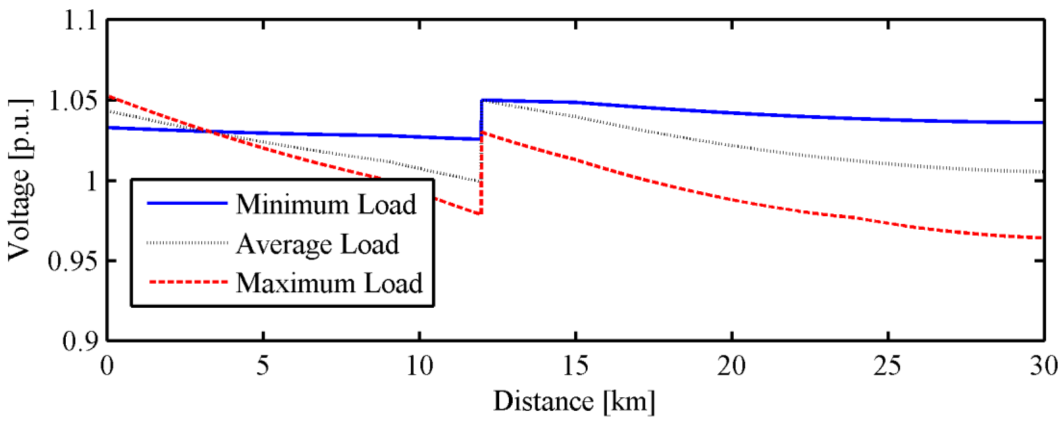

Figure 3.14: Voltage profiles of a feeder for various loading scenarios, with the OLTC equipped with a LDC

A LDC allows the voltage at the substation to vary within a larger band than standard OLTC control. For example, it is possible to set the upper and lower limits for the substation voltage to have a bandwidth of 0.04 p.u. and have the voltage setpoint dynamically adjust within that range.

Voltage regulation using a LDC is more complex when multiple feeders are connected to one busbar. If the feeders have similar load profiles, then a LDC can work well, but if the load profile varies considerably then adequate voltage regulation will be more difficult to implement. During times when the feeders have opposite loading, the load factor difference defines the regulation constraint. When a LDC is configured there are two main limitations that must be adhered to:

1. V_s is less than the maximum voltage defined by the tap zone at the substation busbar
2. The voltage at the end of the feeders or primary side of the VRs is greater than the minimum feeder voltage defined by the network class.

The voltage at the substation when a LDC regulates multiple feeders can be calculated using (3.33), assuming that the regulation point remains the same as in the single feeder case.

$$V_s \approx V_{\text{set}} + \frac{\frac{R_{\text{set}}}{n} P_L + \frac{X_{\text{set}}}{n} Q_L}{V_{\text{nom}}} \tag{3.33}$$

The maximum and minimum secondary voltages of an OLTC can be configured in the controller settings to prevent the LDC from causing over voltages. The increased system complexity when configuring a LDC on transformers with multiple feeders is the main reason that LDCs are rarely used. A more costly option, that provides better voltage regulation for each feeder, is to install a VR close to the substation that is equipped with a LDC. A VR on each feeder allows the voltage to be individually controlled. A secondary advantage is that fewer customers are impacted when maintenance needs to be performed on the OLTC. This option is undesirable in most circumstances, as the operating costs associated with the feeders are increased.

To ensure that the above requirements are met and the calculations provided sensible solutions, simulations assessing worst case scenarios should be performed. These simulations would provide a suitable regulation point for a LDC during the largest load factor difference that can be experienced on a particular feeder.

3.2.4 Capacitor banks

Capacitor banks are installed on feeders to improve the power factor. They reduce the voltage drop along the line due to a reduction in reactive power flow. The capacitors on the Eskom network are typically rated for 1.5-13 kV and 300 kVAr per can but other common sizes are available [17]. Different voltages and power requirements can be met by connecting multiple cans in series and parallel. Capacitors are the easiest and cheapest way to improve the power factor of a feeder in a typical distribution network. The cost is justified by the reduction of transformer loading, line current and voltage drop that results in a loss reduction if suitably controlled. Feeder losses are proportional to the square of the line current and a capacitor can be used to reduce the reactive portion of the current. Capacitors can defer additional capital outlay that would be needed to upgrade the line and transformer.

Capacitor cans have a rated voltage of 110% of the nominal system voltage and can operate up to this voltage with an increased reactive power rating. Capacitor reactive power ratings are supplied for the nominal system voltage. The rated voltage is the rated insulation voltage of the capacitor and the reactive power generated at this voltage can be calculated using (3.34). For example a particular capacitor will produce 100 kVAr at nominal voltage, while at its rated voltage will produce 121 kVAr. Therefore, during periods of high voltages capacitors can exasperate the problem.

$$Q = \left(\frac{V}{V_{\text{nom}}} \right)^2 \times Q_{\text{nom}} \tag{3.34}$$

Q is the produced reactive power, V is voltage the capacitor is operating at, V_{nom} is the nominal voltage and Q_{nom} is the nominal reactive power at the nominal voltage. This shows that the reactive power compensation of a capacitor bank decreases as the voltage decreases. A 5% drop in voltage causes a 9.75% drop in reactive power generation and a 10% drop in voltage causes a 19% drop in reactive power generation. The reduced reactive power output at lower voltages can be a problem when the capacitor is supporting the network voltage. If a disturbance occurs, voltage collapse can follow.

Eskom has standardised on the use of single phase capacitors connected in ungrounded star. A grounded capacitor provides a path for zero sequence currents. The feeder capacitors in the Eskom network are ungrounded to minimise impact on protection devices. If the star point is grounded it would provide a low impedance path for harmonic currents, so operating without a ground limits the impact on the dielectric of the capacitors [17]. The capacitors are either switched or fixed, depending on the load profile and power factor variation of the loads. The switched capacitors are controlled using one of three methods:

- Voltage: The capacitor is switched on when the voltage drops below a certain threshold and off when above a certain threshold. The capacitor controller’s bandwidth must be greater than the step change in voltage caused by the capacitor switching, or else hunting can occur. A VT is required at the capacitors location to measure the voltage.
- Reactive power: The capacitor is switched on and off based upon the reactive power flowing within the branch of the network. A VT and CT are required at the capacitors location.
- Time: The capacitor is switched on/off based upon the time of day. Time switching can only be utilised if the demand profile is predictable. No VT or CT needs to be installed because the control action is based purely on time.

The maximum size of a switched capacitor bank, at a particular location, is limited by the maximum voltage change caused by switching it on or off. Equation (3.12) can be modified by removing the real power component of the equation, because a capacitor produces no real power. The resulting equation that can be used to calculate the approximate voltage change caused by the switching of a capacitor at a certain point λ in the network, is shown in (3.35).

$$\begin{aligned} \Delta V &\approx \frac{X_{\ln.\lambda} Q_{\text{cap}}}{V_{\text{nom}}} \qquad \lambda \le \lambda_{\text{cap}} \\ \Delta V &\approx \frac{X_{\ln.\lambda_{\text{cap}}} Q_{\text{cap}}}{V_{\text{nom}}} \qquad \lambda > \lambda_{\text{cap}} \end{aligned} \tag{3.35}$$

The effect of a capacitor bank on the Eskom distribution network varies depending on the X/R ratio of the particular feeder. The addition of a capacitor bank will probably increase the voltage by 1-4% [17]. The percentage voltage change due to a capacitor switching should be limited based upon how often the switching occurs. Table 3.2 provides indicative rapid voltage change levels.

Table 3.2: Planning levels for rapid voltage change as a function of frequency of occurrence [17]

Number of changes [*r*]	**RVC [%]**
$r \le 1$ per day	6
$1 < r \le 4$ per day	5
$r \le 1$ per hour	4
$1 < r \le 10$ per hour	3

Eskom only makes use of fixed and single stage switched capacitor banks. If various levels of reactive power compensation are required then switched capacitor banks can be placed at different locations along the feeder. Fixed capacitors are usually installed to compensate for minimum load and switched capacitors are used to compensate for the peaks. On feeders with load evenly distributed along the length, a capacitor should be placed approximately 2/3 towards the end of the feeder. Feeder compensation should be considered before substation compensation and if multiple feeder capacitors are needed, they should be placed such that about 50% of the reactive power flows back towards the substation and the other 50% towards the end of the feeder.

3.3 Losses

Losses in a distribution system are affected by a number of variables and are easy to assess with radial power flow. Losses are normally classified into technical and non-technical losses [33]. Technical losses refer to the heat generated from the current flowing through the line. Non-technical losses are a result of theft and meter inaccuracies.

Feeder voltage has an effect on the losses depending on the types of load on the feeder [31]. There are three major kinds of loads. Constant power, constant current and constant impedance:

- Constant power loads will draw reduced current when voltage increases and therefore it will be beneficial to operate the network at the maximum voltage to cause a reduction in losses.
- Constant current loads will change the power drawn with a change in voltage. A variation of the

network voltage causes a negligible change in the losses. It is beneficial for the network operator to run the network at maximum voltage as energy sales will be increased. The increased voltage results in greater energy sales to losses ratio.

- Constant impedance loads will change the power and current drawn with a change in voltage. If voltage is increased, losses will increase as well as energy usage. The energy sales to loss ratio will remain constant. To minimise losses it is beneficial to operate the network at the lowest possible voltage.

The type of load on a particular network should be assessed before any studies are undertaken. The ratio between the three loads will vary between residential, industrial and commercial feeders.

Many of the control methods aim to minimise the losses on the feeder. To minimise the losses, current should be kept to a minimum by optimising the feeder voltage and reducing the reactive power flowing in the feeder.

In PowerFactory the power losses of a feeder are calculated when a load flow is performed. The total energy losses over a period of time can be calculated by running consecutive load flows. Each load flow's calculated losses can be multiplied by the step size for each iteration period and added together. It is easier to compare various network operating scenarios using the total losses rather than instantaneous losses for a single network condition.

For an initial study, the losses can be estimated by using (3.36) assuming that there is a constant voltage along the feeder with equally spaced and sized loads.

$$P_{\text{loss}} = \frac{R_{\text{ln.tot}}}{n}\left(P_L^{\,2} + Q_L^2 + \left(P_L\,\frac{n-1}{n}\right)^2 + \left(Q_L\,\frac{n-1}{n}\right)^2 + \ldots.\left(P_L\,\frac{1}{n}\right)^2 + \left(Q_L\,\frac{1}{n}\right)^2\right) \tag{3.36}$$

P_L and Q_L is the total load of the feeder and n is the number of loads on the feeder. Equation (3.36) can be represented by (3.37).

$$P_{\text{loss}} = \frac{R_{\text{ln.tot}}}{n}\left(P_L^{\,2} + Q_L^{\,2}\right)\sum_{j=1}^{n}\frac{j^2}{n^2} \tag{3.37}$$

The series expansion $\sum_{j=1}^{n} j^2 = \frac{n(n+1)(2n+1)}{6}$ can be used to simplify (3.37) and therefore the per unit losses of a feeder can be approximated using (3.38).

$$P_{\text{loss.ini}} = R_{\text{ln.tot}}\,\frac{P_L^2 + Q_L^2}{n^2}\left(\frac{(n+1)(2n+1)}{6}\right) \tag{3.38}$$

The energy losses of a feeder for a day can be found using (3.39).

$$E_{\text{loss.ini}} = \frac{24}{N}\sum_{i=1}^{N} P_{\text{loss.ini}} \tag{3.39}$$

Where N is the number of sampling periods in a day. For 1 minute resolution there are 1440 sampling periods in a day.

Eskom has a simple way of assessing whether a feeder is economical to operate at a particular load by making use of the economic loading limit for a conductor [29]. The economic loading limit is the maximum load that is economical to operate a particular conductor at for a specific load factor. It accounts for the total life cost of the conductor and includes capital costs, losses and maintenance. If the limit is exceeded, it would be economical to use a thicker conductor. The load factor can be calculated using (3.40).

$$LF = \frac{S_{\text{ave}}}{S_{\max}} \tag{3.40}$$

The line should have an average load less than the economic loading limit, for a particular load factor, and be designed to operate below this level until the seventh year after installation [29]. The economic loading limit is calculated using the typical line capital costs and the forecasted Eskom long run marginal cost of generation. If the load exceeds the economic loading limit, it doesn't necessarily mean that the line should be upgraded. It is mainly a tool that can be used to optimise the additional cost of using a thicker conductor when constructing a new line. DG is expected to reduce the average load and therefore the load factor, but the peak load will remain the same. DG would therefore extend the economic life of a feeder. Figure 3.15 shows the economic loading limit for each conductor as a function of the load factor. This can be used to estimate whether DG will increase or reduce the losses on a particular feeder.

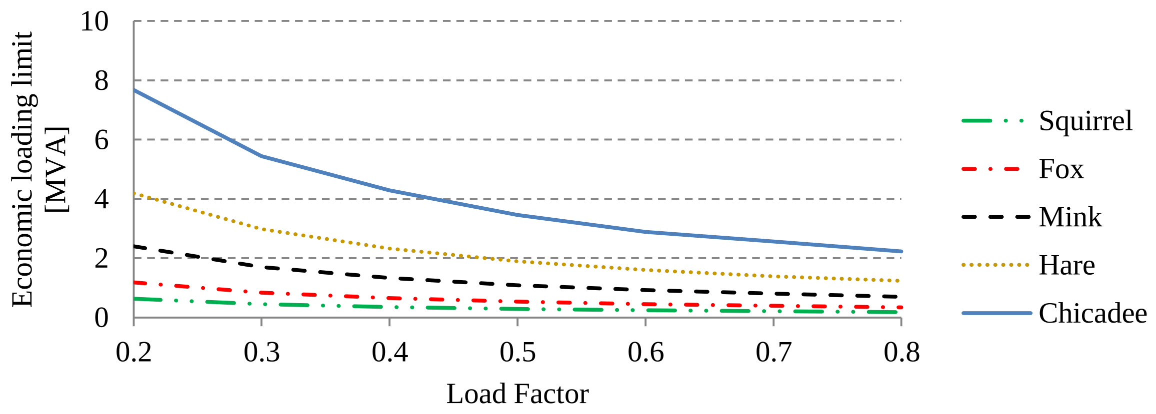

Figure 3.15: Economic loading limit for various conductors operating at 11 kV as a function of the load factor [29]

3.4 Design of the network model

To test various network control methods and to assess the impact of DG on the network, a base network that can approximate a typical Eskom network needs to be developed. It is impossible to cover every feeder design; therefore the various feeder configurations were assessed and combined to create a model that should satisfy most criteria. The model incorporates the devices that are expected to be on the network. The impact of DG can then be assessed using the standard control procedures. The standard control procedures can be compared to various proposed control alterations.

In most studies [6], [33], [39], the MV line lengths were short and conductors with high X/R ratios were used. In these cases, unlike a typical rural Eskom network, the thermal rating of the line is more of an issue than voltage regulation and voltage change.

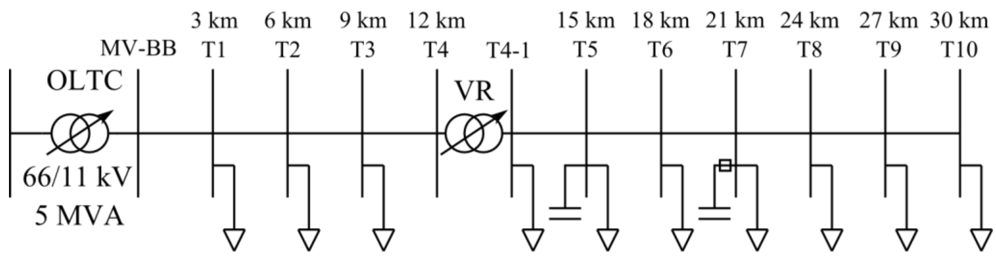

Figure 3.16: Feeder model

The overview of the feeder model is shown in Figure 3.16. This section will cover the thought process and logic used when making decisions about the choice of voltage level, lines, transformers, voltage regulators, loads, power factor and capacitors. The design methodology of the feeder will follow a systematic approach to create a feeder with an optimal voltage profile and minimal losses. Simulations have to be performed at different stages during the design of the network model. These simulations are given in a later section.

3.4.1 Voltage Level

The voltages used in distribution networks are most commonly 11 and 22 kV. In certain cases 33 kV can be used. A model for 11 kV will be made. Typically 22 kV is used when there is a greater load or the lines are longer than 11 kV can cope with. The results obtained on 11 kV will be similar to those obtained on a 22 kV network.

The HV side of the substation will be at 66 kV as this is the most commonly used voltage level to supply substations with lower power levels.

3.4.2 HV Fault level

The fault level of the HV network is specified at 480 MVA because it was found that this value is the average fault level for 66 kV substation busses [2].

3.4.3 Lines and busses

The lines most commonly used on the Eskom network were shown in Table 3.1. The majority of rural distribution lines on the Eskom network in the 11/22 kV range consist of Hare lines for the first 6-10 km, Mink for the next section from 10-30 km and Fox or Rabbit at greater distances from the substation. Chicadee is used in certain cases where there is a large load. Most of the t-offs from the main line are Fox or smaller conductor. Thinner conductors are used further away from the substation to reduce costs, because there is reduced load and lower fault level [29].

The backbone line length varies considerably between different feeders, but is usually between 20-50 km for 11 kV and 30-100 km for 22 kV when measured from the substation. There are exceptions because certain feeders exceed 200 km. Urban distribution lines are typically 5-10 km. A 30 km feeder length is selected for the 11 kV model network with the busses spaced at 3 km intervals. The model uses Hare line for the first 9 km and Mink for the last 21 km.

The voltage variations will correspond well with those experienced on the Eskom network. The small conductors allow for the line to be upgraded for increased loading or generation. These assessments would typically be made by a network planner if the load is predicted to increase in a particular area.

The typical number of feeders at a substation varies from 1 to 4 and in some cases more can be connected to a single bus bar. In this study a single feeder will be investigated.

3.4.4 Loads and power factor

The location and size of loads are difficult to determine as they vary considerably from feeder to feeder, day and time of year. The types of load depend whether the feeder is comprised of industrial, residential or commercial customers. The loads on a feeder can include motors, heating, lighting and power electronics. These can be classified into a ratio of constant power, constant current and constant impedance loads. The majority of small DG will be connected on farmer’s feeders. Farmer’s feeders contain a large amount of induction motors that are used for irrigation and refrigeration. Up to 80% of the load on a farmer’s feeder is induction motor load, with 20% being urban load.

The easiest way to model the entire feeder load, is to distribute it evenly along the feeder and for each load to contain the same ratio of the three load types. There are 10 busses in the 30 km feeder and a load is connected to each bus. In PowerFactory a complex load model can be defined as a ratio of the three load types and induction motor load. The load is modelled as 80% induction motor and 20% constant power, because constant power loads have the greatest impact on the voltage profile. For basic calculations it is assumed that constant power loads are used for simplicity.

The typical load profile of the feeder model is shown in Figure 3.17. The peak load for the 11 kV feeder is 2.5 MW at 21:00 and the lowest load is 0.5 MW at 03:00. Both extremes were not experienced on the same day but these values are used for worst case scenario calculations. The average load during the day is around 1.9 MVA and the feeder operates at an uncompensated power factor of 0.85. The 10 loads are assigned a base value of 200 kVA and are varied based upon the total feeder load. This work focused on a single typical day for analysis and the low load scenario is the lowest load experienced during the year.

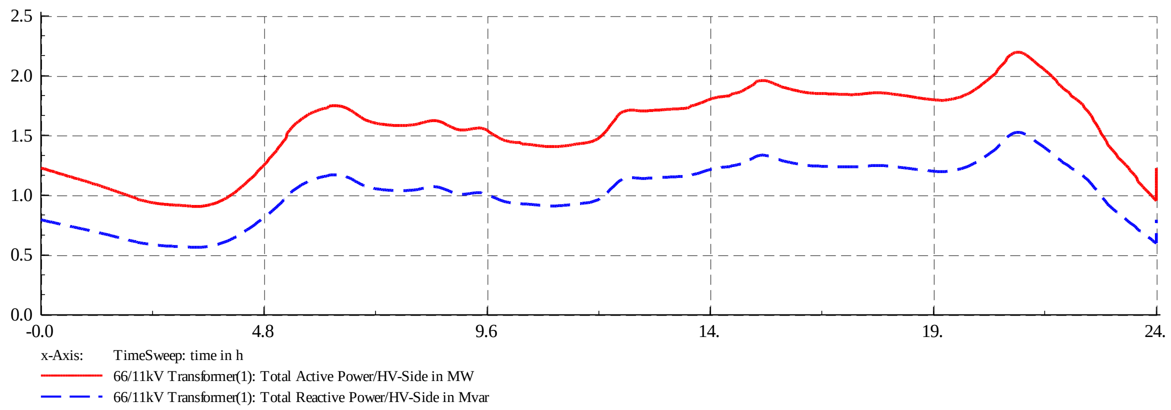

Figure 3.17: Typical load profile of the feeder under study

3.4.5 Transformers and voltage regulators

Transformer size is specified based upon the number of feeders, loading and future load growth expected at the substation. For this study a 5 MVA transformer is selected for the 11 kV model. 5 MVA corresponds to the maximum current carrying capacity of a feeder with Hare conductor at 11 kV. It will provide the worst case voltage regulation because of the higher impedance than a larger transformer. In many cases Eskom is working towards N-1 capability in distribution substations. Parallel transformers will result in a reduced impedance and increased fault current. N-1 capability means that a single piece of equipment can be removed from service and normal operation can be upheld. The single transformer operating between 20 to 50% of its rated load will cause increased voltage changes with a change in load due to the increased impedance and will represent the worst case scenario. Each transformer is equipped with an OLTC that provides ±10% regulation. The transformer has an impedance of 2.1 ohms with an X/R ratio of 9.5. The worst case voltage profile with the OLTC is shown in Figure 3.18 and is generated using (3.18). The worst case voltages are shown for high load and low load. Therefore, the source voltage is at a minimum for high load and a maximum for low load.

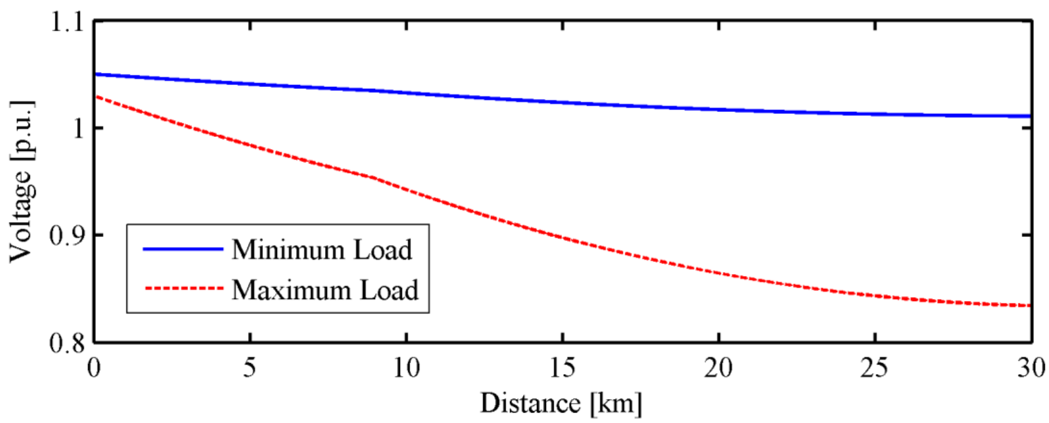

Figure 3.18: Voltage profile of the feeder with an OLTC at the substation

The VRs are connected in open delta to provide +-10% regulation. For the feeder under study, a single voltage regulator did not provide adequate regulation as can be seen in Figure 3.19 and therefore capacitors were also used. The voltage regulator is placed at 12 km in combination with a switched and fixed capacitor as described in the next section. Voltage regulators are placed where the voltage drops to around 0.96 pu under highest load conditions in combination with the capacitors. Some MV feeders do have two VR's but these configurations are not studied in this work.

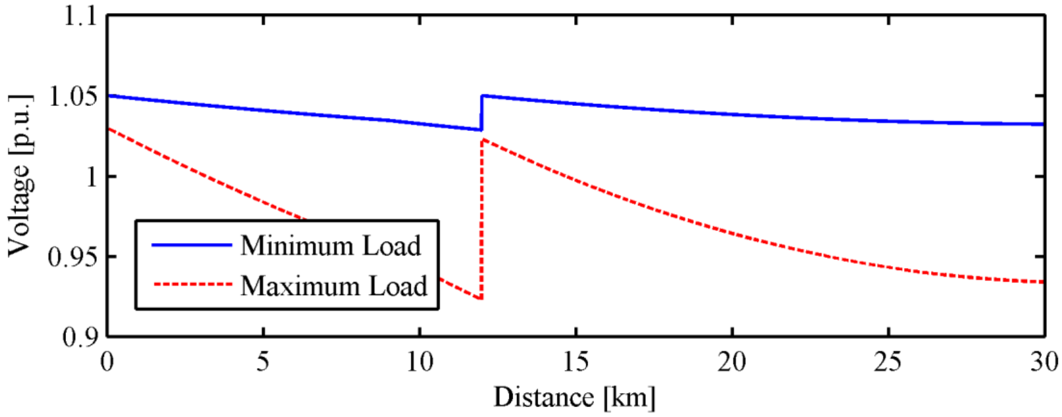

Figure 3.19: Voltage profile of the feeder with an added VR at 12 km

3.4.6 Capacitors

Capacitors are placed by following the Eskom guidelines in [17] and only standard sized capacitors will be used. A simulation of maximum and minimum loading was done to determine the reactive power flow and voltage levels. A fixed capacitor bank is placed halfway down the feeder with $Q = 1.5 \times Q_{\min}$. The feeder voltage profile is assessed at maximum load with the fixed capacitor. It was determined that an additional capacitor is needed, therefore a switched capacitor is placed two thirds down the feeder at the closest standard capacitor size such that $Q_{\text{switched}} < Q_{\max} - Q_{\text{fixed}}$.

For this feeder, the minimum reactive power is 0.3 MVAr and maximum reactive power is 1.55 MVAr. A fixed capacitor bank of 0.45 MVAr is placed halfway down the feeder and a switched capacitor bank of 0.9 MVAr is placed 2/3 down the feeder. The 0.45 MVAr fixed capacitor increases the feeder voltage by a maximum of 2.55%, if the impedance of the transformer is taken into account. The OLTC of the transformer adjusts for any long term voltage changes and therefore the long term feeder voltage change caused by the fixed capacitor is 1.8%.

These values were used as a starting point to minimise the feeder losses. A simulation was done for the typical day and the losses were found to be 2.6 MWh. The load profile was assessed and the maximum reactive power requirement is only for a short period. With a capacitor of 0.9 MVAr the feeder was operating at a leading power factor for most of the day when it is switched on. The switched capacitor banks size was reduced to 0.6 MVAr to provide much better reactive power support for most of the day. The reduced capacitor size resulted in a daily loss of 2.4 MWh and the voltage profile of the feeder is still acceptable. The maximum change in voltage caused by switching the capacitor, before any compensation by the VR or OLTC, is 4.8%

and therefore should be switched fewer than 4 times per day. Once the OLTC and VR have compensated for the capacitors voltage change, the capacitor will change the voltage by 1.5% at its location. The improved voltage profile with the added capacitors is shown in Figure 3.20. The minimum voltage is improved to just above 0.955 p.u.

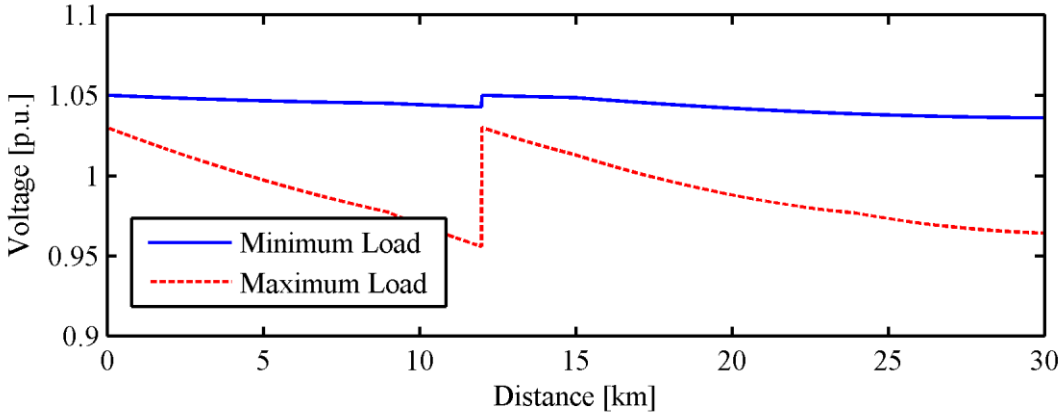

Figure 3.20: Voltage profile of the feeder with the addition of the fixed and switched capacitor

3.4.7 LDC

The effectiveness of using a LDC is evaluated by controlling T1 between 1.03 p.u. and 1.05 p.u. The voltage profile of the feeder with a LDC is shown in Figure 3.21. The substation voltage is controlled to be close to 1.05 p.u., at minimum and maximum load. The voltage profile of the feeder, up until the voltage regulator, is improved when there is high loading because the minimum voltage, with standard OLTC control, at the substation was 1.03 p.u. The VR could be equipped with a LDC, but the control of the switched capacitor would be more difficult, as the voltage variation at its terminals would be reduced.

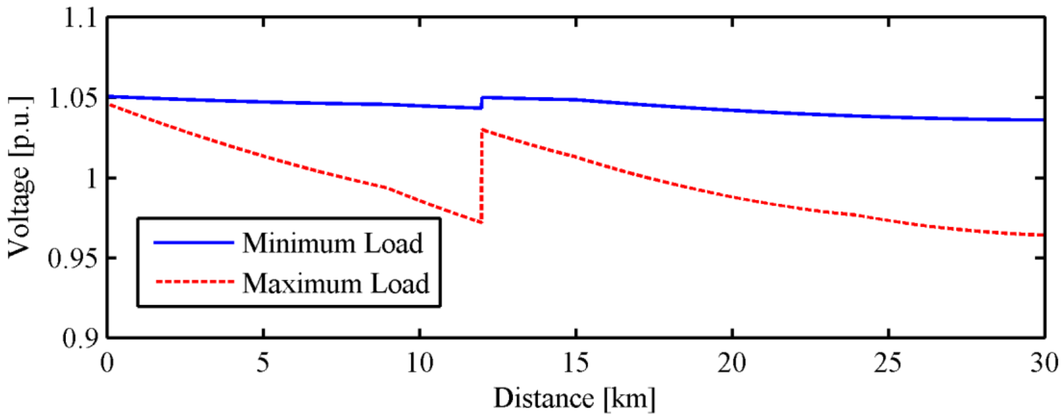

Figure 3.21: Voltage profile of the feeder with the OLTC equipped with a LDC

3.4.8 Limitations

The network model is simplified when compared to a typical distribution network. A real feeder will have many T-offs and sub sections; a variety of load types; unbalanced loading; different sized transformers; different sized loads; loads that are not evenly distributed along the feeder and a greater variety of conductor sizes. The infinite number of network design and operation possibilities, means that the concepts tested on this simplified network will need some engineering analysis when applying them to a real network. For example, if a large percentage of the load is close to the substation, with only light loading towards the end of a feeder, the voltage drop at the end of the feeder will be less than with evenly distributed loads. The basic principles related to the network control and operation will stay the same. New control techniques can be tested on the simplified network to determine the viability and effectiveness, without having to worry about the increased complexity as the principles stay the same.

3.5 Network operation

The control of a classical distribution network involves the proper co-ordination of the OLTC, voltage regulator and feeder capacitors. Normally there is no communication between the devices so they are locally controlled. The theory behind each of the devices as well as the basic control strategies were covered in previous sections, so the coordination of the devices will be covered here. The methods used to co-ordinate each device and the local control strategies are discussed in the Eskom documents [17], [29].

If a feeder incorporates the use of an OLTC and a VR, the controllers should have a different time delay to operate with the minimum number of tap changes. The delay difference between devices should be at least 15 s [37]. A tap change in an upstream regulator affects the entire feeder and might solve the voltage problems experienced at the end of the line. A downstream regulator will no longer need to compensate for the voltage problem and will not tap change [16]. The time delays of the local controller shall be set as $td_{OLTC} < td_{vr1} < td_{vr2}...$ if multiple tap changing devices are installed along the feeder.

There are a variety of distribution system control methods that have different objectives. The various objectives include reduction of OLTC and capacitor switching operations, voltage and reactive power optimisation, flattening the voltage profile, reducing power usage and loss minimisation. These objectives have to be achieved within certain constraints that limit how each can be optimised. The total number of tap changes by a device (*DT*) during a simulation can be calculated using (3.41).

$$DT = \sum_{i=1}^{N} \left| TAP_i - TAP_{i-1} \right| \tag{3.41}$$

Where DT is the total number of tap changes, and *TAP* is the tap position of the device. *N* is the number of simulations that are performed. The total number of tap changes by all devices (*TT*) on the network is calculated by adding each device’s total for the simulation period using (3.42). The VR consists of two transformers that tap change individually, but are considered as a single device.

$$TT = DT_{VR} + DT_C + DT_{OLTC} \tag{3.42}$$

The voltage control equipment needs to be controlled in a manner that allows for optimal control of the network voltage, with the minimum number of switching operations. The test network is a class 3 network and is operated in TZ1. This means the voltage at the substation bus and the voltage regulator should be controlled between 1.03-1.05 p.u. The minimum allowed voltage at any point on the MV feeder during normal operation is 0.955 p.u, but should be controlled closer to the nominal voltage.

As previously discussed, capacitors can be fixed, voltage controlled, time controlled or reactive power controlled. Voltage control is the simplest method to control a capacitor if the time control is not adequate and is the most commonly used. A switched capacitor should only operate when reactive power consumption is high, therefore the set point needs to be suitably adjusted such that the capacitor switches on during periods of high demand and off during periods of low demand. The low X/R ratio of typical distribution networks can cause problems with voltage control systems because the voltage, at the capacitor connection point, is mostly dependant on real power flow. In these cases it is usually assumed that during periods of high demand, reactive power consumption is high.

During periods of high demand and increasing load, the secondary side of the voltage regulator keeps the voltage at the lower limit. The turn on voltage is calculated to be the voltage at the capacitor when the voltage regulator's output is at V_{LB} minus the voltage drop between the VR and capacitor at a certain load. Similarly, the turn off voltage is calculated to be the voltage at the capacitor when the voltage regulator's output is at V_{UB} minus the voltage drop between the VR and capacitor at a certain load. This is demonstrated in Figure 3.22.

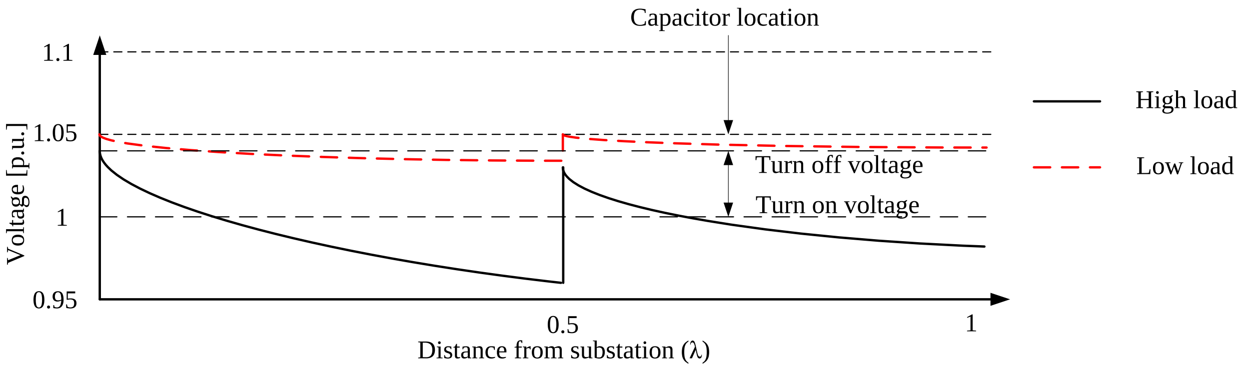

Figure 3.22: Capacitor turn on and turn off voltage calculation

The bandwidth of the capacitor control should be greater than the change in voltage caused by the capacitor switching. The capacitor should be configured to operate before the OLTC and VR so the time delays (*td*) are $td_{cap} < td_{OLTC} < td_{vr1}$. It will directly increase the voltage at the substation busbar and along the entire feeder because of the reduced reactive power flowing though the transformer. The voltage control devices must be properly configured to minimise the number of tap changes. The voltage set points and time delay for each device is shown in Table 3.3.

Table 3.3: Voltage and time delay set point for network control

	OLTC	**VR**	**Capacitor**	**OLTC LDC (3 km)**
V_{UB}	1.05	1.05	1.04	1.04
V_{LB}	1.03	1.03	0.99	1.02
td	45 s	60 s	30 s	45 s

Various network operation strategies are evaluated using the load profile in Figure 3.17. The voltage profile, losses and voltage regulation between minimum load and maximum load are compared between the different network configurations. The results show that the logic and analytical results used in designing the network model provide good results. The results of the simulations are shown in Table 3.4. The total number of tap changes includes the OLTC, VR and capacitor.

Each subsequent simulation makes use of an additional component and the simulations are numbered as follows:

Case 1) OLTC
Case 2) OLTC and VR
Case 3) OLTC and capacitors
Case 4) OLTC, VR and capacitors
Case 5) LDC, VR and capacitors

Table 3.4: Simulation results for various network configurations

Case	V_{min} **[p.u.] Maximum Load**	V_{min} **[p.u.] Minimum Load**	**%VR**	E_{loss} **[kWh]**	E_L **[MWh]**	E_{loss}/E_L **ratio [%]**	TT
1	0.84 (T10)	1 (T10)	16	2620	32.1	8.2	2
2	0.91 (T4)	1.01 (T4)	9.9	3024	34.5	8.7	18
3	0.88 (T10)	1.02 (T10)	13.7	2247	33.8	6.7	2
4	0.956 (T4)	1.03 (T10)	7.8	2427	35.1	6.9	26
5	0.96 (T4 & T10)	1.03 (T4)	6.8	2421	35.2	6.9	28

Case 1 makes use of an OLTC to regulate the substation secondary voltage. The feeder has a poor voltage profile, with low voltages experienced during moderate to high loading. The loss load ratio is high since no reactive power compensation is performed and the voltage regulation is poor. The energy usage is low because the load power has a large dependence on the voltage.

Case 2 adds a VR at 12 km. The simulation showed an improved voltage profile and higher energy usage. The improved voltages along the feeder result in a higher profit per day but the power loss to load ratio increases. The voltage regulation is improved by 50% when compared to case 1.

Case 3 adds a fixed capacitor at 15 km and a switched capacitor at 24 km. The addition of capacitors improves on case 1 by reducing the loss load ratio. The voltage levels are inadequate under high loading as shown by the poor value of the voltage regulation.

The network cannot be operated utilising just one compensation device and therefore a VR and capacitor must be used together. Case 4 combines the OLTC, VR and capacitors. The combination provides an improved voltage profile, voltage regulation and lower losses along the feeder. The method of feeder voltage control in case 4 is typically how feeders are operated. Figure 3.23 shows the voltages at selected busses over a typical day for the feeder. The voltages at each bus are relatively well controlled and fall within a narrow band. As can be seen, the capacitor is on during most of the day when the load of the feeder increases to 1.6 MW for the morning peak and switches off during the period with low load in the late evening. For each operation of the switched capacitor, the VR has to tap change to compensate for the 3% change in voltage caused by the capacitor at the VRs location.

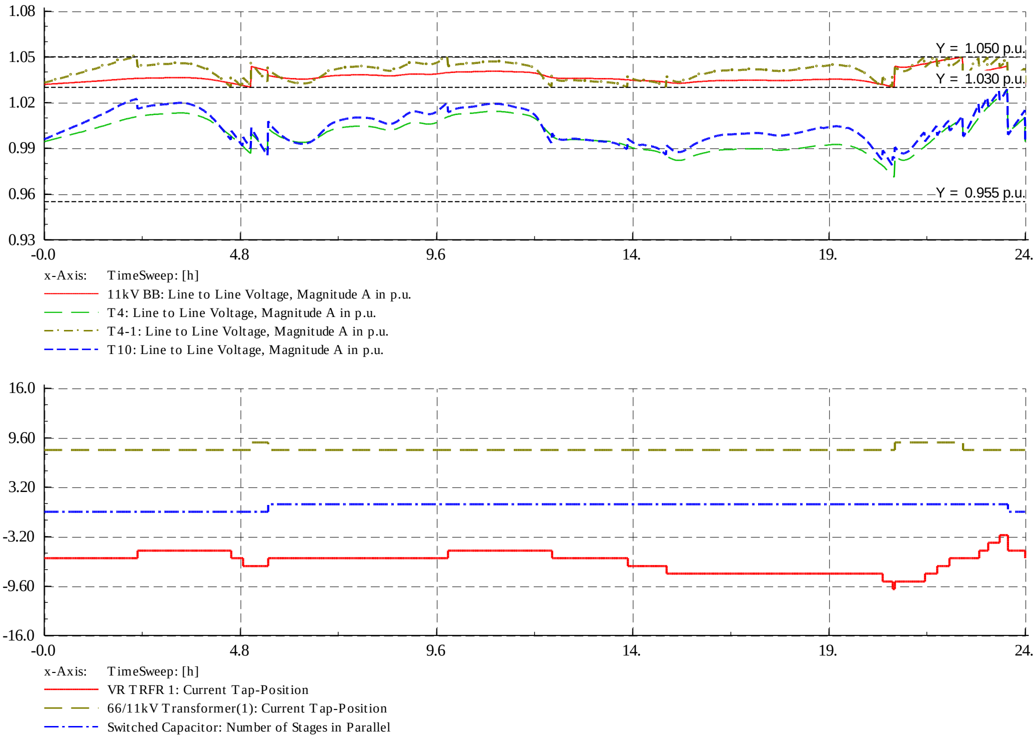

Figure 3.23: Voltages and tap positions of the voltage control devices for case 4

In case 5, the LDC is configured to regulate a point 3 km from the substation. Using the LDC provides a voltage closer to the nominal voltage for the first portion of the feeder during periods of low load. There is only a minor reduction in losses and increase in energy usage. The LDC could increase the number of times the OLTC tap changes per day. It is no longer only compensating for the voltage variations of the HV network and transformer, but also 3 km of the MV network. The LDC causes the VR to tap change less, because the primary side voltage of the VR varies within a narrower band and reduces the compensation required by the VR.

The VR can also be equipped with a LDC, however it conflicts with the capacitor’s control. The voltage at the terminals of the capacitor will never vary enough for the on and off setpoints to be reached. If the VR's LDC is enabled, the capacitor would need to use reactive power control to turn on correctly.

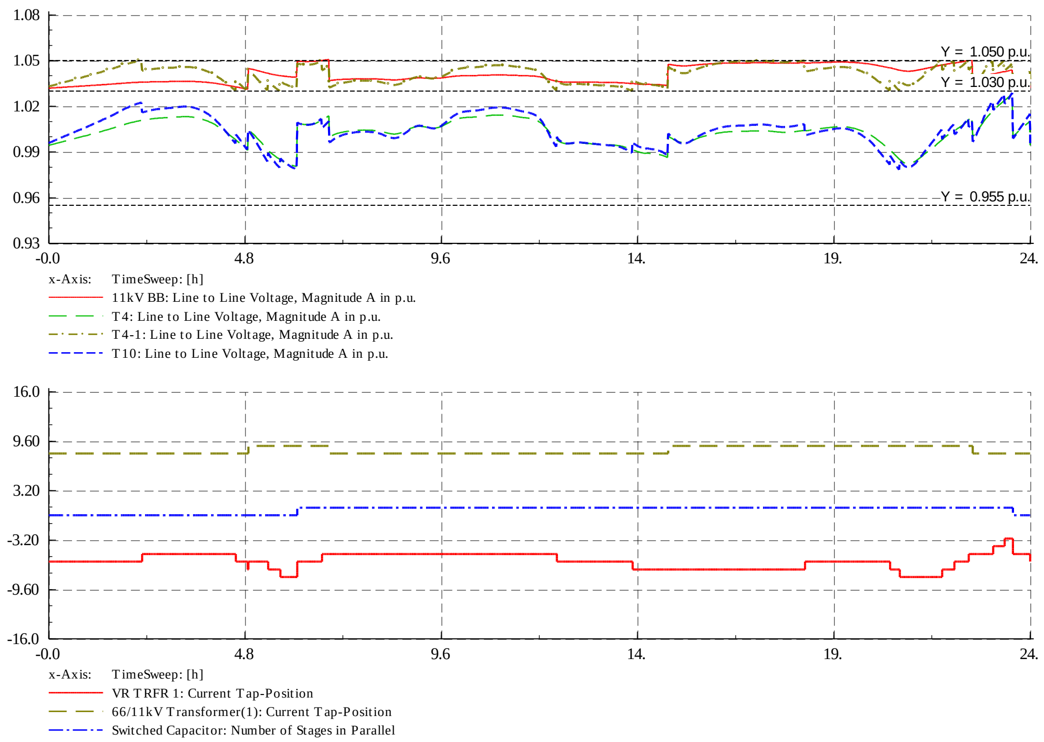

Figure 3.24:Voltage and tap positions of the voltage control devices for case 5

3.6 Conclusion

In this chapter, the method to calculate line parameters and model the lines in simulation software was shown. A rule of thumb method for calculating the voltage drop over a section of line and to calculate the entire feeder's voltage profile was provided.

The basic theory and operation for the different types of voltage control equipment, used on distribution systems, was covered. Models for an OLTC, VR, LDC and capacitor were developed, along with their basic control methods and their effect on a feeder's voltage. The function of each of the components under study was explained at a level relevant for power system studies.

A brief explanation of feeder losses was given. The three load types were compared and changing the network voltage varies the power usage of each load. Optimal network operating conditions were given for each load type. A basic method that can be used to estimate a feeder's losses at a specific load power was given and the concept of the economic loading limit of a conductor was explained.

Finally a test network that aims to include as much of the typical distribution network's characteristics was developed and the method to control it was discussed. A method to calculate the voltage control device's setpoint was discussed. It was found that a suitable method for voltage profile optimisation and loss minimisation made use of all of the voltage control devices discussed in this chapter. The typical losses of the feeder, for a standard day, was found to be about 2400 kWh and the daily tap changes, for all voltage regulation devices, was 26.

4 Distributed generation on conventional distribution systems

In this chapter the influence of distributed generation on conventional distribution systems is investigated. The influence of PV plant size is investigated to determine if a PV plant could cause flicker. Geographically dispersing multiple plants is investigated to see how the average power fluctuation is affected and the influence on the expected number of tap operations. The maximum penetration level for DG connected to the base network model is found. Issues that could arise with feeder reconfiguration and the influence of DG on voltage control equipment is shown.

4.1 Introduction

The main purpose of DG is to produce active power and inject it into the grid. Ideally the control method should maximise the amount of active power generated. It should also maintain good power quality, grid stability and reduce the losses. In this chapter steady state voltage control limits will be assessed to determine the long term impact on the grid. Steady state implies that the power system is operating in a fixed, stable condition. The worst case loading or generation cases that will seldom occur will be assessed and the maximum DG penetration level limited by these cases will be provided.

Natural variation of DG power output caused by clouds passing overhead is investigated. The active power output could vary between 20% and 100%, over a period of several seconds to minutes. The frequency and rate of change of the solar irradiation can cause increased wear on voltage regulators and tap changers [39]–[41]. The increased wear is one of the reasons for the 1% voltage variation limit specified by EPRI [10].

A PV plant acts as a low pass filter for irradiance changes, measured at a single point of the PV plant, and the plants power output for small time scales (<20 s). The time required for a cloud to move over all the panels can take several seconds and the power output will not drop instantaneously [42]. Multiple PV plants that are spaced a few kilometres apart have a similar power smoothing effect over longer time scales. The net output power of all the PV plants combined varies less than that of a single plant, due to the effect of geographical dispersion [43].

4.2 Photovoltaic power generation modelling

4.2.1 PV model

Photovoltaic generators can be modelled using a static generator in PowerFactory. The generator is modelled such that it meets the grid code requirements. PV power output fluctuations need to be modelled so that the dynamic impact on the grid by a PV plant can be assessed.

4.2.2 Recorded Solar profile

The solar profiles used in these simulations were recorded on a sunny and a cloudy day. The sunny day was recorded at Stellenbosch on 16/12/2012 and the cloudy day was recorded at Stellenbosch on 15/12/2012. The solar profile was recorded as solar irradiance in W/m² at a single point and converted to a per unit power output with a base the size of the PV plant installed. The data has a resolution of one minute. The normalised power output of the PV plant assumes that the peak output, at 1000 W/m², corresponds with rated output of the plant and that the peak DC rating of the panels has been adjusted suitably for the temperature of the location. Most PV plants operate with a DC to AC power ratio of 1.2-1.3 to compensate for the de-rating of the panels and other losses in the plant [42]. Figure 4.1 shows the power output over a day if the solar plant has fixed PV panels. The power output steadily rises until about noon and then steadily falls without having a period of relatively constant output.

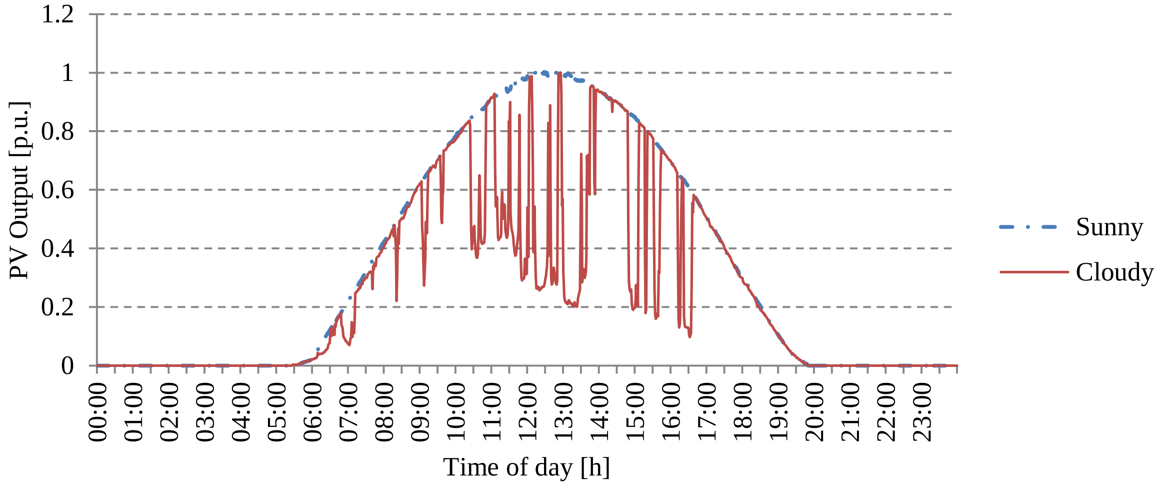

Figure 4.1: Power output of PV plant with fixed solar panels

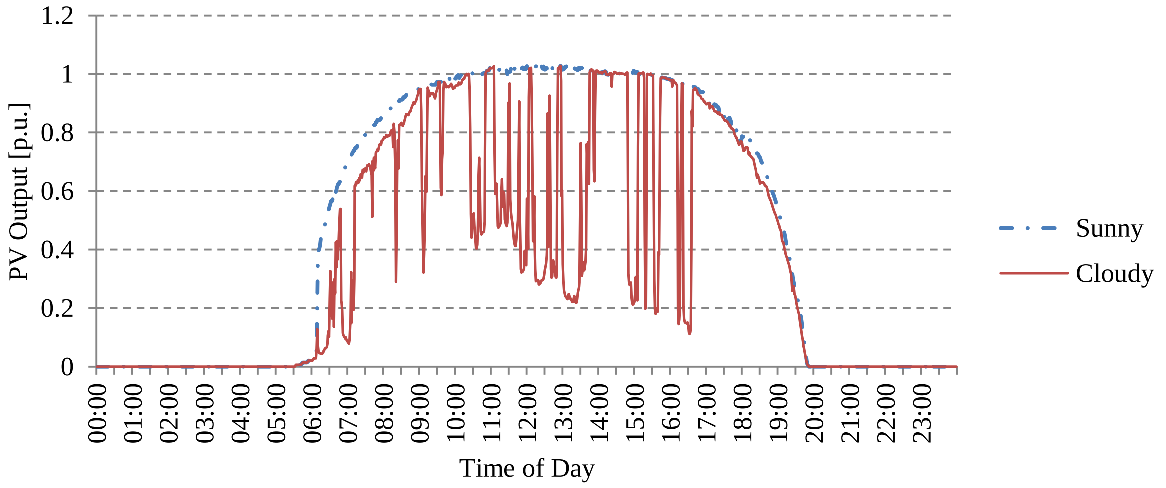

Figure 4.2: Power output of PV plant with solar tracking panels

In these simulations it is assumed that the panels will have solar tracking built in and the profile is shown in Figure 4.2. It is evident when comparing Figure 4.1 and Figure 4.2 that the solar tracker provides substantial gains in energy output over the period of a day. Solar tracking is more economical in locations with a high solar irradiance such as South Africa where there are greater returns on investment; due to the increased cost of building the solar tracker. A solar tracker can provide 30-40% more energy than the fixed axis solar panel [44].

4.2.3 Plant size

The size of a PV plant has a large influence on the rate of change that its output power varies. Clouds that move over a PV plant will block the sun and reduce the irradiance on a PV panel. The rate that the power output of a plant changes depends on how quickly the sun covers all of the panels. The time taken for a cloud to cover a PV plant depends on the area of the plant and the speed that the cloud is moving. Thus, a PV plant acts as a low pass filter for short time scales when the change of irradiance is measured at a single point and compared to the instantaneous power output change of the plant. High risk days for power fluctuations are ones that are partly cloudy with high wind speeds [12]. In [42] an equation (4.1) was developed to relate the area of the plant to the low pass filter cut off frequency. The equation was developed from a year's recording of irradiance related to output power.

$$f_c = 0.021.A^{-0.5} \text{ [Hz]} \tag{4.1}$$

Where f_c is the filter cut off frequency and A is the area of the plant in hectares.

From the cut off frequency, a transfer function (4.2) was developed for an entire PV plant that relates the normalised irradiance to the power output [42].

$$G(\alpha,\beta) \rightarrow \boxed{\frac{K}{\frac{1}{2\pi f_c}s+1}} \rightarrow P \tag{4.2}$$

Where G is the measured irradiance of the sun, normalised to 1000W/m² in p.u., at a vertical angle α and horizontal angle β; K [m²] is the energy gain of the plant that relates the transformer power to the irradiance (P_{trfr}/G) and P is the output power of the plant in p.u. The low pass filter effect is only significant for periods less than 20 seconds with a declining influence up to 1 minute, except for very large PV plants.

The plant peak power output can be related to the area by assuming that the power per area is around 180-220 kWp/ha. The simulated response of different plant sizes was compared in [12] to the actual recordings at multiple PV plants in Spain. In most cases the results corresponded, but the authors found that a small PV plant of 48 kWp could, in extreme cases, change its power output by 80% over 2 s. The simulated maximum change over the same period is only 30%. Thus, modelling the plant as a low pass filter adequately determines the average power fluctuations in RMS simulations; however, more detailed studies are required to determine the instantaneous maximum power change for a PV plant. The smoothing effect of PV plant size is limited when observing power fluctuations over a time scale greater than 20 s. The clouds have enough time to cover the entire plant over the longer periods and the power output would be more directly related to the instantaneous irradiance [45]. The maximum power change of a PV plant cannot be calculated using (4.2) with a step change in irradiance, so a more general equation (4.3) can be used to determine the maximum power fluctuation that falls within the 99th percentile [43].

$$99^{th}\left[\Delta P_{\Delta t,1}\right]=b.A^{-c}, \quad b,c>0 \tag{4.3}$$

The values of *b* and *c* for different sampling periods are shown in Table 4.1.

Table 4.1: Parameters values for *a*, *b* and *c;* as calculated in [43] for different sampling periods, that are used to calculate the maximum power change

Δt	*a*	*b*	*c*
1 s	0.77	25.55	0.49
5 s	0.75	64.09	0.29
20 s	0.71	88.2	0.11
60 s	0.63	91.6	0.05
600 s	0.46	94.07	0.02

Equation (4.3) was developed from data recorded in Spain and the results obtained by the equation were verified with data recorded in Hawaii [46]. The calculated maximum power fluctuations were found to be very similar for vastly different locations. The maximum power change for a certain time period is shown in Figure 4.3.

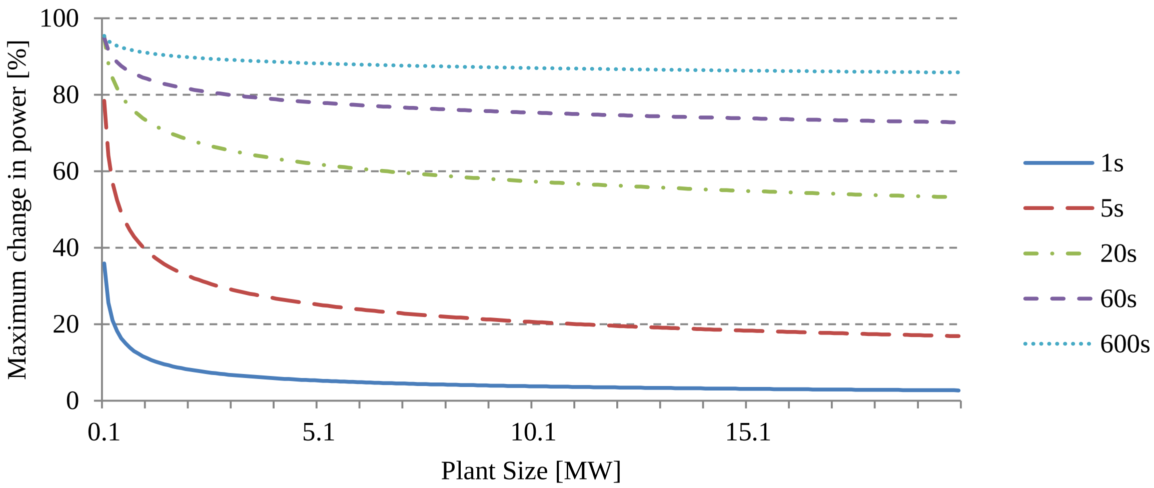

Figure 4.3: Maximum power change that falls within the 99th percentile, for single PV plants, from 0.1 to 20 MW over different time scales

As can be seen by the figure, the plant size has only a minimal effect in smoothing the PV plants output power, for periods greater than a minute. The maximum expected power change that can occur over a 60 s time period is about 73% for a 20 MW plant and up to 85% over 600 s. Plants with a size greater than about 2 MW do not dramatically reduce the maximum expected power change further for the short time periods.

The maximum power change that falls within the 90th percentile can be calculated using (4.4) [12]. The 90th percentile power changes will have more of a direct impact on power quality as they will occur more frequently.

$$90^{th}\left[\Delta P_{\Delta t}\right] = 90\%.\left(1-e^{-0.24.\Delta t}\right).A^{-c} \tag{4.4}$$

The low pass filter effect needs to be simulated when performing RMS and EMT simulations, for example in a flicker study, but becomes negligible when performing load flows with an interval of one minute or more. For simulation periods greater than a minute the power output of the plant would have reached its steady state level. For load flows with time periods between 1 and 10 minutes, the geographical location of multiple plants needs to be considered.

4.2.4 Geographical dispersion

It was shown in the previous section that the size of the PV plant can smooth output power variations for a small time scale. The time scale for the power smoothing effect can be increased if there are multiple PV plants, as the distance between multiple PV plants can smooth out power fluctuations over a greater time scale. The reason for this is that multiple PV plants situated a few kilometres apart are not influenced by the same clouds at the same time. It will take a while for a cloud to move from one PV plant to another. A cloud moving at a relatively fast speed of 60 km/h takes one minute to travel one kilometre. To put that into perspective, a cloud will cover a square area of 1 ha within 10 s under the same circumstances. In most cases, the wind speed will be substantially slower than this and the clouds will take a longer period to cover the same area.

On a permanently overcast day, the clouds will lower the output of all PV plants in an area. On a partly cloudy day, a PV plant in one location could be in full sun and another a few kilometres away could be in the shade. A distance of 6 km between two PV plants was shown to provide similar power output smoothing over a period of 600 s to two PV plants spaced hundreds of kilometres away [12]. It should be emphasised that the smoothing for plants spread out over a geographical area extends beyond long sampling times of 600 s. The combination of plants grouped together were shown to have no effect on the magnitude of the smoothing and only the number of plants considered mattered. Increasing the number of PV plants on a system smoothed out power variations substantially and it was found that if 100 plants were installed in a geographical area, the addition of more plants did not reduce the total power fluctuations further [12].

The results of the research in [12] imply that it is better to install multiple smaller plants distributed over a geographical area than a single large plant with the same power output. A large plant will act as a low pass filter for short time periods, but multiple plants will act to reduce power fluctuations over a greater length of time.

The estimated maximum power change that falls within the 99th percentile can be calculated for multiple plants using (4.5) [12].

$$99^{th}\left[\Delta P_{\Delta t,N}\right]=99^{th}\left[\Delta P_{600,1}\right].\left(1-e^{-0.24.\Delta t}\right).A^{-c}.N^{-a} \tag{4.5}$$

Where N is the number of PV plants and a and c can be found in Table 4.1. Using (4.5), the maximum power change of many plants over a time period can be calculated. Therefore, the maximum expected voltage change caused by multiple plants can be approximated. Figure 4.4 shows how geographical dispersion greatly reduces the maximum expected power output changes for 0.1 MW PV plants over all time periods. The most notable reduction is for a period of 600 s where the power change is reduced from 96% for a single plant to 34% for 10 plants and is less than 20% for more than 32 plants.

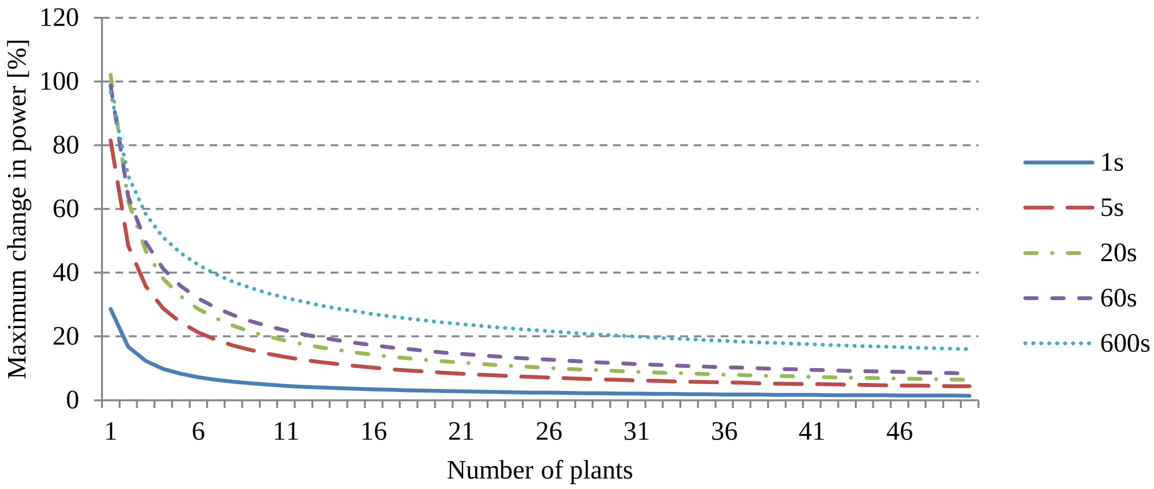

Figure 4.4: Maximum power change that falls within the 99th percentile for multiple 0.1 MW PV plants

The solar profile used to calculate the power output, of a PV plant in Figure 4.2, is calculated from the reading of solar radiation at a single point. On a real distribution feeder, the solar radiation will vary from point to point and the variation will be spread out over several minutes. On the test feeder, the plants are spread out over a distance of 30 km. This distance is small enough that on a permanently cloudy day, the output power of the entire fleet will be reduced and on a partly cloudy day, the power output of each plant will vary independently. The days where the output power of the entire fleet is high or low are not a major concern, as the voltage will not vary substantially and the feeder will operate as normal. The days that are cloudy will cause many power fluctuations and hence voltage variations, that could put network equipment under strain.

4.3 Voltage along a radial feeder with DG

The effect of DG on the voltage profile is investigated in this section. A basic substation, line and load model with a DG is shown in Figure 4.5. The DG reduces the current flowing through the line and therefore affects the voltage drop. DG can be modelled as a negative load if it operates at a fixed power and power factor.

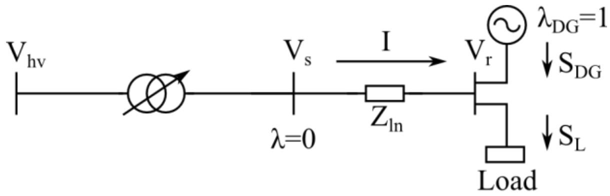

Figure 4.5: Basic line model with DG connected to the load bus

The voltage drop along the line can be calculated similarly to (3.12). The DG's real and reactive power is included in (4.6).

$$\Delta V \approx \frac{R_{\ln}\left(P_L - P_{DG}\right) + X_{\ln}\left(Q_L - \left(\pm Q_{DG}\right)\right)}{V_r} \tag{4.6}$$

As shown by (3.12) and (4.6) the DG causes an increase in the voltage at the POC and hence influences the voltage along the entire feeder. It is possible for DG to improve the voltage profile of a feeder if a limited amount is connected. If too much DG is connected to a feeder, over voltages can occur and the voltage profile can be negatively impacted. DG can either raise or lower the voltage depending on the X/R ratio of the line and amount of reactive power it generates or absorbs.

The change in the voltage magnitude at a point λ, caused by a generator installed at λ_{DG}, can be calculated using (4.7). The long term change in voltage, calculated in (4.7), can be added to the voltage, calculated in (3.17), to get the new voltage profile.

$$\begin{aligned} \Delta V &\approx \frac{R_{\ln.\lambda} P_{DG} + X_{\ln.\lambda} Q_{DG}}{V_{\text{nom}}} & \lambda \leq \lambda_{DG} \\ \Delta V &\approx \frac{R_{\ln.\lambda_{DG}} P_{DG} + X_{\ln.\lambda_{DG}} Q_{DG}}{V_{\text{nom}}} & \lambda > \lambda_{DG} \end{aligned} \tag{4.7}$$

The instantaneous change in voltage caused by the sudden disconnection of a generator can be calculated by including the source resistance and reactance, R_{source} and X_{source}, as shown in (4.8). The source resistance and reactance includes the network impedance and the impedance of the substation transformer.

$$\Delta V_{RVC} \approx \frac{R_{\text{source}} P_{DG} + X_{\text{source}} Q_{DG}}{V_{\text{nom}}} + \frac{R_{\ln.\lambda_{DG}} P_{DG} + X_{\ln.\lambda_{DG}} Q_{DG}}{V_{\text{nom}}} \tag{4.8}$$

The ΔV_{RVC} of the generator, calculated in (4.8), is known as the rapid voltage change (RVC) level of the generator. The term RVC can be defined here as the maximum variation of voltage, that will occur at a point along the feeder, when DG is suddenly added or removed. If DG causes a 3% RVC upon connection, the voltage at the POC and the voltage towards the end of the feeder will rise by 3%, before any control action has been performed by an OLTC or VR [47].

Another one of the constraints that limit the amount of DG that can be connected to a feeder is the voltage headroom at minimum load. The concept is shown in Figure 4.6.

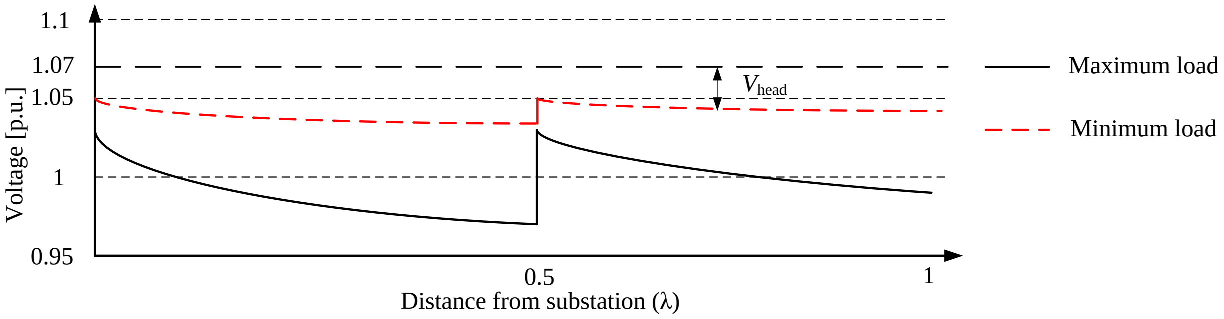

Figure 4.6: DG voltage headroom

The maximum amount of generation that can be installed at a point on a feeder, when limited by the voltage headroom (V_{head}), can be calculated by rearranging (4.7) to get (4.9).

$$P_{DG.\max} = \frac{\Delta V . V_{\text{nom}} - Q_{DG} X_{\text{ln}.\lambda}}{R_{\text{ln}.\lambda}} \tag{4.9}$$

Where ΔV can be substituted with V_{head} and can be calculated using (4.10).

$$\begin{aligned} V_{\text{head}} &= V_{\max} - V_{UB} - \Delta V_{L.\min} \\ &= V_{\max} - V_{UB} - \frac{R_{\text{ln}.\lambda} P_L + X_{\text{ln}.\lambda} Q_L}{V_{\text{nom}}} (1 - 0.5\lambda) \end{aligned} \tag{4.10}$$

By substituting (4.10) into (4.9) it is possible to estimate the maximum DG size at minimum load when limited by the voltage headroom using (4.11).

$$P_{DG.\max} = \frac{\left(V_{\max} - V_{UB} - \frac{R_{\text{ln}.\lambda} P_L + X_{\text{ln}.\lambda} Q_L}{V_{\text{nom}}} (1 - 0.5\lambda) \right) V_{\text{nom}} - Q_{DG} X_{\text{ln}.\lambda}}{R_{\text{ln}.\lambda}} \tag{4.11}$$

The calculation of $P_{DG.\max}$ assumes that the load is evenly distributed along the feeder.

If a VR is installed along the feeder, the voltage headroom beyond the regulator is increased and can be calculated using (4.12).

$$P_{DG.\max} = \frac{\left(V_{\max} - V_{UB} - \left(\frac{R_{\text{ln}.\lambda} P_L + X_{\text{ln}.\lambda} Q_L}{V_{\text{nom}}} \right) (1 - 0.5\lambda) + aTAP \right) V_{\text{nom}} - Q_{DG} X_{\text{ln}.\lambda}}{R_{\text{ln}.\lambda}} \tag{4.12}$$

If the $P_{DG.\max}$ calculated in (4.12) is greater than the $P_{DG.\max}$ calculated at the VR location, then the maximum DG power that can be installed is limited by the voltage headroom at the VR.

Voltage rise and RVC are the main limiting factors for DG connection on long lines. On short lines or lines with a large amount of distributed generation, placed close to the substation, the current carrying capacity can be exceeded before the voltage regulation limitations are exceeded. The definition of a long or short line varies for the type of conductor, voltage level and current carrying capacity. Figure 4.7 shows a guideline voltage drop per kilometre for the lines listed in Table 3.1. The line voltage is 11 kV and the load is increased from zero to the rated apparent power of the line using a power factor of 0.975. The power transfer for a specified voltage drop can be doubled when referring to a 22 kV line.

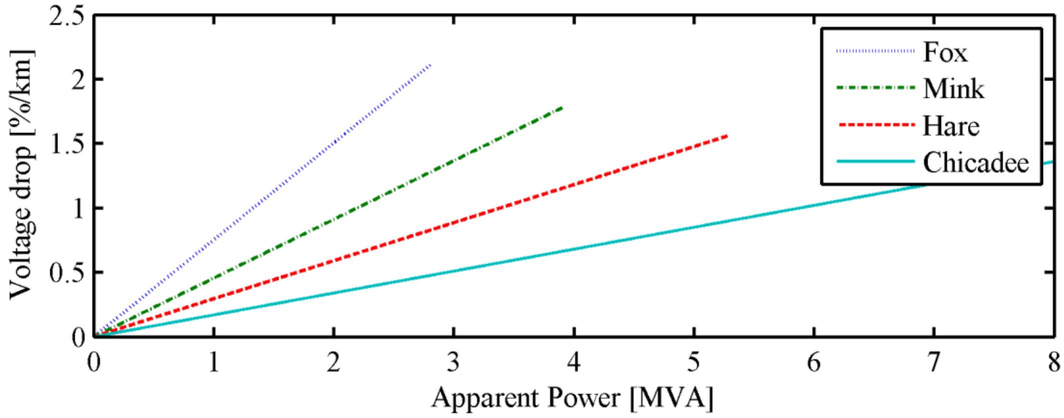

Figure 4.7: Voltage drop per kilometre as a function of apparent power for various conductors

It is easy estimate the voltage drop from the graph for a particular conductor and load. For example on a network with Hare conductor at 11 kV, the difference in voltage between a DG and substation will be approximately 2.4% if the DG is situated 3 km from the substation and generates 3 MVA. The graph provides a simple graphical method to get a basic idea of how much load or generation can be situated a certain distance away from the substation.

4.4 Maximum DG penetration level

The following maximum penetration levels are specified for the 11 kV feeder model that was developed in the previous chapter. The aim of this section is to provide an upper bound of the DG penetration that satisfies the constraints. The estimated RVC and voltage headroom, at the steady state limit of DG penetration, will be used to evaluate the amount of DG that can be installed at a point. The DG penetration level can be calculated using (4.13).

$$PL_{DG} = \frac{P_{DG}}{P_{L.\max}} \times 100 \quad [\%] \tag{4.13}$$

Where PL_{DG} is the DG penetration level and $P_{L.\max}$ is the maximum load of the feeder. The effectiveness of the voltage regulation methods will be assessed in the next chapter by comparing the increase in penetration to the base penetration level defined here. The base penetration level is taken as the point where adding more generation to the feeder causes one of the constraints to be exceeded. The base penetration level assumes the DG operates at unity power factor and no modifications to the control of OLTCs, VRs or capacitors have been made.

There are three main constraints that will be assessed when determining the steady state penetration level of a feeder:

1. The maximum current carrying capacity of a line at a certain temperature
2. The maximum and minimum voltages of the feeder
3. The maximum rapid voltage change level

According to the NRS048-2-2008, the maximum voltage for both MV and LV, for two consecutive 10 minute intervals, is 110% of the nominal voltage. The minimum voltage, that a low voltage event is defined, is 85% of the nominal voltage. In practice, the voltages should be limited by the compatibility level and for MV is within ±7.5% of the nominal voltage during normal operation. In the previous chapter the voltage limits of feeders with DG were discussed and are allowed to reach a level of 2% above the maximum tap zone voltage. The maximum 2% voltage rise can only occur during minimum load and maximum generation conditions; providing the combination occurs for less than 5% of the year [27]. With PV generation, the peak occurs around midday and the load at that time on a farmer's feeder is usually not at a minimum, however, for this work the penetration is limited by the voltage rise at minimum load.

The maximum DG penetration that is based on the above rules is shown in Figure 4.8. The maximum DG size is shown based upon the rapid voltage change, calculated using (4.8); and the voltage headroom, calculated using (4.11) and (4.12). In this case the DG is operating at unity power factor.

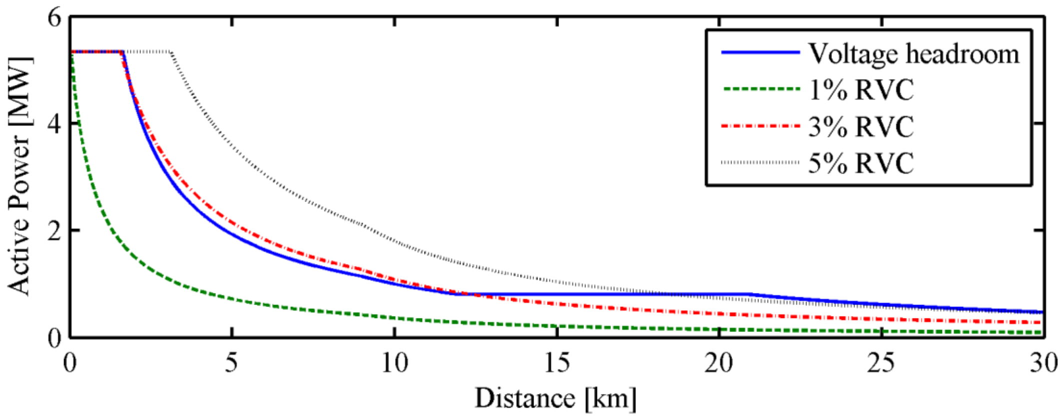

Figure 4.8: Maximum DG size as a function of distance from the substation for the base feeder model

Figure 4.8 shows the EPRI and Eskom RVC limit of 1% and 3% for fluctuating DG; and the Eskom/EPRI RVC limit of 5% for DG with a controllable energy source. The 3% RVC limit, suggested by Eskom, is more lenient than EPRI's, but this limit will need to be assessed. The 5% RVC limit for DG allows for a high penetration level and voltage rise issues can be a greater concern. At a 3% RVC limit, both the voltage rise and the RVC are the limiting factor, depending on the location of the feeder. The voltage rise limits DG penetration up to 12 km from the substation and after that RVC limits penetration.

If multiple DG plants are connected to a feeder then (4.14) can be used to calculate the total RVC at the end of the feeder (ΔV_{tot}) by summing up each individual plants change in voltage (ΔV_k) for each bus that DG is connected.

$$\Delta V_{\text{tot}} = \sum_{k=1}^{n} \Delta V_k \tag{4.14}$$

A simulation is done to investigate the impact of DG sizing, based upon the number of units installed and the units' position on the feeder. There is a detailed description of the algorithm in the appendix. The base penetration level for each scenario is shown in Table 4.2. The DG size is the total amount of DG installed along the feeder. The OLTC and VR are set to regulate the voltage to 1.05 p.u. This is done to limit the influence of the controller bandwidth, on the voltage of the feeder between simulations and assumes the maximum voltage that can be experienced at the substation busbar. The maximum DG penetration level is specified as the point where: the voltage at any point of the feeder exceeds 1.07 p.u.; or the current exceeds the thermal rating of the line; or the RVC level for an individual generator exceeds 3%. In practice, the voltage at the substation will fall between the regulation bandwidth and the load will not be at a minimum when the generation is running at full power. Therefore the upper voltage limit is assessed for the worst case scenario. The different placement cases are defined below:

Case 1) DG is placed 3 km from the substation at T1 (Single DG - Figure 4.9)

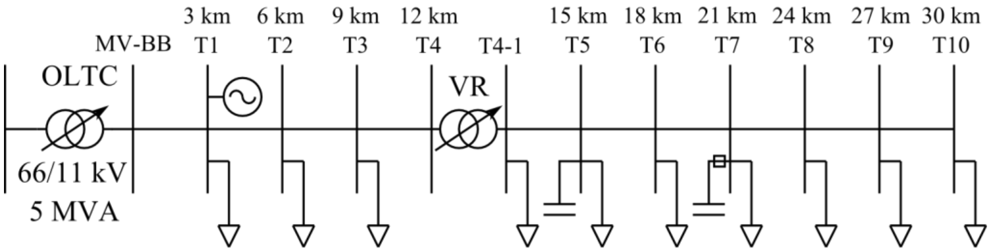

Figure 4.9: Feeder model for case 1

Case 2) DG is placed midway along the feeder at T5 or 15 km (Single DG - Figure 4.10)

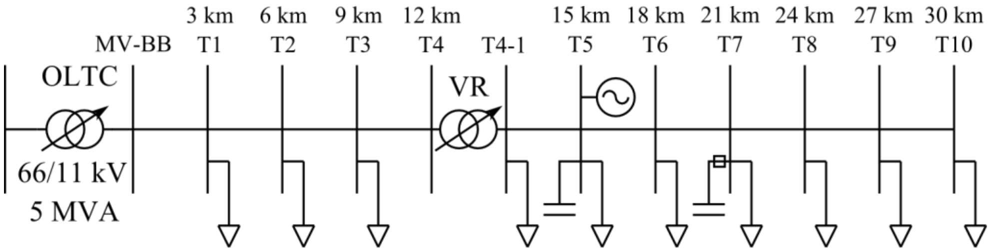

Figure 4.10: Feeder model for case 2

Case 3) DG is placed at the end of the feeder at T10 or 30 km (Single DG - Figure 4.11)

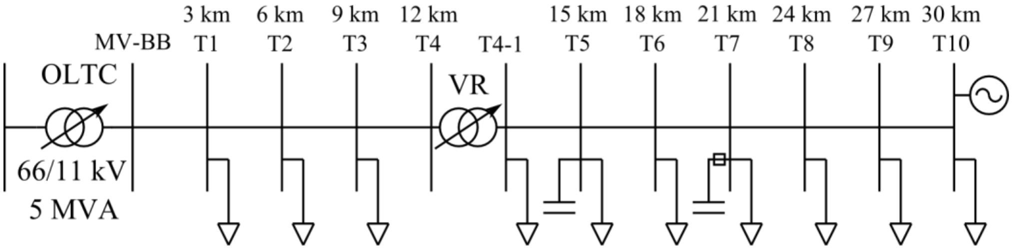

Figure 4.11: Feeder model for case 3

Case 4) DG is placed at all terminals and equally sized (Ten DGs - Figure 4.12)

Case 5) DG is placed at all terminals and sized such that the voltage change caused by each unit is equal (Ten DGs - Figure 4.12)

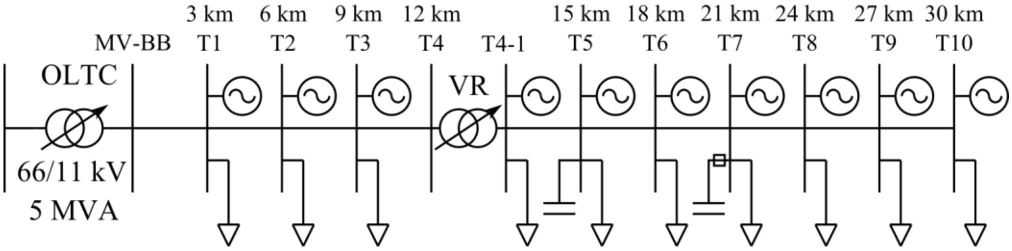

Figure 4.12: Feeder model for case 4 and 5

The maximum DG size is calculated using the minimum load, maximum generation scenario. The losses and daily number of tap changes are calculated using the load profile for a clear day, as shown in Figure 4.2.

Table 4.2: Base DG penetration level for different DG locations on a clear day

Case	P_{DG} **[kW]**	**Limiting factor**	$V_{\max}$ **Terminal**	$V_{\max}$ **[p.u.]**	ΔV_{tot} **[%]**	E_{loss} **[kWh]**	TT	PL_{DG} **[%]**	**Increase DG [%]**
1	3425	OV T1	T1	1.07	2.6	2443	36	137	N/A
2	686	RVC	T4	1.064	3	1721	30	27	N/A
3	300	RVC	T10	1.06	3	1917	26	12	N/A
4	1090	OV	T4	1.07	5.2	1640	32	44	N/A
5	1570	OV	T4	1.07	4.26	1750	32	63	N/A

The results obtained in Table 4.2 provide an outlook into the different DG placement methods and confirm the results obtained in Figure 4.8. It is evident that DGs should be connected close to the substation to maximise installable capacity and to limit RVC. The only simulation where the RVC level is not the limiting factor for a single DG is in case 1. Due to the relatively flat voltage profile at low load, the voltage headroom limits the DG size until RVC becomes the limiting factor after T4. When DG is spread out along the feeder, the total DG voltage change is acceptable for each individual plant, but the total voltage change combined is greater than the 3% limit. This implies that the further away DG is connected from the substation, steady state voltage problems become less of a concern and dynamic output fluctuations need to be investigated further.

The daily losses in all cases, except case 1, are reduced when compared the case with no DG. The line in case 1, between the substation and DG, carries more current with the added DG and the current flow beyond the DG connection point is unaffected. The DG equally sized at all terminals resulted in the lowest losses because the power supplied by the DGs supply most of the local load.

4.5 Effect on voltage variations and tap changes on cloudy days

The operation of the feeder, with DG on a clear day, does not dramatically increase transformer tap changes and voltage fluctuations on the feeder. The life of the VR could be reduced by about 15% based upon the percentage increase in tap changes. This is evident when comparing results between Table 3.4 and Table 4.2. To assess the maximum recommended voltage change level for multiple DGs on the same feeder, the operation of the feeder on a partly cloudy day must be investigated. The effect that geographical dispersion has on smoothing net voltage fluctuations will be investigated.

Two scenarios are compared for case 4. In case 4a, the voltage fluctuations experienced along the feeder are shown if all of the DGs output power varies at the same time, according to the cloudy profile in Figure 4.1. The second case 4b includes the effect of geographical dispersion. To simulate the effect of geographical dispersion, the output power of each DG is randomly offset, between -10 and 10 minutes, from the base profile. It would be expected that the variations would be over a greater time period on a real feeder, but actual recordings will be necessary to confirm this. A conservative value of 20 minutes should show worst case scenarios for power output change on a cloudy day over a distance of 30 km.

Table 4.3: Voltage fluctuation percentage and number of tap changes on a cloudy day

Case	**Average voltage fluctuation [%]**				***DT***			**E_{loss} [kWh]**	**Q-gen [kVAr]**
	MV BB	T4	T4-1	T10	OLTC	VR	Cap		
1	0.29	1.22	1.23	1.37	4	58	2	2342	0
2	0.2	1.14	1.14	1.49	4	56	2	1860	0
3	0.14	0.68	0.77	1.56	2	24	2	2051	0
4a	0.23	1.37	1.3	2.18	4	74	4	1859	0
4b	0.15	0.77	0.9	1.4	2	38	2	1847	0
5	0.17	0.82	0.95	1.2	2	40	2	1934	0

The results in Table 4.3 show the average voltage fluctuation, for a few locations on the feeder and the number of tap changes for each device, on a cloudy day. Lower numbers are better and indicate improved voltage regulation along the feeder. DG that is distributed equally across the entire feeder causes the greatest change to the number of tap changes per day, if geographical dispersion is not considered. The high RVC level of all of the generators combined causes the largest voltage variations.

The DG in case 1 and 2 also increases the number of tap changes substantially on cloudy days, when compared to the DG situated further away. The number of tap operations is increased by 100% for case 1 and 2. This could potentially be a problem and could mean that the maximum recommended RVC of generators connected close to the substation or near to VR, should be limited to about 2%. In these cases, the voltage variation at the primary side of the VR is greater than the bandwidth of the controller. The number of times the VR operates can be reduced by increasing the bandwidth of the controller to be greater than the average voltage fluctuation at the VR location. The disadvantage with increasing the bandwidth of the controller is reduced voltage regulation at the end of the feeder. It would need to be determined how many cloudy days are expected at the DG's location so that the average number of tap changes per day, over a longer period of time, could be calculated.

The DG in case 3 doesn't influence the VR and OLTC, because the voltage variation at the VR is less than the controller bandwidth. At these levels of DG penetration, for DG connected far from the substation, it is evident that excessive tap changing of voltage control devices is not a major concern. DG that often causes greater than 2% fluctuation, at the primary side of the VR, causes the total number of tap changes per day to be about double the amount with DG on a sunny day.

The DG impacts the control of the switched capacitor, because of the increased voltage when it is generating power. The capacitor's upper bound voltage can be increased, but this could result in the capacitor remaining on when it is not needed. DG causes the capacitor to be kept off during the periods of high reactive power demand. The network has higher losses, than it would have, if the capacitor was controlled with a reactive power controller. The increased lagging reactive current, which would have been compensated for by the capacitor, places additional strain on the transmission network. The reduced real current component and increased reactive current component, reduces the lagging power factor of the feeder. This causes the feeder to operate at a very poor power factor, ranging between 0.5 and 0.8.

Figure 4.13 shows the results for case 4a and Figure 4.14 shows the results for case 4b. It is evident that including the effect of geographical dispersion dramatically reduces the voltage variations on the feeder. Many of the large voltage dips evident in Figure 4.13, between 10:00 and 14:00, are completely smoothed out in Figure 4.14. The number of tap changes is halved and the difference in tap changes between a cloudy and sunny day is only ten.

A potential problem with the VRs tap changing can be observed in Figure 4.14. The VR tends to operate within a very narrow band of tap positions when compensating for the voltage variations caused by the PV plant. The increased use of a few tap positions could lead to accelerated wear, because the calculated life with four tap changes per tap position is easily exceeded.

Using (4.5) the maximum power change, that falls within the 99th percentile over a 10 minute period, is calculated to be 34% for the case of ten 109 kW PV plants. Evidently, the DG plants connected to the weakest part of the network will cause a greater voltage change with the same level of power change. When compared to the total voltage change, caused by fluctuating DG output power of a single PV plant limited to a 3% RVC, the combined RVC level of multiple plants on a feeder can be increased depending on the number of distributed plants. It is estimated that for ten equally sized plants, an acceptable value for feeder RVC is about 4-4.5%, for the number of tap operations to not be increased on a cloudy day.

From the figures it is evident that high voltage is not an issue with these levels of DG penetration, during typical feeder operation. If the capacitor is configured with a reactive power controller, it can be switched on during the day when the voltage is supported by the generators. This will reduce the feeder losses further and cause the voltage profile to be more flat.

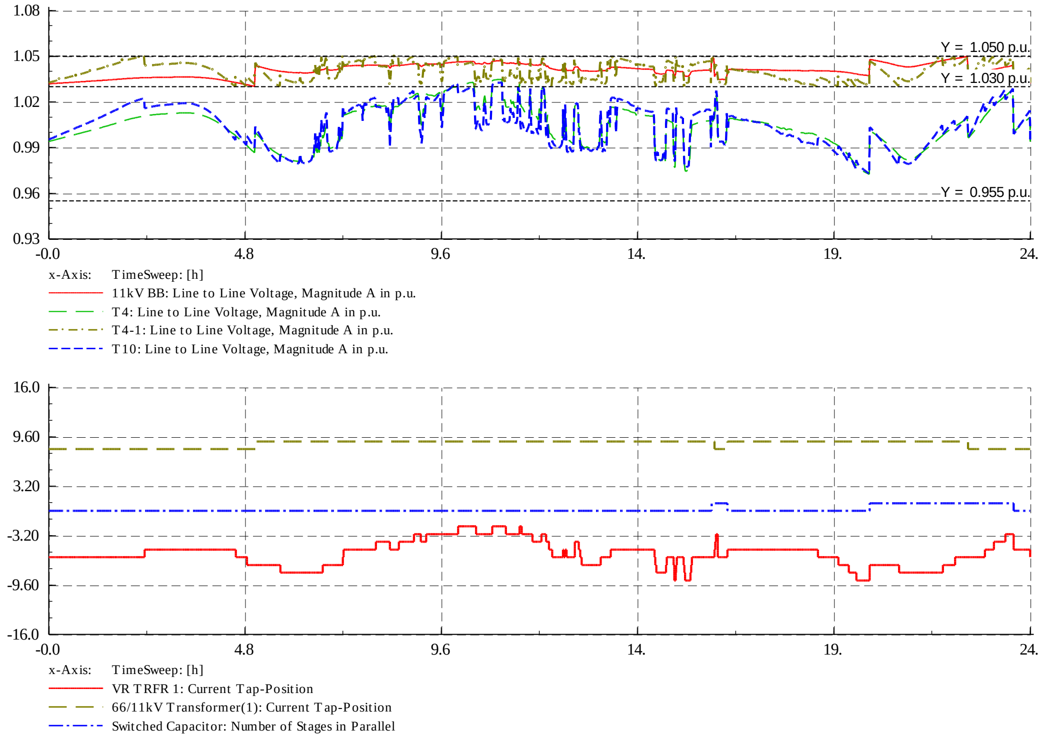

Figure 4.13: Voltages and tap positions on a cloudy day ignoring geographical dispersion for case 4a

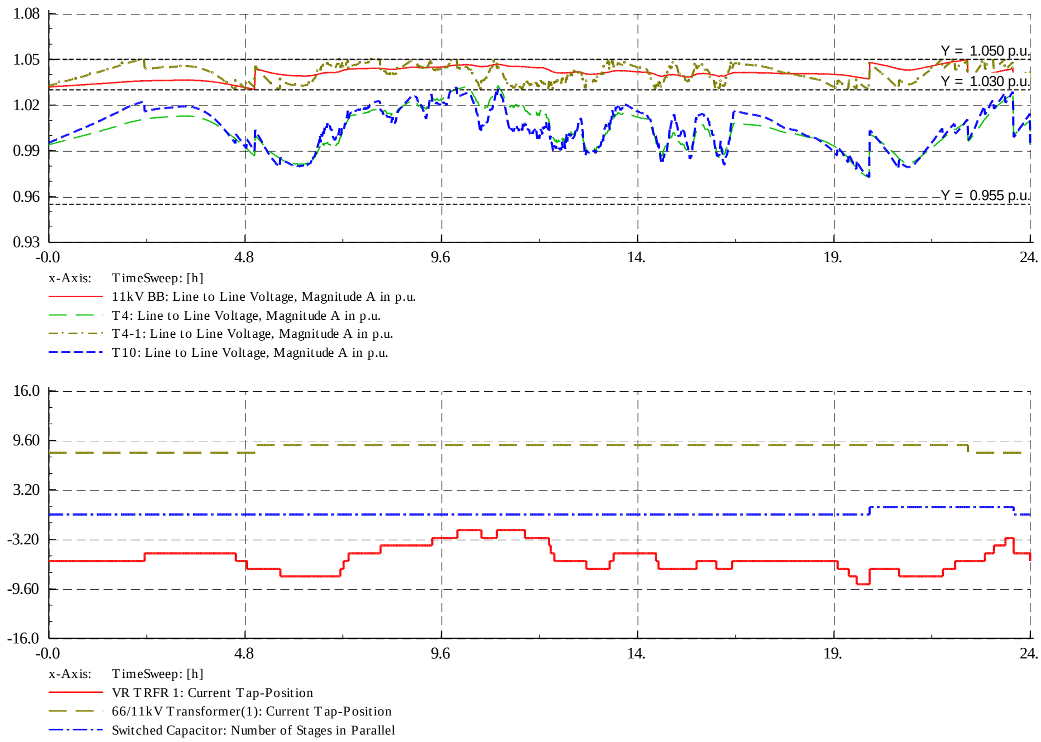

Figure 4.14: Voltages and tap positions on a cloudy day considering geographical dispersion for case 4b

From this point when multiple PV plants are under assessment, geographical dispersion will always be considered and case 4b will be referred to as case 4.

4.6 Loss minimisation

There is a specific amount of DG penetration, for each connection case, that reduces the losses of the feeder to a minimum. In [48], (4.15) was developed that allows for the losses of a feeder to be calculated if a single DG is connected to a feeder.

$$P_{\text{loss}} = P_{\text{loss.ini}} + R_{\text{ln.tot}}(k)\frac{P_{DG}}{pf_{DG}} \times \ldots$$
$$\ldots\left(\frac{P_{DG}}{pf_{DG}} - 2\frac{|S_L|}{n}\left(pf_L\, pf_{DG} - \sqrt{1-pf_L^{\;2}}\sqrt{1-pf_{DG}^{\;2}}\right)\left(\frac{(2n+1-k)}{2}\right)\right) \tag{4.15}$$

Where n is the number of terminals with loads and k is the terminal that DG is connected to. The approximate power for a single DG to give minimum losses at unity power factor can be calculated by differentiating (4.15) with respect to P_{DG} and equating to zero, as shown in (4.16).

$$P_{DG.\min\text{losses}} = \frac{P_L(2n+1-k)}{2n} \tag{4.16}$$

The choice of P_L in (4.16) is critical to provide accurate results. For the case of PV generation, power is only produced during the day. The average load during the day can be used to approximate P_L. It can be assumed that if the PV plant has tracking solar panels that the generation profile is relatively flat. It is assumed that the test feeder has an average load of 1.6 MW during the day.

The minimum losses over a 24 hour period are evaluated from the base penetration level of Table 4.2. The losses are iteratively evaluated by reducing the maximum DG power from the base penetration level and finding the losses for each power level. The maximum DG power level, with the lowest losses, is found at the point where reducing DG power further causes the losses to increase. It was found that the DG power level that results in the lowest losses could be greater than the base penetration level, so the point of minimum losses might need to be calculated by ignoring the integration rules. A detailed description of the algorithm to determine the DG size for minimum energy losses can be found in the appendix. The algorithm that calculates the penetration level for loss minimisation can be evaluated until the objective function (4.17) is met.

$$J = \mathrm{Min}\left(E_{\mathrm{loss}}\right) \tag{4.17}$$

The DG power level that had the lowest losses is found for the different cases and is shown in Table 4.4. The estimated power level using (4.16) is compared to the results obtained using the algorithm.

Table 4.4: Power operating point for minimum losses on a sunny day

Case	**Estimated P_{DG} [kW]**	**Actual P_{DG} [kW]**	**Percentage of base power [%]**	**E_{loss} [kWh]**	**Loss reduction [%]**	***TT***
1	1600	1590	47	2201	10	30
2	1280	1358	198	1506	12.5	38
3	880	900	293	1531	20	32
4	-	1800	190	1479	10	38
5	-	2420	184	1630	7	38

The DG power that causes the minimum losses on the feeder is found to be greater than the base penetration level for all cases, except for case 1. The power for minimum losses in this case is found to be 1.59 MW and the losses are reduced to 2201 kWh. This is a loss reduction of 242 kWh/day or 10%, but at the cost of limiting the DG size to 47% of its original value. The network operator would have to decide if the reduction of generation is a worthwhile trade off to reduce the losses. For the other cases the losses were at a minimum with between 184% and 293% more DG connected to the network. In most cases it would be beneficial if a way could be found to increase the DG penetration level beyond the base penetration level so that the network losses can be reduced. The DG power estimation using (4.16) is shown to provide a good estimation when compared to the PowerFactory calculation of the DG power.

4.7 Voltage regulator operation

The addition of DG to a network with voltage regulators can cause problems if the voltage regulator is not configured to operate in the correct control mode, for the current network conditions. During normal network operation without DG, bi-directional mode can be used because reverse power flow will only occur if the network configuration changes. The source side can change by closing a normally open point on the load side, so power is supplied from the opposite direction. If the bi-directional control mode is used when DG is installed downstream of the VR, the VR will assume that the source side has changed and attempt to regulate the actual source side voltage. The VR is unable to control the source side voltage and the VR will change taps to its limit and an over voltage will occur on the load side, as shown in Figure 4.15a and Figure 4.15c. Conversely if a regulator is configured to operate in co-generation mode and the source side changes, the regulator will attempt to regulate the new source side voltage and will cause under voltage on the new load side as shown in Figure 4.15b and Figure 4.15c.

This illustrates the need for a method to easily switch between regulator control modes. Many networks are expected to operate with reverse power flow during contingencies. Remote control of regulators is a possibility where the mode could be changed by the network control. Local control could be performed by operators, however this would add to the period of time that customers are without power.

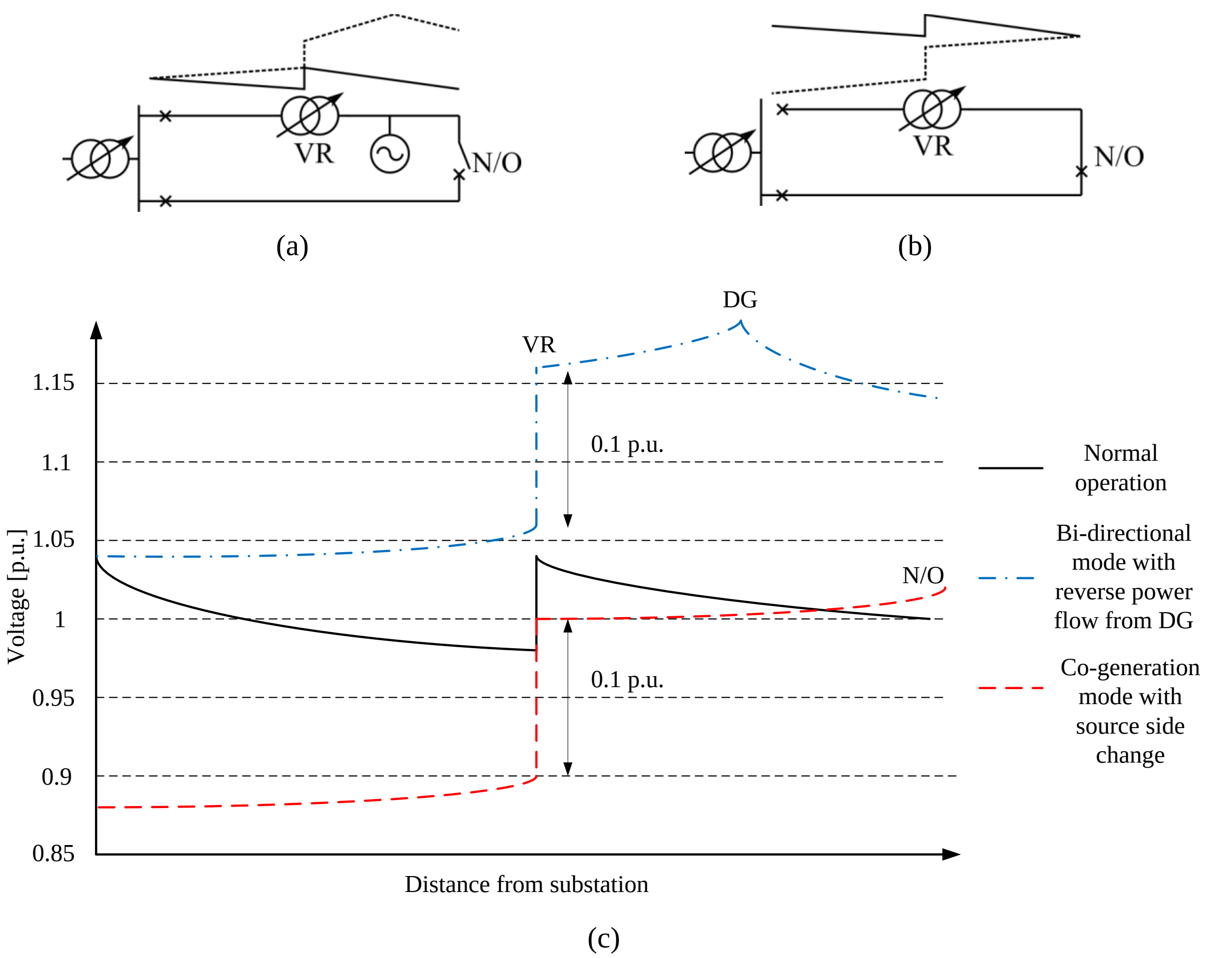

Figure 4.15: a) DG and VR operated in bi-directional mode with reverse power flow. b) Reverse source with VR operated in co-generation mode. c) Voltage profile of feeder operational modes

4.8 Flicker

Short term voltage variations caused by PV will be investigated in this section. The most severe short term voltage variations are noticed as flicker and some sources suggest that flicker could be introduced by PV systems [10], [49], [50]. Flicker could be introduced from a square voltage change of 2%, 20 times an hour and it is undetermined whether PV could introduce these changes. The flicker curve assumes that there is a sudden step change of voltage. PV generation is not expected to cause step changes, but rather voltage variations over several seconds or minutes.

The authors in [50] state that flicker can be observed at the end of a feeder but an analysis of this study shows that they have not defined what they term as flicker and provide no calculations to show that flicker will be a problem. It appears that their definition of flicker is any voltage variation, but flicker is the term used to describe noticeable rapidly fluctuating light levels due to voltage fluctuations.

In [51] the flicker caused by PV inverters on the distribution network is analysed for cloudy days using an irradiance based voltage flicker study. The authors analysed irradiance data in Hawaii to determine the maximum power change of a 5 MW PV plant. They determined the most extreme ramp rates and used these values to determine the power changes to use in their flicker study. Their results were compared to the GE flicker curve but no calculation was made using the IEC 61000-4-15 method to calculate flicker. The authors concluded that a step change in voltage was not suitable for a flicker analysis with PV inverters. Another study concludes that flicker, caused by PV generators, is not expected to pose many problems [49]. A power quality study found that flicker is not an issue with PV systems but that harmonic outputs and voltage unbalance of PV plants at low power levels was more of a concern [52].

Flicker is a phenomenon that is quantifiable based on human perception and is only a problem if people are there to observe it [53]. Historically flicker has been characterised by the visible changes in light output by an incandescent 60W lamp bulb. Current lighting technologies such as CFL were found to have similar or greater levels of flicker than incandescent bulbs for certain frequencies [54]. In particular inter-harmonics and odd harmonics were found to cause the most problems, but are not taken into account with current flicker measurement standards [55].

The IEC 61000-4-15 standard specifies the function and method to measure flicker for incandescent light bulbs. Flicker can be calculated based on long or short term measurements and the short term measurement is calculated using (4.18) [56].

$$P_{st} = \sqrt{(0.0314 P_{0.1s} + 0.0525 P_{1s} + 0.0657 P_{3s} + 0.28 P_{10s} + 0.08 P_{50s}} \tag{4.18}$$

Where $P_{0.1s}$, P_{1s}, P_{3s}, P_{10s} and P_{50s} are the flicker levels exceeded from 0.1 to 50% of the time during the observation period. The subscript *s* indicates that smoothed values should be used and are defined as follows [56]:

$$P_{50s} = \frac{P_{30} + P_{50} + P_{80}}{3} \tag{4.19}$$

$$P_{10s} = \frac{P_6 + P_8 + P_{10} + P_{13} + P_{17}}{5} \tag{4.20}$$

$$P_{3s} = \frac{P_{2.2} + P_3 + P_4}{3} \tag{4.21}$$

$$P_{1s} = \frac{P_{0.7} + P_1 + P_{1.5}}{3} \tag{4.22}$$

The IEC specification [56] states that the flicker is acceptable for loads if P_{st} is below 1. For generation P_{st} should be kept below 0.5.

The GE flicker curve is shown in Figure 4.16 and is representative of instantaneous step changes in voltage due to switching operations. There are curves that relate the GE step change curve to pulses, ramps, sinusoidal and triangular changes [57].

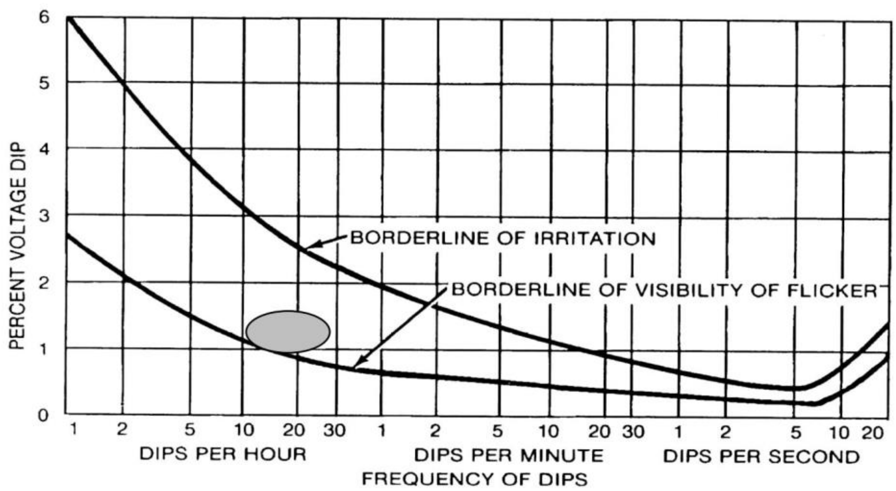

Figure 4.16: Flicker Curve [56]

The influence of a PV plant on the dynamic voltage changes that could cause flicker is investigated. The penetration level that could potentially cause flicker will be determined, based upon worst case analysis and a recorded irradiance profile. For the initial study the PV plant is placed at the end of the feeder at T10 and is sized according to the base penetration level of 300 kW. The 300 kW PV plant causes a 3% RVC on the MV network. The output of the PV plant is varied according to Figure 4.17 where the PV plant is switched in and out every 10 s. The switching is repeated for 10 minutes because this is the minimum simulation time for the flicker meter to calculate P_{st}. It should be kept in mind that RVC limits are defined for switching operations that occur beyond the 10 minute window used to calculate P_{st} [50].

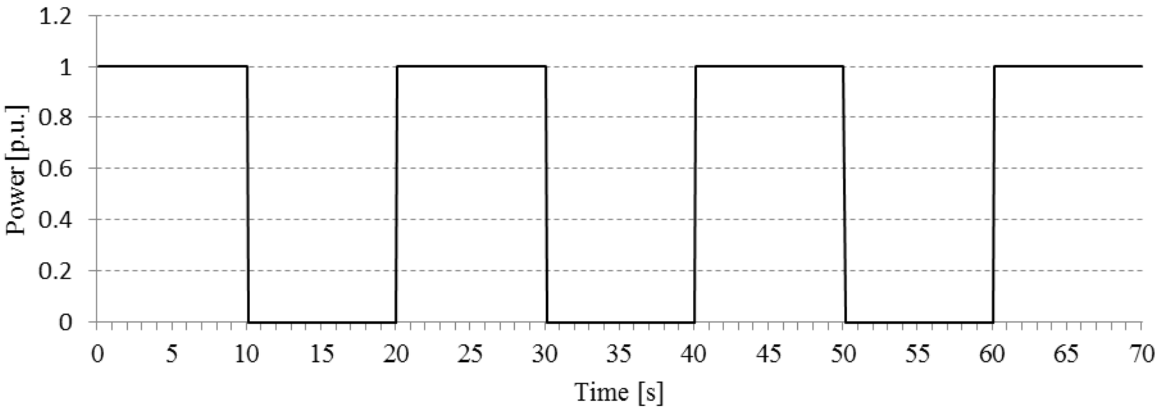

Figure 4.17: Switching of PV plant

With the 3% RVC of the generator, the P_{st} was found to be 1.61 for the generator voltage at bus 10. The value equates to 60, 3% RVC's over the 10 minute period. The RVC was evaluated at 16 Hz and therefore the generator's power changes over a period of 0.0625 s. In practice, it would not be expected for a PV plant's output to have such a large ramp rate or so many consecutive switching operations. The 100% ramp would be caused by a plant trip and is not representative of a flicker analysis.

A more realistic approach would be to investigate the maximum expected power change over a period of time. The change of a PV plants power output over 1 s is found to be less than 30% for 99 % of power changes for a 300 kW plant. This would provide a more realistic measure to determine RVC levels. The worst case variation of the PV output power would be multiple 30% variations in succession. To test the level that PV the flicker could potentially pose a problem the PV plants power is ramped up and down at a rate of 30%/s according to Figure 4.18.

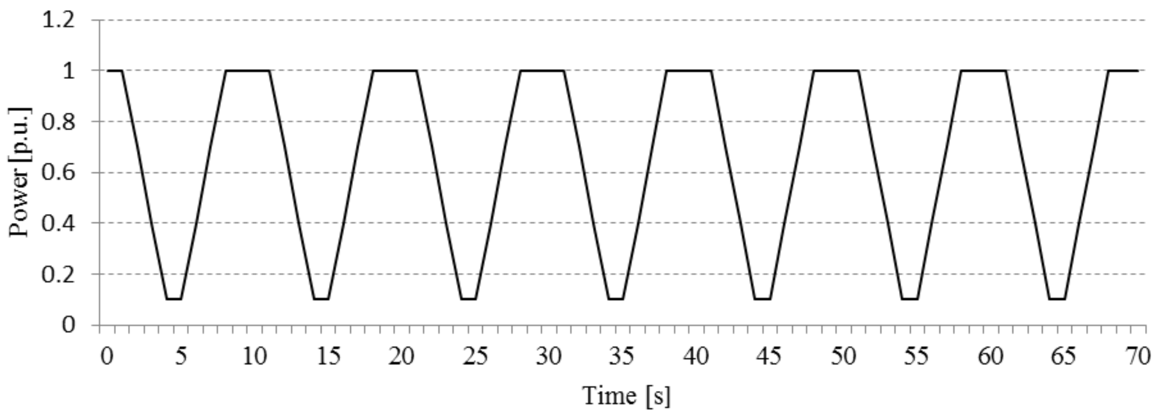

Figure 4.18: Ramping of PV plant

The short term flicker for the 30% ramp rate is found to be 0.21 for a 3% RVC plant. This value is still an over estimation of the expected flicker values that might be experienced for short periods a few times per year. In [51] it was found that the extreme ramp rates would normally occur during the same time period, but over a few minutes rather than seconds. In most cases the ramp rates were below 100 W/m²s or approximately 10%/s but for a few occasions could be over 800 W/m². The periods with high ramp rates will be ignored due to their relative infrequency. The power level that causes the flicker level to exceed the recommended P_{st} value of 0.5 is found to be 800 kW or an 8% RVC. A recorded irradiance profile is used to determine the flicker severity for a typical cloudy day. The irradiance was recorded with one second accuracy over a week period and a 30 minute portion is selected for the flicker study as shown in Figure 4.19. The irradiation is typical of a partly cloudy day with many irradiance changes in the 30 minute period.

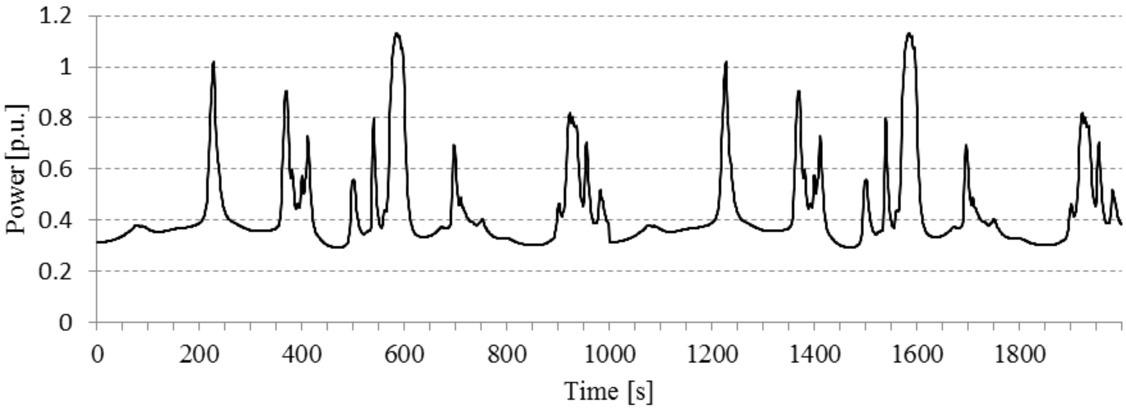

Figure 4.19: Recorded 30 minute irradiance profile

The three short term flicker levels and the long term flicker level is calculated for the 30 minute period. For the first 10 minutes the flicker level cause only by the PV plant is 0.09, the second 10 minutes is 0.06 and the last 10 minutes is 0.09. The long term level is 0.08. These values are well below the calculated worst case for the 800 kW PV plant.

In the NRS 048-2-2008 standard [14], it is stated that the voltage variations that cause flicker do not affect other equipment as severely as they do the light bulb. The power quality of the network, due to voltage variations, is satisfactory if the flicker level is below 1.

From these results, it can be concluded that PV will not cause significant flicker. Switching operations should occur infrequently and providing there is no other reason, such as over voltage that limits the penetration level of PV, the RVC level of a generator can be increased beyond 3%. In the previous section it was shown that the 3% RVC level provided a good limit when voltage regulators are installed on the network. The number of tap changes increased substantially if more generation was added. Therefore, the RVC limit of all of the generators that are installed beyond a voltage regulator could be increased, providing that the RVC of all of the generators, measured at the primary side of the regulator, is below 3%. If a generator that causes a large RVC is connected to a remote part of a network, the generator must have active power curtailment to limit the possibility of over voltage during periods of low demand.

The voltage of the network should still vary within the upper and lower bound limits defined by the network class and tap zone. The generator that is connected to the remote portion of the network will not cause a large increase in tap changes at the substation transformer and will not contribute to flicker. The voltage rise along the feeder will be equivalent to the generators rapid voltage change and therefore the voltage headroom must be assessed during low and high load.

4.9 Conclusions

In this chapter the effect of DG on a conventional distribution system has been investigated. In the simulations it was assumed that the DG relies on the classical network voltage control devices to keep the voltage within the required limits.

The idea of modelling a PV plant as a low pass filter, for short time power fluctuations, was investigated. It was shown that for simulations with a resolution of greater than one minute, the power output smoothing is negligible except for PV plants that cover a very large area. The geographical dispersion of multiple PV plants was shown to smooth out power fluctuations over a greater time period of up to 10 minutes.

The standard control methods, used by a conventional distribution system, allow a penetration level between 12% and 137% on the test feeder. The penetration level was influenced by the point of connection and number of generators installed. The losses were reduced in all but one of the connection cases. It was shown that the generation impacts the capacitors control. The voltage does not reach the turn on value when the generators are supplying active power.

It was suggested that the total feeder RVC level can exceed 3% if there are multiple smaller PV plants that are suitably distributed along the feeder. A value of 4-4.5% was suggested to minimise the increase in the number of tap changes during a cloudy day. It is apparent on a partly cloudy day that there is a relatively constant generation reduction, when the PV plants are geographically spaced apart. On average the total power output, of all the plants combined, varies within a much smaller range when compared to an individual plant. For the 10 generators in the test case, the power fluctuation is expected to be reduced to 34% of the equivalently sized PV plant.

It was shown that it is necessary to investigate methods that can be used to increase the penetration level of DG plants on distribution feeders. It was shown that the constraints, limiting DG penetration, also limit the amount that the feeder losses can be reduced. In most cases it will be beneficial to increase the DG penetration level, by between 100% and 200% of the base penetration level, to reduce the losses to a minimum.

Flicker was shown to not be an issue with PV generation. The low pass filter effect, between the rate of irradiance change and the plant power output, is enough to smooth out power variations that have the potential to cause flicker. The typical cloudy day operating scenario was shown to have a flicker contribution of 0.1 and is well below the limit of 0.5 for generators. It is suggested that the RVC limitation of generators, connected to remote parts of the feeder, can be increased if there are no voltage control devices on the feeder.

5 Technologies to increase the penetration level of DG

In the previous chapter, the maximum DG penetration was found for the test feeder. The limits were found assuming that DG plays no part in the voltage control of the network and that the control of the existing voltage control devices were left unchanged. In this chapter various methods are investigated that can be used to increase the DG penetration levels, that were established in Chapter 4 Table 4.2, without negatively impacting power quality. Any changes that can be made to increase DG penetration are assessed individually, to determine the most practical to implement and the extent that the modification improves the penetration level. After each technology is individually assessed, two control strategies that combine the various technologies are suggested.

5.1 Modification of on load tap changer, voltage regulator and line drop compensator settings

An OLTC is the most common voltage regulation device that is used for voltage regulation on a MV network. Much of the literature recommends increasing the intelligence of the controllers or modifications of the setpoint voltages. In [1] and [12], an OLTC with a line drop compensator (LDC) is used to regulate the line voltage. The LDC can be used to increase the DG penetration while keeping the voltage within the upper and lower limits. There are a few disadvantages when using a LDC, such as a decrease in performance when the power factor changes. The LDC can also impact neighbouring feeders, if there is a high load factor difference between them [6].

A VR can be operated in co-generation mode, while still making use of a LDC. This allows the voltage to be regulated at the same point along the line, irrespective of the direction of power flow. The regulator would need to have some logic to vary between co-generation and bidirectional control when used on networks with ring feeds as discussed in the previous chapter [58].

There are a few problems when solely relying on OLTCs and VRs to control the network voltage [39]. There is an increase of the daily tapping operations, especially on days with variable power output. Under high levels of DG penetration, the excessive tap changing can shorten the tap changers lifespan. The voltage control performed by a tap changer is executed in discrete steps and often cannot compensate for the short term power fluctuations experienced with high levels of penetration.

The base penetration level for a single DG, in Table 4.2, is constrained by the rapid voltage change level of the generator; except for case 1, where the constraint is voltage rise. The OLTC secondary voltage upper bound is 1.05 p.u. and therefore the voltage rise is limited to 2%. The first step to attempt to increase the steady state DG penetration level in those cases is to modify the control settings of the equipment already installed. The aim of the control modifications is to allow a greater voltage rise along the feeder so more DG can be installed for case 1, 4 and 5.

5.1.1 Reduction of OLTC and VR set point voltage

Adjusting the OLTC tap settings will increase the steady state DG limit by increasing the voltage headroom. Reducing the OLTC tap setting might cause low voltages during times when there is no generation but maximum load. Figure 5.1 shows how the constraint changes to RVC for the entire length of the feeder when the OLTC setpoint is reduced by 0.01 p.u.

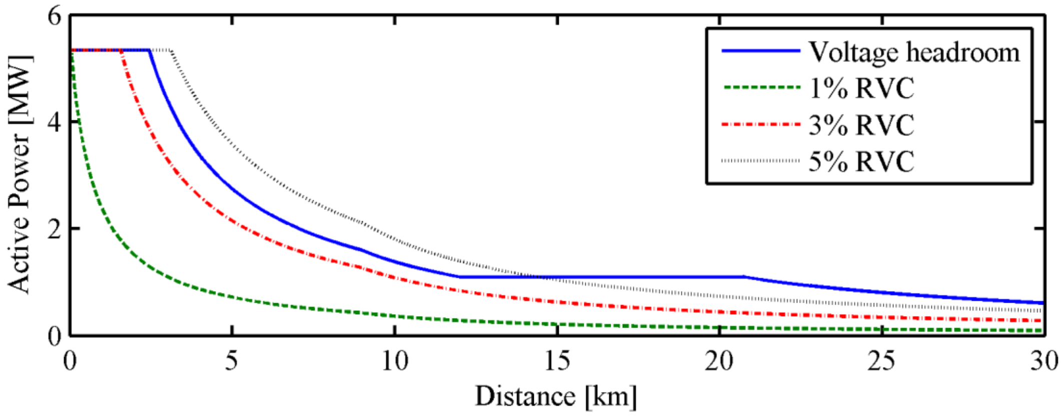

Figure 5.1: Maximum DG size as a function of distance from the substation with OLTC and VR setpoint reduction of 0.01 p.u.

The effect of reducing the OLTC and VR regulation set point to 1.04 p.u. is simulated and the results are shown in Table 5.1. The capacitor's turn on and off voltage had to be reduced by 0.01 p.u. for the control to function as expected. There are increased penetration levels in cases 4 and 5, but the voltage change percentage caused by the increased generation could lead to more power quality problems. On the test network the reduction of OLTC and VR setpoints did not lead to under voltage, during the normal load profile conditions; but it would lead to a 0.01 p.u. under voltage, at T4, during peak loading conditions.

Table 5.1: DG penetration level with the OLTC and VR setpoint reduced by 0.01 p.u.

Case	P_{DG} [kW]	Limiting factor	V_{max} Terminal	V_{max} [p.u.]	ΔV_{tot} [%]	E_{loss} [kWh]	TT	PL_{DG} [%]	Increase DG [%]
1	4034	RVC	T1	1.06	3	2679	36	161	18
2	665	RVC	T4	1.05	3	1713	32	27	-3
3	300	RVC	T10	1.05	3	1911	28	12	0
4	1480	OV	T4	1.07	6.8	1487	38	59	36
5	2075	OV	T4	1.07	5.5	1630	38	83	32

The results in Table 5.1 confirm that the reduction of OLTC and VR regulation setpoints can be beneficial if DG capacity is limited by voltage rise. The increased penetration level for case 1 results in increased losses, because the base penetration level is already above the point of minimum losses. In case 4, the setpoint reduction allows for 36% more DG to be connected to the feeder. A benefit to the increased DG penetration is the reduction of losses, as the DG can supply more of the load during the day. The total feeder rapid voltage change increased by 30% and it still needs to be determined whether 6.8% is a suitable level for total feeder voltage change. Another concern is that if all of the DG suddenly disconnects due to a fault, then the voltage at the end of the feeder drops by 6.8%. This sudden change of power could lead to temporary under voltage during periods of high load. The network voltage will be restored to suitable levels once the switched capacitor is turned on and the VR has adjusted to the correct tap position.

Figure 5.2 shows the voltage profile and tap positions with the increased penetration level for case 4. On a partly cloudy day, the voltage could vary towards the end of the feeder by up to 5% over a period of a few minutes. The average voltage fluctuation at T-4 is 0.9 and the number of daily tap changes by the VR is increased substantially to 50. This could potentially lead to power quality issues however it is expected to be more of a concern to the utility than the customer. The average voltage fluctuation at the end of the feeder increases from 1.4% to 1.66%. These comparisons indicate that the VR will be placed under additional strain when the average voltage fluctuation at T-4 exceeds about 0.7-0.8%. Therefore, the average voltage fluctuations at the terminals of voltage regulators on a cloudy day should be limited to be below 0.7%. The voltage variations are the worst around midday, when the irradiance varies by the greatest amount over a short time period. Based on this simulation, a total feeder RVC level of 4.5-5% would be the upper limit for DG penetration, when at least ten DGs are installed. This is slightly higher than the amount specified in the previous section of 4-4.5%.

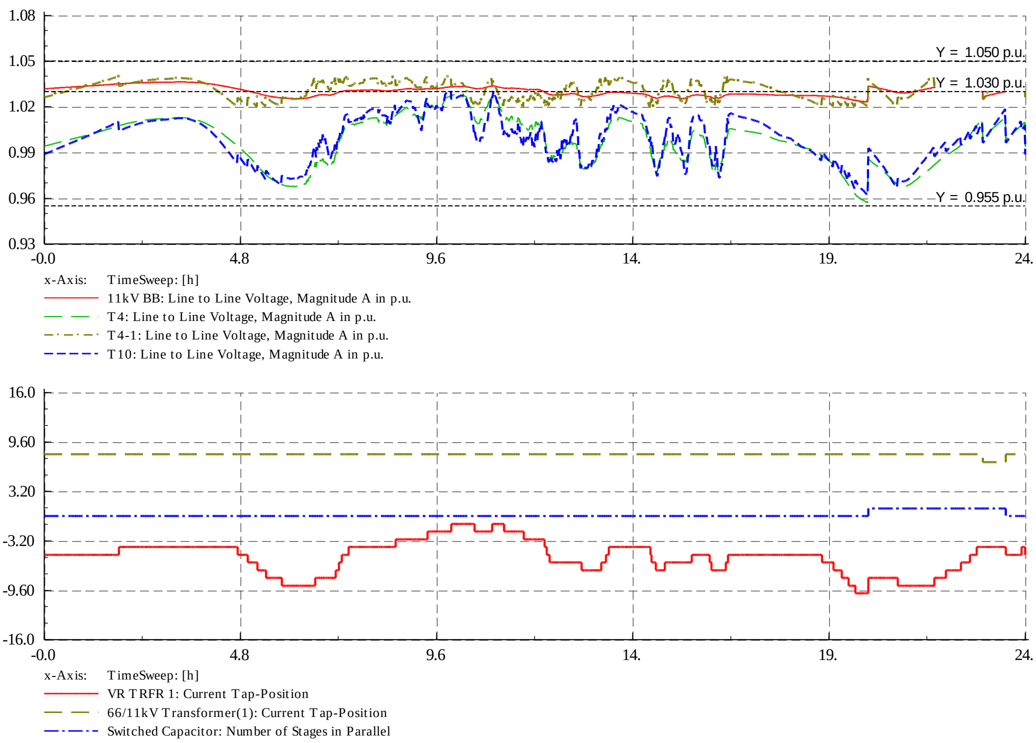

Figure 5.2: Voltages and tap positions for case 4 with OLTC setpoint reduction on a cloudy day

5.1.2 LDC control

It was shown in the previous chapter that a LDC is quite complicated to configure and the addition of DG increases the complexity further. DG affects the control of a LDC in the following ways:

- When DG is connected before the LDC, the LDC will see the effect of the DG on its source; therefore it will have no impact on the control or load centre voltage.
- When DG is connected after the load centre of the LDC, the LDC and the load centre both see the effect of the DG. The changed current flow affects the entire feeder and therefore the LDC correctly compensates the voltage at the load centre.
- If DG is connected between the LDC and the regulation point, the DG will cause problems when trying to regulate the load centre voltage. The DG will reduce the current sensed by the LDC and the control will cause the VR/OLTC lower the voltage. The control action can cause low voltage at the load centre [58]. The LDC assumes that the current reduction is seen along the entire length of the feeder. This assumption is incorrect as the current flow after the DG is the same as it would have been prior to the DG being installed.
- A LDC on the substation transformer connected to a busbar with multiple feeders will encounter regulation problems if one or more of the feeders contain a large percentage of DG. The DG could supply some of the load of the other feeders and reduce the current though the transformer. The LDC sees this as a load reduction on all feeders and will lower the voltage of the busbar. This can result in low voltages on feeders that do not have DG.

The change in voltage caused by a DG on a feeder equipped with a LDC can be calculated using (5.1) [11].

$$\begin{aligned} \Delta V &\approx \frac{\left(R_{\mathrm{ln}.\lambda} - R_{\mathrm{set}}\right)P_{DG} + \left(X_{\mathrm{ln}.\lambda} - X_{\mathrm{set}}\right)Q_{DG}}{V_{\mathrm{nom}}} & \lambda \le \lambda_{DG} \\ \Delta V &\approx \frac{\left(R_{\mathrm{ln}.\lambda_{DG}} - R_{\mathrm{set}}\right)P_{DG} + \left(X_{\mathrm{ln}.\lambda_{DG}} - X_{\mathrm{set}}\right)Q_{DG}}{V_{\mathrm{nom}}} & \lambda > \lambda_{DG} \end{aligned} \tag{5.1}$$

Figure 5.3 shows a possible scenario with a single substation transformer regulating multiple feeders. The DG on feeders 1 and 2 supply the load of all of the feeders and the transformer has power flowing in the reverse direction. The LDC assumes the power flows in reverse, from all of the feeders, and compensates for the expected high voltage at the regulation point V_r. If feeder 3's load requires a high substation voltage, to ensure adequate voltage along the feeder, the use of a LDC will not provide suitable regulation. DG effectively increases the load factor difference between feeders and can cause LDC regulation to be ineffective. The problem can be partly solved by reducing the distance to the regulation point or relying on standard OLTC regulation. Another alternative would be to use cancellation CTs, on certain feeders, to effectively remove the feeder from the LDC's calculations [59].

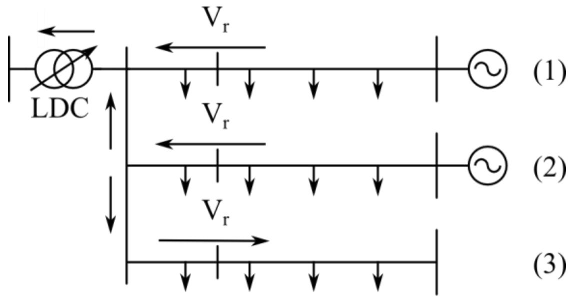

Figure 5.3: LDC regulation with DG

In most cases where the minimum feeder voltage is not a major limitation, the dynamically adjusting setpoint voltage allows for more generation to be connected to a feeder. The voltage regulation of the feeder is also improved, as illustrated by a simple two feeder scenario with the voltage profiles of each feeder shown in Figure 5.4. The upper voltage profile is of a feeder at high generation and minimum load and the lower profile shows no generation and maximum load. The LDC's regulation capabilities are reduced when compared to the single feeder case, but the overall regulation is better than standard OLTC control.

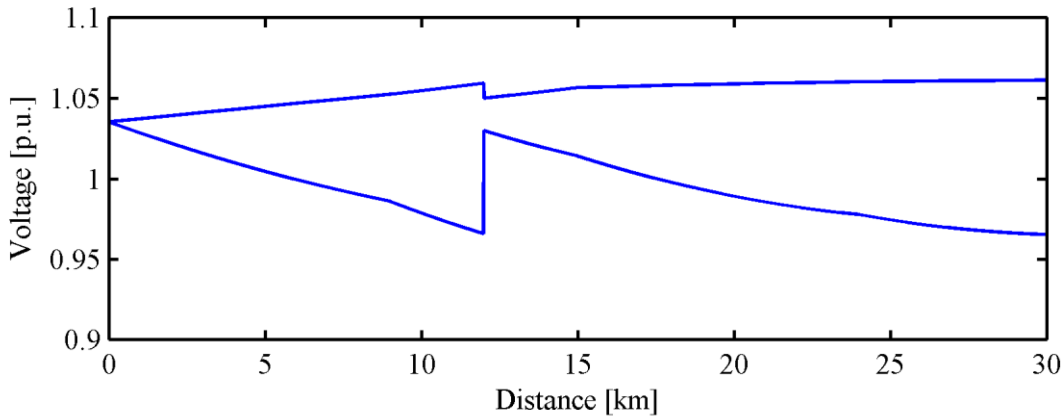

Figure 5.4: Voltage profile of two feeders fed off of the same busbar. One feeder is at maximum load, no generation and the other feeder is at minimum load, maximum generation.

Like OLTC setpoint reduction, the LDC can be used to increase DG penetration levels if over voltage is the limiting factor. The advantage of equipping the OLTC with a LDC, on the single feeder setup, is that that the voltage of the MV busbar is adjusted for the current amount of generation and load. This allows for a much greater voltage rise from the substation voltage when compared to OLTC setpoint reduction. The LDC can effectively compensate for periods with high load and no generation or low load and high generation at the cost of extra daily tap changes.

The LDC of the OLTC is configured to regulate the voltage 3 km from the substation on the test feeder. The LDC settings are shown in Table 5.2 and the simulation results are shown in Table 5.3:

Table 5.2: LDC settings for the single test feeder

V_{set}	V_{UB}	V_{LB}	R_{set}	X_{set}	CT ratio	VT ratio
1.03	1.04	1.02	0.88	0.86	1	1

Table 5.3: DG penetration level with the OLTC configured with a LDC

Case	P_{DG} [kW]	Limiting factor	V_{max} Terminal	V_{max} [p.u.]	ΔV_{tot} [%]	E_{loss} [kWh]	TT	PL_{DG} [%]	Increase DG [%]
1	3858	RVC	T1	1.04	3	2601	30	154	13
2	665	RVC	T4	1.05	3	1707	30	27	-3
3	300	RVC	T10	1.05	3	1909	26	12	0
4	1878	OV	T4	1.07	8.4	1470	36	75	72
5	3130	OV	T4	1.07	7.9	1742	38	125	100

In all of the simulations, the number of times the OLTC tap changed during the day increased from about two to between four and eight. In certain simulations, the number of times the VR had to tap change is reduced, as the OLTC helped to compensate for more of the voltage changes. The number of tap changes does not increase substantially on a sunny day. On a cloudy day, the voltage variations cause the number of times the VR and OLTC tap change to increase to 52 taps for the VR, and 8 for the OLTC. This is shown in Figure 5.5 where there are many large voltage variations throughout the day.

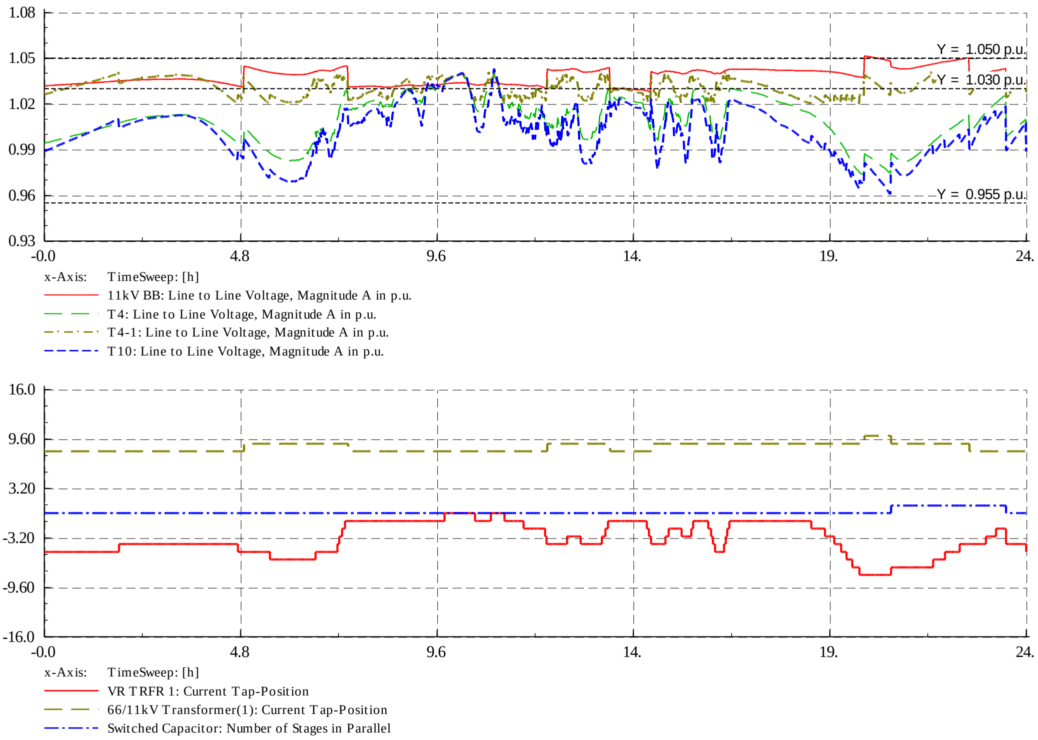

Figure 5.5: Voltages and tap positions for case 4 with OLTC configured with a LDC on a cloudy day

As can be seen, the VR in particular struggles to keep the voltages within the required range. Over voltage is not a concern with the normal daily load profile with 1878 kW of generation. It is evident from the large voltage changes that the penetration levels calculated for case 4 and 5 are unreasonable due to the high RVC level of all of the generators.

5.2 Reactive power control

Reactive power control (RPC) has been proposed and well documented in many sources [5], [6], [19], [22], [25], [40]. Generators with RPC are able to supply or absorb reactive power to offset some of their impact on the network voltage. RPC is implemented in DGs by varying the phase angle between its injected current and the grid voltage.

There are limitations to the amount that the network voltage can be controlled using RPC. Typical overhead distribution lines have a low reactance to resistance (X/R) ratio, of about one, that results in an equal voltage change being caused by active and reactive power. For an inverter to supply reactive power when operating at rated power, it will need to be oversized to supply the additional current [5]. A DG's reactive power can be implemented using constant reactive power, power factor or droop control. A droop controller is used to share the reactive power support among many generators and prevent control interactions between them [60]. In [26], a voltage control method using multiple distribution static synchronous compensators (DSTATCOMs) is proposed. The authors recommend using a piecewise linear droop line to provide the best voltage control along the feeder while minimising losses and voltage variability.

The reactive power that a DG can supply when generating rated power depends on the inverter overrating. It is zero if the power electronic converter is rated to the real power. The available reactive power for an inverter with rated current I_{DG} and line voltage V_{DG} is shown in (5.2).

$$Q_{DG.\max} = \sqrt{\left(V_{DG} I_{DG.\max}\right)^2 - P_{DG}^2} \tag{5.2}$$

Figure 5.6 shows the per unit reactive power that can be generated by an inverter if it is over rated, when supplying rated power.

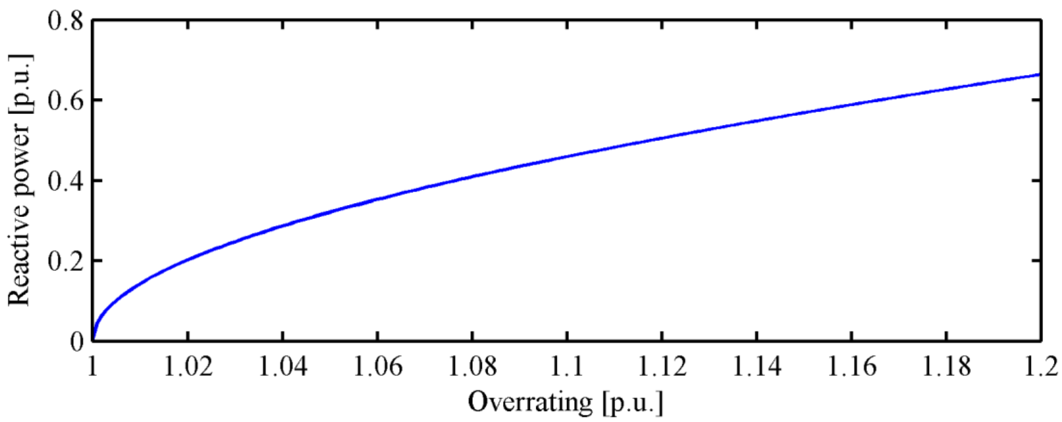

Figure 5.6: Reactive power generation as a function of converter overrating

Reactive power control can be economical to help regulate the voltage variation, as the cost to over rate a converter is small. A converter is required to provide 5.3% more current to operate at a power factor of 0.95. The maximum converter current is calculated using (5.3).

$$I_{DG.\max} = \frac{S_{DG.\text{rated}}}{V_{DG.\text{rated}}} \tag{5.3}$$

In South Africa the grid code specifies that the inverters must be able to supply rated power at a power factor of 0.95 (Category A and C) or 0.975 (Category B). This means that for each megawatt of active power connected to the grid, the DG must be able to provide 328 kVAr or 222 kVAr respectively.

Figure 5.7 and Figure 5.8 show how the penetration level is increased when reactive power control is used for power factors of 0.975 and 0.95.

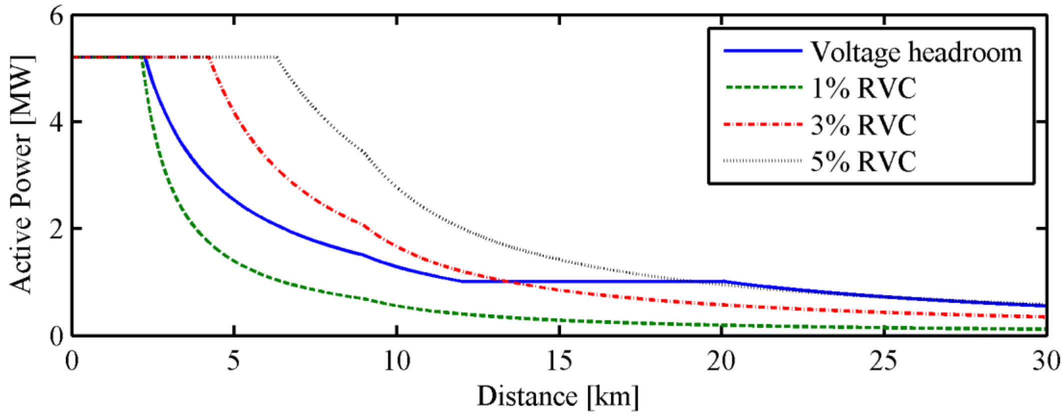

Figure 5.7: Maximum DG penetration when making use of reactive power control at a power factor of 0.975

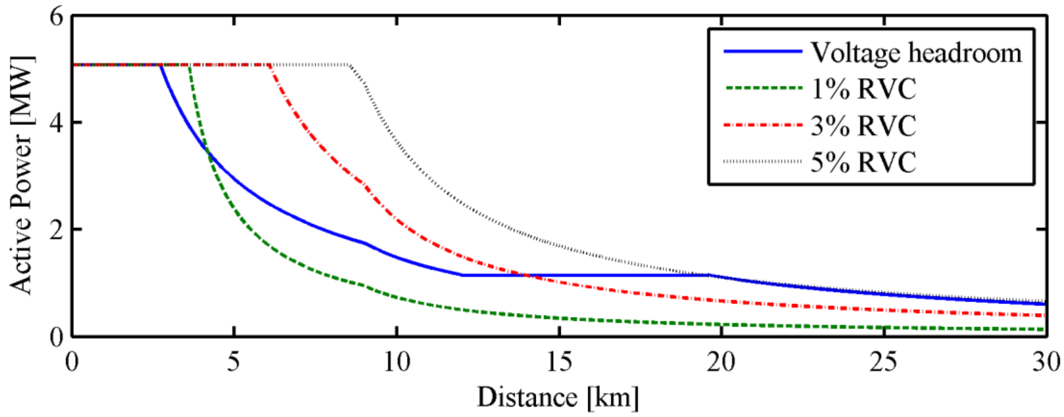

Figure 5.8: Maximum DG penetration when making use of reactive power control at a power factor of 0.95

Reactive power control has limited functionality on MV networks when compared to HV networks, due to the low X/R ratio of between 0.4 and 1.5. Figure 5.7 and Figure 5.8 show the difference between the maximum DG penetration levels for different power factors. It is clearly seen that the reduced conductor size from Hare to Mink at 9 km from the substation reduces the voltage controllability and limits the penetration level increase with RPC. Even with the low X/R ratio, reactive power control by a DG can increase penetration by 20-45% at a power factor of 0.975 and 40-70% at a power factor of 0.95.

As conductor thickness increases, resistance decreases while the reactance remains relatively constant. The reduced resistance results in greater current carrying capacity and therefore a smaller voltage drop under the same conditions. The magnitude of the voltage change per unit of reactive power remains relatively constant with increasing conductor thickness.

Lagging reactive power control should not be used continuously to increase DG penetration, as the increased line current can cause increased losses. The reactive power absorbed by the DG also needs to be supplied from an alternate source. Reactive power absorption provides no benefits to reduce the voltage rise if the reactive power is locally supplied from a feeder capacitor. It does however reduce the RVC so the reactive power can supplied locally using capacitors or a DSTATCOM. The need to supply the reactive power comes at increased cost, but the installation of DG should not place additional strain on the transmission network. It is possible to make use of certain DG units connected to the network to supply some of the reactive power when required.

While DG is typically controlled to absorb reactive power, it can be configured to supply reactive power to reduce the losses, if voltage rise is not a concern. With communication to each DG, a reactive power controller can be installed at the substation to minimise the current flowing through the transformer. The controller specifies each DG's reactive power output and can be configured to equally distribute the reactive power load among the generators or apply a weighting algorithm.

5.2.1 Constant power factor control

The simplest method for a DG to offset the voltage rise with reactive power is to operate at a constant power factor. Operating at a constant power factor reduces the voltage change per unit of active power injected into the grid. The penetration levels found using constant power factor control determine the upper limit that the DG penetration can be increased with reactive power control. The reactive power absorbed or supplied by a generator can be found by relating the reactive power generation to active power using (5.4).

$$Q_{DG} = P_{DG} \tan \phi_{\mathrm{set}} \tag{5.4}$$

Where ϕ_{set} is the power factor angle setpoint. The sensitivity of the voltage magnitude to a change in real power can be calculated using the chain rule as shown in (5.5).

$$\left.\frac{d|V|}{dP}\right|_{Q=f(P)} = \frac{\partial|V|}{\partial P} - \frac{\partial|V|}{\partial Q}\frac{dQ}{dP} \tag{5.5}$$

The change in reactive power caused by a change in active power can be found by differentiating (5.4) to get (5.6).

$$\frac{dQ}{dP} = \tan \phi_{\mathrm{set}} \tag{5.6}$$

(5.6) is substituted into (5.5) to get (5.7).

$$\left.\frac{d|V|}{dP}\right|_{Q=f(P)} = \frac{\partial|V|}{\partial P} - \frac{\partial|V|}{\partial Q}\tan\phi_{\text{set}} \tag{5.7}$$

Therefore, the change in voltage can be approximated using (5.8).

$$\Delta V = \Delta P_{DG} R - \Delta P_{DG} X \tan\phi_{\text{set}} \tag{5.8}$$

A simulation is done to investigate how much reactive power control can increase DG penetration. The same study case is used as in Table 4.2 and assumes the OLTC and VR upper voltage setpoint is 1.05 p.u. The DG is set to operate at a fixed power factor of 0.975 for the results in Table 5.4.

Table 5.4: DG penetration level at a power factor of 0.975 for a sunny day

Case	P_{DG} **[kW]**	**Limiting factor**	$V_{\max}$ **Terminal**	$V_{\max}$ **[p.u.]**	ΔV_{tot} **[%]**	E_{loss} **[kWh]**	***TT***	PL_{DG} **[%]**	**Increase DG [%]**
1	4411	OV	T1	1.07	0.90	3050	28	176	29
2	940	RVC	T4	1.065	3	1675	30	38	37
3	384	RVC	T10	1.06	3	1896	24	15	28
4	1374	OV	T4	1.07	4.67	1697	30	55	26
5	2425	OV	T4	1.07	3	1976	30	97	55

To determine the effect of allowing DG to operate at different power factors the DG is set to operate at a fixed power factor of 0.95 in Table 5.5.

Table 5.5: DG penetration level at a power factor of 0.95 for a sunny day

Case	P_{DG} **[kW]**	**Limiting factor**	$V_{\max}$ **Terminal**	$V_{\max}$ **[p.u.]**	ΔV_{tot} **[%]**	E_{loss} **[kWh]**	***TT***	PL_{DG} **[%]**	**Increase DG [%]**
1	5200	OV	T1	1.07	-0.27	3751	30	208	52
2	1140	RVC	T4	1.07	3	1677	32	46	66
3	440	RVC	T10	1.06	3	1899	24	18	47
4	1571	OV	T4	1.07	4.5	1807	30	63	44
5	2457	OV	T4	1.07	2.7	2039	30	98	56

The results obtained in the simulation confirm that it is possible to use reactive power control to increase penetration levels. On the simulated network with a low X/R ratio, penetration levels could be increased between 28 and 55% by operating at a power factor of 0.975. If the power factor is increased to 0.95 then the increase is between 44 and 66%. The reactive power offsets the voltage rise caused by the active power generation and therefore lowers the RVC level for the same active power. Reactive power control allows for increased DG penetration when the RVC and upper voltage limits are exceeded. This is unlike the OLTC and VR setpoint adjustment that can only increase DG penetration if the upper voltage limits are exceeded.

The RVC level of case 1 at a power factor of 0.975 is reduced substantially, even with greater injected active power, because of the close proximity to the substation transformer. The reactive power causes a large voltage drop through the transformer, because of the high transformer reactance. The tap changer compensates for the voltage drop in the steady state. When the DG disconnects, the voltage only changes slightly because the reactive power offsets the active power voltage rise. For case 1, at a power factor of 0.95, the voltage increases when the generation disconnects. The reactive power decreases the voltage more than the active power raises the voltage.

Operation at the maximum penetration limits with a constant power factor, for cases 2 and 3, causes the RVC level to remain the same as unity power factor. As a result, the number of tap changes per day and the average voltage fluctuation remains very similar with the higher penetration levels. The increased penetration reduces the losses, particularly if the amount of DG that is installed is less than the amount that gives lowest losses as calculated in Table 4.4. Increasing DG penetration with reactive power control lowers losses if the increased DG size reduces the net current in certain circumstances. This is discussed in more detail in the next section. For case 1 and 5, the losses are increased substantially because of the large amount of generation that is connected close to the substation. Generation connected close to the substation does not reduce the current flowing in the rest of the feeder and therefore has limited potential to reduce the feeder losses.

5.2.2 Loss and RVC reduction with reactive power control

It is typically understood that reactive power absorption will increase the losses of a feeder; however it was shown in the previous section that it can result in a net reduction in losses. Operating a generator at unity power factor will result in the lowest possible losses, if it causes a RVC of less than 3%. If the DG penetration is limited by RVC then the penetration level can be increased by using reactive power control. The 3% RVC limitation of a generator, at unity power factor, is often well below the point of minimum losses on weak parts of the network. This can be illustrated by plotting constant loss and constant RVC curves shown in Figure 5.9 to Figure 5.11. They are calculated using (4.15) and (4.8) for a specific power factor and DG power.

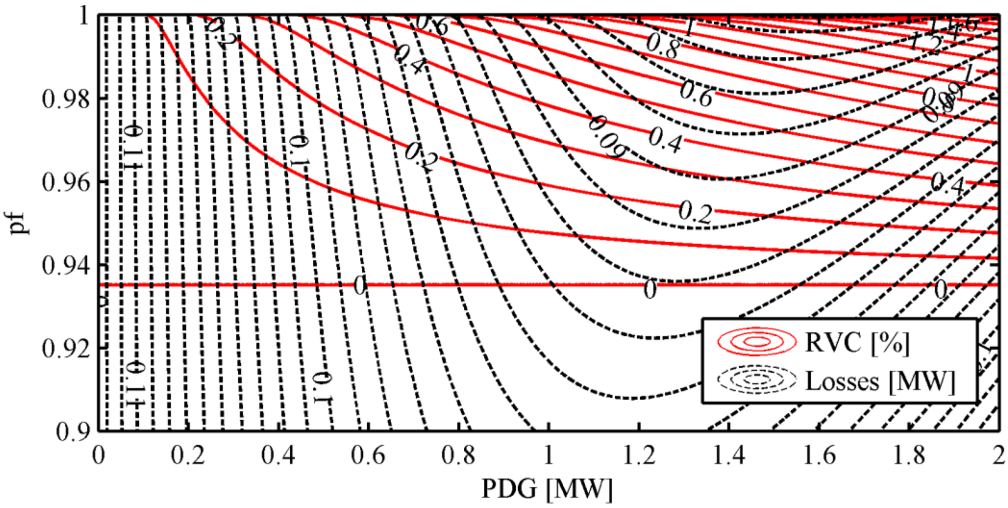

Figure 5.9: Constant loss and constant RVC curves of the test feeder for case 1

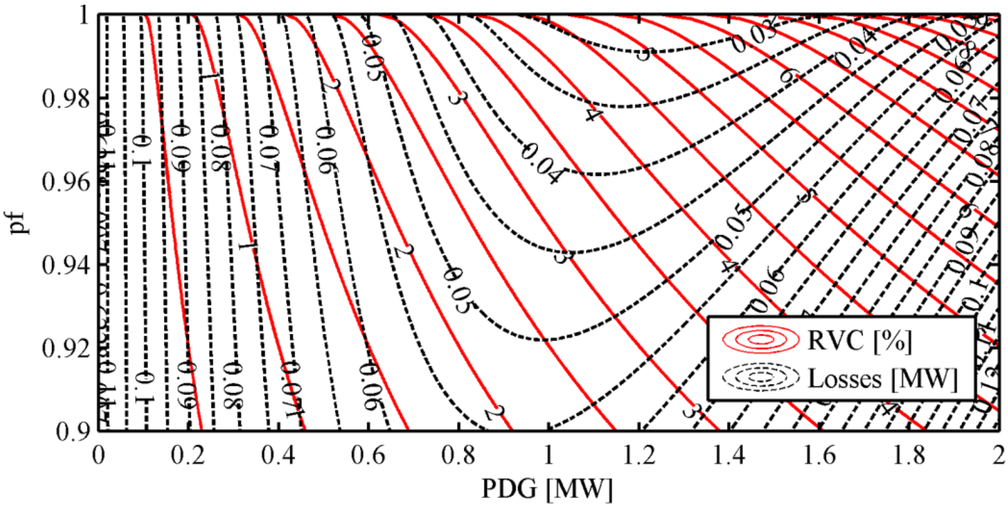

Figure 5.10: Constant loss and constant RVC curves of the test feeder for case 2

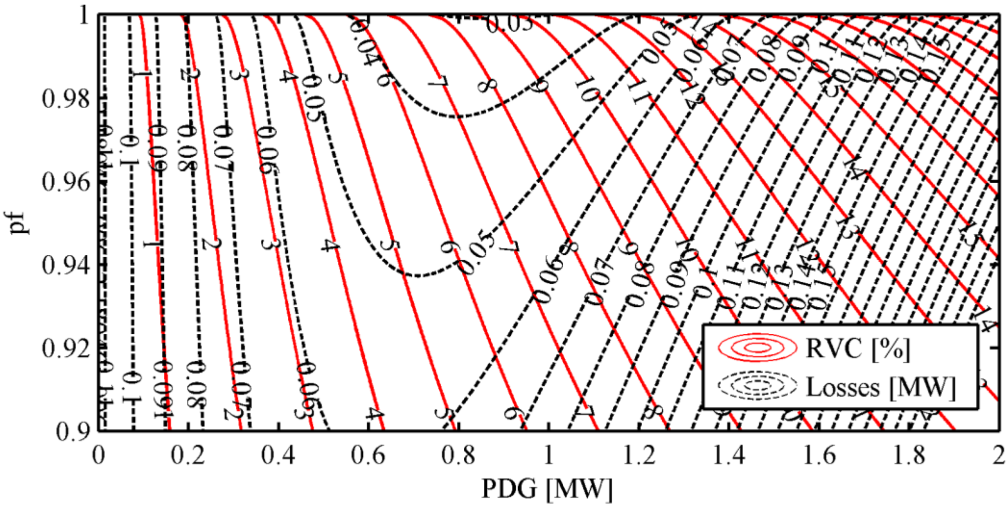

Figure 5.11: Constant loss and constant RVC curves of the test feeder for case 3

Figure 5.9, Figure 5.10 and Figure 5.11 show how the same RVC level can be maintained at higher DG power levels. It demonstrates how the losses are reduced up until a point, where increasing the power factor and DG power cause the losses to increase. In Figure 5.9 it is evident that reactive power control is not necessary for lowest losses operation, due to the strong connection to the grid. In Figure 5.10 RPC causes a loss reduction of around 10% at a RVC level of 3%, if operated at a power factor of 0.975. Similarly Figure 5.11 shows that RPC causes a loss reduction of about 9% at a power factor of 0.93.

While the losses are reduced on the test feeder, they might not be on other feeders. The loss reduction depends on the operating power factor of the feeder. If the feeder is operating at a low power factor, then reactive power absorption will increase the losses. Absorbing reactive power can lower the losses of a feeder, if the power factor of the feeder is high. One method of achieving a good feeder power factor is by installing an additional switched capacitor at the DG's location and controlling any switched capacitors with a reactive power controller instead of voltage control. The capacitor will supply the reactive power absorbed by the generator in the steady state and will place no additional strain on the transmission system. If the generator disconnects, the reactive power change is positive and the RVC of the generator is reduced. If the capacitor causes the feeder to export reactive power when the generator disconnects, then the capacitor can be switched out after a predetermined time period. This principle can be used to ensure that upon the disconnection of a generator during an auto-reclose operation, the voltage is supported by the capacitor until the generator is reconnected. As an example, consider Figure 5.12.

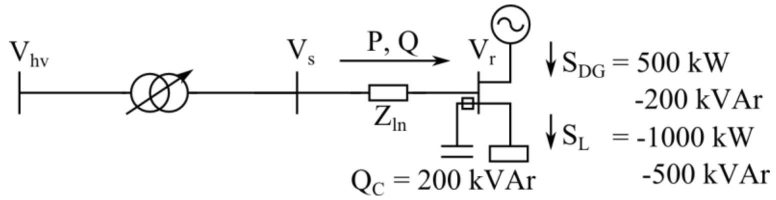

Figure 5.12: Line model and generator with locally supplied reactive power

When the generator is operating, the total load of the feeder is 500 kW and 500 kVAr. If the capacitor is installed with the generator, the generator places no additional reactive power requirements on the feeder. If the generator were to disconnect, the load of the feeder would change to 1000 kW and 300 kVAr. Therefore, the voltage drop from the sudden loss of active power will be compensated for by the reduced reactive power demand.

These results illustrate that it cannot be assumed that reactive power absorption by DGs will always causes an increase in the losses of a feeder. If the DG size that gives the lowest losses is greater than the calculated maximum DG size, then reactive power control can be beneficial to reduce losses.

5.2.3 Reactive power droop control

Droop control does not increase the penetration level when compared to constant power factor control, but it can reduce the use of reactive power by the DGs when it is not needed. The reduction of the reactive power requirement, in most operating conditions, results in reduced losses when compared to constant power factor control [10]. The voltage versus reactive power graph, for droop control, is shown in Figure 5.13. The terminology droop is specified as a percentage. It can also be represented by a droop coefficient *m* that is the droop percentage divided by 100. A 5% droop means that if the network voltage is differs by more than 5% from the setpoint voltage, the DG will either supply or absorb its maximum reactive power. The reactive power direction depends on whether the network voltage is above or below the setpoint.

Reactive power droop control of DG is traditionally implemented using a steady state droop line. By using a droop line, multiple DGs on a single feeder will share the load of the voltage regulation between them without causing instability [60]. In [26] a solution was provided to incorporate droop control when multiple DSTATCOMS are connected to a feeder.

The reactive power can be controlled using a proportional controller to a linear droop line. This results in a slow response for the DG to settle onto the line as it hunts for a stable operating point. The solution suggested by [26] is to use an integral controller to force the DG to operate on the droop line.

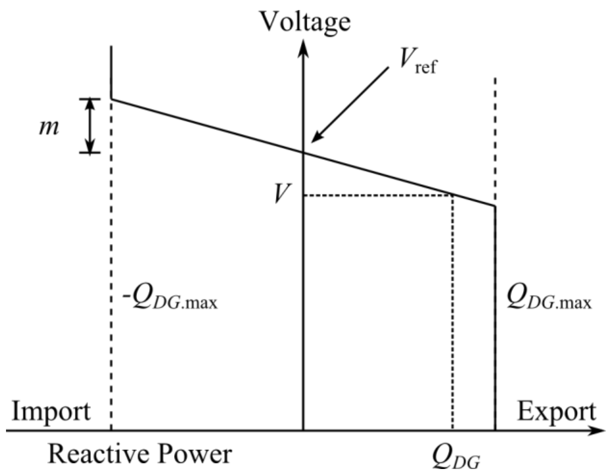

Figure 5.13: Reactive power droop control

The reactive power reference with droop control can be calculated using (5.9).

$$Q_{DG} = \frac{V_{\mathrm{ref}} - V}{m} \sin \phi_{\mathrm{r}} \tag{5.9}$$

Where V is the network voltage, V_{ref} is the reference voltage, m is the droop coefficient and ϕ_{r} is the rated power factor angle of the DG. The maximum reactive power can be related to the rated power of the DG and can be calculated using (5.10). A maximum power factor of 0.975 and 0.95 is selected for droop control.

$$Q_{DG.\max} = P_{DG.\max} \tan \phi_r \tag{5.10}$$

The sensitivity of the voltage magnitude to a change in real power can be found by including the DG power rating into (5.9) to get (5.11).

$$Q_{DG} = -\frac{V_{\mathrm{ref}} - V}{m} P_{\mathrm{r}} \tan \phi_{\mathrm{r}} \tag{5.11}$$

Differentiating (5.11) with respect to V gets (5.12).

$$\left.\frac{dQ}{d|V|}\right|_{V=f(P)} = \frac{dQ}{d|V|}\frac{d|V|}{dP} = \frac{1}{m} P_r \tan \phi_r \frac{d|V|}{dP} \tag{5.12}$$

Therefore the change in voltage with respect to a change in power can be represented by (5.13) and rearranged to get (5.15).

$$\left.\frac{d|V|}{dP}\right|_{Q=f(V=f(P))} = \frac{\partial |V|}{\partial P} - \frac{\partial |V|}{\partial Q}\frac{dQ}{d|V|}\frac{d|V|}{dP} \tag{5.13}$$

$$\left.\frac{d|V|}{dP}\right|_{Q=f(V=f(P))} \left(1 + \frac{\partial |V|}{\partial Q}\frac{dQ}{d|V|}\right) = \frac{\partial |V|}{\partial P} \tag{5.14}$$

$$\left.\frac{d|V|}{dP}\right|_{Q=f(V=f(P))} = \frac{\frac{\partial |V|}{\partial P}}{\left(1+\frac{\partial |V|}{\partial Q}\frac{dQ}{d|V|}\right)} \tag{5.15}$$

Substituting (5.12) into (5.15) we can find the voltage sensitivity for a single generator configured with droop control.

$$\Delta V = \frac{R\Delta P_{DG}}{(1+\frac{X}{m}P_r \tan\phi_r)} \text{if } \Delta V < m \tag{5.16}$$

In many cases droop control is used when there are multiple generators connected to the network. A single generator's change in active power will cause a voltage change at all other points on the network. Therefore, the reactive power contribution of all of the generators must be taken into account. A typical radial feeder with *n*-busses is shown in Figure 5.14. In this example there is a change in active power at the node V_{n-1}.

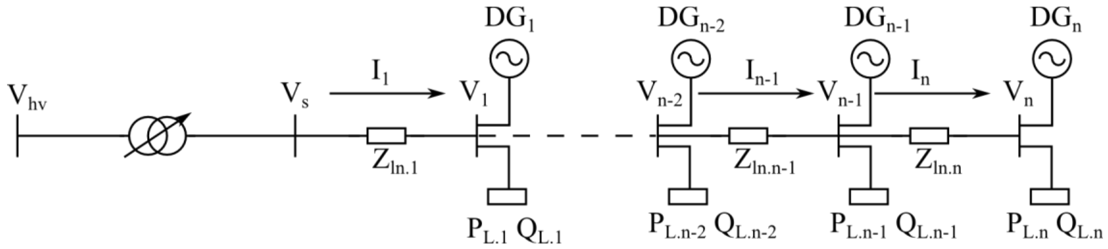

Figure 5.14: Feeder with many generators

The change in voltage can be calculated similarly to the way (5.16) was calculated. The voltage support of all of the generators on the feeder can be approximated using (5.17).

$$\begin{aligned}\Delta V_{n-1} &= R_{n-1}\Delta P_{n-1} - \frac{\Delta V_{n-1}X_{n-1}}{m_{n-1}}\tan\phi_{\mathrm{r}.n-1}P_{r.n-1} - \frac{\Delta V_1 X_1}{m_1}\tan\phi_{\mathrm{r}.1}P_{r.1} \\ &\quad .... - \frac{\Delta V_{n-2}X_{n-2}}{m_{n-2}}\tan\phi_{\mathrm{r}.n-2}P_{r.n-2} - \frac{\Delta V_n X_{n-1}}{m_n}\tan\phi_{\mathrm{r}.n}P_{r.n}\end{aligned} \tag{5.17}$$

The voltage change at all other locations on the network must be related to ΔV_{n-1}. It was shown in (4.7) that the change in voltage caused by a generator is equal at any location beyond the generator and proportional to λ before, assuming that the conductor is the same.

$$\begin{aligned}\Delta V_1 &= \frac{\lambda_1}{\lambda_k}\Delta V_{n-1} \\ \Delta V_n &= \Delta V_{n-1}\end{aligned} \tag{5.18}$$

Therefore (5.18) can be substituted into (5.17) to get (5.19).

$$\Delta V_{n-1} = R_{n-1}\Delta P_{n-1} - \frac{\Delta V_{n-1} X_{n-1} P_{r.n-1}}{m_{n-1}} \tan\phi_{\mathrm{r}.n-1} - \frac{\frac{\lambda_1}{\lambda_k}\Delta V_{n-1} X_1 P_{r.1}}{m_1}\tan\phi_{\mathrm{r}.1}$$
$$.... - \frac{\frac{\lambda_{n-2}}{\lambda_k}\Delta V_{n-1} X_{n-2} P_{r.n-2}}{m_{n-2}}\tan\phi_{\mathrm{r}.n-2} - \frac{\Delta V_{n-1} X_{n-1} P_{r.n}}{m_n}\tan\phi_{\mathrm{r}.n} \tag{5.19}$$

Rearranging (5.19) and solving for ΔV_{n-1} gives (5.20).

$$\Delta V_{n-1} = \frac{R_{n-1}\Delta P_{n-1}}{1 - \frac{X_{n-1}P_{r.n-1}}{m_{n-1}}\tan\phi_{\mathrm{r}.n-1} - \frac{\frac{\lambda_1}{\lambda_k}X_1 P_{r.1}}{m_1}\tan\phi_{\mathrm{r}.1} ... - \frac{\frac{\lambda_{n-2}}{\lambda_k}X_{n-2}P_{r.n-2}}{m_{n-2}}\tan\phi_{\mathrm{r}.n-2} - \frac{X_{n-1}P_{r.n}}{m_n}\tan\phi_{\mathrm{r}.n}} \tag{5.20}$$

Therefore the general form to (5.20) is shown in (5.21).

$$\Delta V_k = \frac{R_k \Delta P_k}{1 + \sum_{i=1}^{k} \frac{\lambda_i X_i}{\lambda_k m_i} P_{\mathrm{r}.i}\tan\phi_{\mathrm{r}.i} + \sum_{i=k+1}^{n}\frac{X_k}{m_i}P_{\mathrm{r}.i}\tan\phi_{\mathrm{r}.i}} \tag{5.21}$$
$$\text{if } \Delta V < m \text{ at all generators}$$

Each PV plant must be configured to regulate to a certain setpoint voltage with a specified droop. If all of the PV plants are configured with the same setpoint voltage, some of the DGs will absorb reactive power to lower the voltage and others will supply reactive power to raise the voltage. Alternatively, a unique setpoint voltage can be specified for each generator but that can pose a problem for the network operators. A unique voltage setpoint and droop coefficient could be calculated for each DG individually but they would need to be updated with any network changes.

A comparison between constant power factor control and droop control is shown in Table 5.6 with a total DG power of 1374 kW. The base case of 1090 kW of DG at unity power factor is given for comparison. In the simulations with droop control, each DG is configured with a setpoint voltage of 1.03 p.u.

Table 5.6: Voltage fluctuation percentage and number of tap changes on a cloudy day for different reactive power control strategies

Total generation configuration	**Average voltage fluctuation [%]**				***DT***			**E_{loss} [kWh]**	**Q-gen [kVAr]**
	MV BB	T4	T4-1	T10	OLTC	VR	Cap		
1090kW unity	0.15	0.77	0.9	1.4	2	38	2	1847	0
CPF 0.975	0.13	0.70	0.82	1.38	2	32	2	1844	-2758
CPF 0.95	0.15	0.61	0.7	1.24	2	24	2	1913	-3980
5% droop 0.975	0.1	0.68	0.76	1.25	2	32	2	1700	1055
5% droop 0.95	0.1	0.62	0.67	1.13	2	28	2	1688	1445

Both constant power factor control and droop control reduce the losses and average voltage fluctuation of the feeder with increased generation. Droop control provides the best voltage control of the feeder and the lowest losses. It allows for the DG to support the voltage during periods of high load and no generation. As a result of configuring each DG to regulate the voltage to 1.03 p.u., the net reactive power flow through the transformer is reduced. The DG's towards the end of the feeder supply reactive power while the DGs near the OLTC and VR absorb reactive power. Allowing the DGs to operate up to a power factor of 0.95, with droop control, provided substantial benefits to the feeder voltage control and reduces the losses.

The following figures show the issues with relying on only constant power factor control or standard droop control. In Figure 5.15 the DG is operated in constant power factor mode. The ratio of the voltage change caused by a change in active power is constant and only the DG that has a change in active power has a change in reactive power. A DG in constant power factor control mode cannot support the voltage during periods it does not generate active power. With constant power factor control each DG does not assist with reducing voltage changes caused by other generators' or loads' power changes.

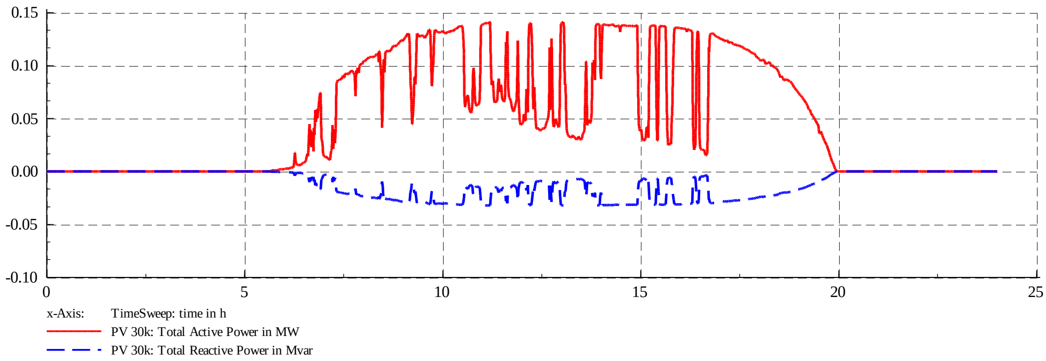

Figure 5.15: PV-30 km active and reactive power with constant power factor control at a power factor of 0.975

Droop control partially solves the problems of constant power factor control by distributing the voltage support among the generators on the network. The weakness with droop control is that generators, connected to strong sections of the network, do not compensate for their active power change as much as the generators connected to remote locations. Operating an individual generator with droop reactive power control, with a large droop coefficient, does not reduce the voltage variations as much as if it operated at a constant power factor.

For a generator to supply 100% of its rated reactive power with droop control, the voltage needs to change by the droop percentage specified for that generator. To allow each generator to offset its voltage change by supplying reactive power, the droop coefficient will have to be very small and custom configured for each generator. The droop coefficient will have to be calculated based upon the generator's rapid voltage change and the network sensitivity to active and reactive power changes at its location. The remote generators have to supply or absorb much more reactive power and there is an unequal sharing of reactive power support. This is demonstrated in Figure 5.16 where the reactive power of the generator at 3 km hardly varies even with large changes in active power. In Figure 5.17 the reactive power of the generator at 30 km varies much more with each change in active power.

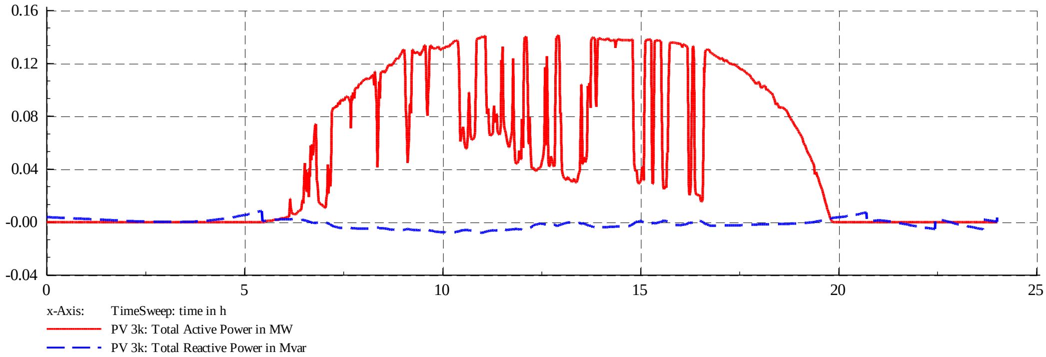

Figure 5.16: PV-3 km active and reactive power when using droop control with a maximum power factor of 0.975 on a cloudy day

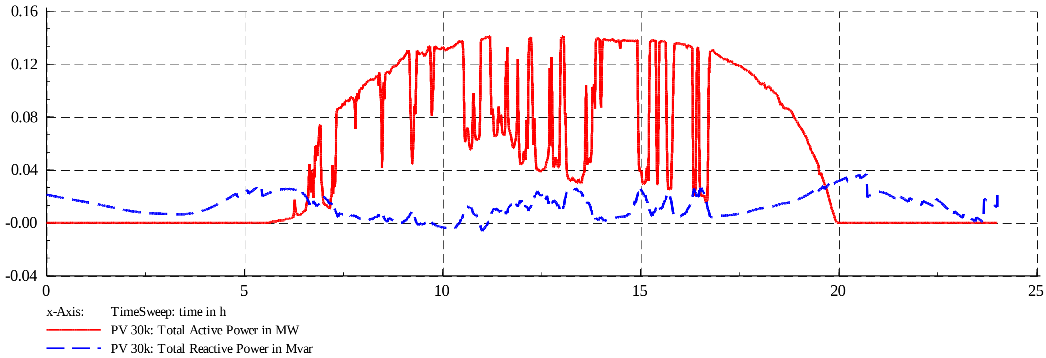

Figure 5.17: PV-30 km active and reactive power when using droop control with a maximum power factor of 0.975 on a cloudy day

5.2.4 Droop control modifications

It has been shown that standard droop control is beneficial to the operation of the test network, but it does have some disadvantages. These problems will be minimised with a few simple droop control modifications.

There are improvements that can be made to reduce the voltage variations further, while minimising reactive power drawn. Some of the methods that can be used to improve upon the basic droop control include:

1. Adapt the setpoint voltage based on current network operating conditions
2. Specify a power factor setpoint for droop control not equal to unity
3. Decrease the droop coefficient

The network operator would prefer the DGs to operate at unity power factor. The first of the modifications can be used to adjust the setpoint voltage for the droop control, based upon the average voltage of the DG for a defined period. By adjusting the setpoint voltage to the average voltage, the control aims to drive the reactive power to zero if the network is operating at a stable voltage. The DG will still respond to voltage variations caused by fluctuating power output. It will adjust the reactive power accordingly for short term voltage changes, but will ultimately rely on other voltage control devices for long term voltage control. An upper and lower bound can be specified for the setpoint voltage. When the voltage reaches the voltage constraints specified by the network operator, the generator provides the maximum amount of reactive power support.

The second modification allows for the DGs to operate at a specified power factor in the steady state, but also use a droop controller to limit voltage variations. The adjustment of the DG to operate with an offset droop line, allows for the RVC of the generator to be reduced in all operation cases. Operating a DG with an offset reactive power setpoint combines the advantages of constant power factor control with droop control and can further reduce the voltage variations. It also allows for easy network expansion if a single DG is initially connected to a feeder. The DG can be specified to operate in constant power factor mode with droop control. When additional DGs are connected to the network, they will each be able to support their own voltage and provide reactive power support for any voltage changes on the network. The modified reactive power setpoint can be calculated using (5.22).

$$Q_{DG} = P_{DG}.\tan\phi_{\text{set}} + \frac{V_{\text{ref}} - V}{m} P_{\text{r}} \tan\phi_{\text{r}} \qquad (5.22)$$

Where ϕ_{set} is the setpoint power factor angle.

Similarly to (5.16), the voltage sensitivity for a single generator can be calculated using (5.23).

$$\frac{d|V|}{dP} = \frac{R - X\tan\phi_{\text{set}}}{(1 + \frac{X}{m} P_r \tan\phi_r)} \text{if } \Delta V < m \qquad (5.23)$$

The voltage sensitivity due to a change in power at a certain generator, with voltage support contributions from the other generators, can be calculated using (5.24).

$$\frac{d|V|_k}{dP_k} = \frac{R_k - X_k \tan\phi_{\text{set}.k}}{1 + \sum_{i=1}^{k} \frac{\lambda_i X_i}{\lambda_k m_i} P_{\text{r}.i} \tan\phi_{\text{r}.i} + \sum_{i=k+1}^{n} \frac{X_k}{m_i} P_{\text{r}.i} \tan\phi_{\text{r}.i}} \qquad (5.24)$$
$$\text{if } \Delta V < m \text{ at all generators}$$

The droop slope can be modified so that the DG can supply or absorb more reactive power for smaller changes in voltage. The droop is often specified as 5% but can be decreased to further reduce the voltage variations. For example, a 5% droop can be specified based on the nominal apparent power of the DG, so that a 1.1% voltage difference from the setpoint causes the DG to operate at rated reactive power. The disadvantage of a reduced droop coefficient is that the DG will supply or absorb more reactive power for small deviations from the setpoint voltage. If the voltage setpoint is poorly configured, the network losses could be increased and the generator could permanently operate at rated reactive power. The voltage control capability could be limited if the voltage difference from the setpoint voltage constantly exceeds the droop. Ideally, the droop should be greater the further away the generation is placed from the substation, but for simplicity the droop is the same for all generators.

All of these modifications can be combined, thereby allowing the DG to operate at a fixed reactive power during steady state generation and zero reactive power when not producing active power. The droop controller allows the DG to provide reactive power support if a large voltage change were to occur.

Simulations are performed to determine the improvements that are made with the above modifications. The setpoint voltage is varied in the simulations with "AS" in the description and the setpoint can be varied between 1 p.u. and 1.04 p.u. Each generator has a rated power of 0.137 kW and power factor ϕ_r of 0.975. The power factors specified in the table indicate the fixed power factor setpoint ϕ_{set}. In each of the simulations the droop percentage is specified. The results of the simulations for case 4 are shown in Table 5.7.

Table 5.7: Voltage fluctuation percentage and number of tap changes on a cloudy day with the droop control modifications

Total generation configuration	**Average voltage fluctuation [%]**				***DT***			***E*** $_{loss}$ **[kWh]**	**Q-gen [kVAr]**
	MV BB	**T4**	**T4-1**	**T10**	**OLTC**	**VR**	**Cap**		
AS 5% droop unity	0.11	0.7	0.79	1.28	2	38	2	1730	-2
5% droop CPF 0.975	0.13	0.54	0.6	1.08	2	22	2	1797	-1376
2.5% droop	0.11	0.59	0.64	1.12	2	24	2	1682	1701
AS 1.1% droop	0.16	0.45	0.48	0.85	2	24	2	1727	-21
AS 2.5% droop CPF 0.975	0.15	0.5	0.56	0.99	2	24	2	1837	-2576
AS 2.5% droop CPF 0.9875	0.14	0.50	0.57	0.99	2	24	2	1806	-1892
AS 1.1% droop CPF 0.9875	0.16	0.4	0.44	0.80	2	22	2	1792	-1763

The results show that the voltage control of the feeder is improved with each of the modifications. The number of VR tap changes is substantially reduced when compared to the standard droop. It is evident from the simulations that the best voltage control improvement comes with the reduction of the droop percentage. The adaptive setpoint allows for the reduced droop percentage to be effective across the wide range of voltages experienced during a typical day and requires almost no total reactive power. Operating the generators with fixed power factor and droop settings reduced the voltage variations slightly more but required substantially more reactive power. It would have to be decided if it would be preferred to operate the generators with a larger droop percentage with a power factor setpoint of unity or to have the constant power factor setpoint with droop.

The reactive power demand of the entire feeder combined does not vary nearly as much as each of the individual generators when looked at individually. The droop control ensures that the reactive power change of the entire feeder is minimised even when there are large changes in active power. If the power profile of the substation transformer in Figure 5.18 is compared to the profiles of the PV-3 km plant in Figure 5.20 and the PV-30 km plant in Figure 5.19, it is evident that the reactive power of each generator varies significantly more than the transformer's reactive power over short time periods.

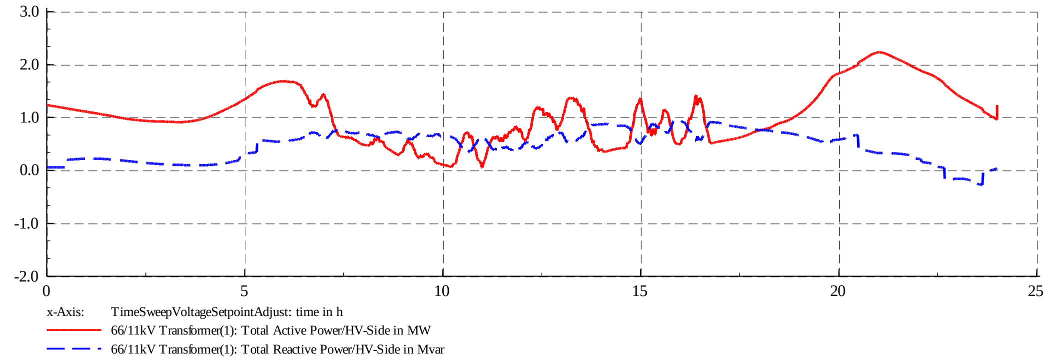

Figure 5.18: Reactive power requirements of the feeder for adaptive voltage setpoint at a power factor of 0.9875 and droop percentage of 1.1%

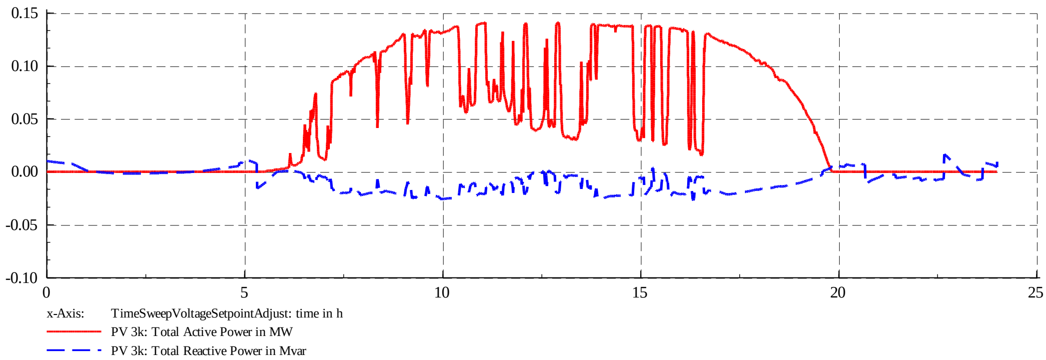

Figure 5.19: PV-3 km active and reactive power with adaptive voltage setpoint at a power factor of 0.9875 and droop percentage of 1.1%

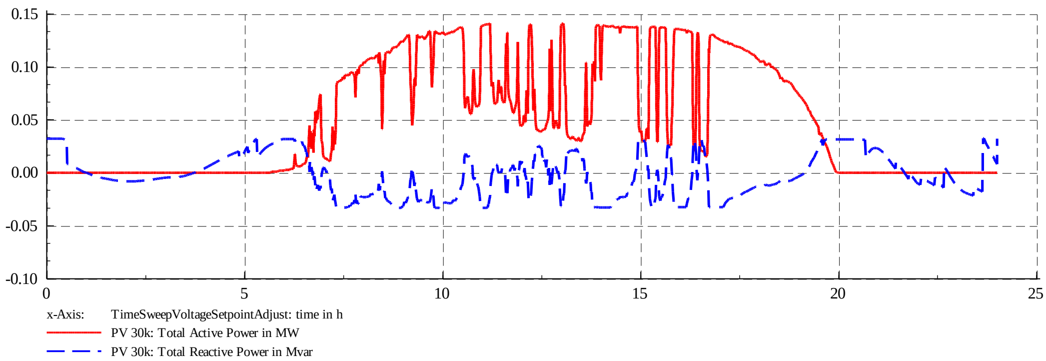

Figure 5.20: PV-30 km active and reactive power with adaptive voltage setpoint at a power factor of 0.9875 and droop percentage of 1.1%

The reactive power control improvements still cause the generators towards the end of the feeder to provide most of the reactive power control contributions, but Figure 5.20 shows that the fixed power factor of the PV-3 km generator allows it to compensate for more of its voltage changes. The PV-30 km generator in Figure

5.20 has effectively double the reactive power control capability with the increased droop because the generators reactive power can vary from a leading to lagging power factor to compensate for voltage changes.

The voltage profile of the feeder is improved from both the standard droop control and constant power factor control. Figure 5.21 shows the voltages and tap positions of the feeder when the generators rely on constant power factor control. Figure 5.22 shows the voltages with the improved droop control. The voltages vary a lot less than when using constant power factor control. The reduction of the VR tap changes during the day can also be seen clearly in Figure 5.22. The total number of tap changes is reduced and the use of a few taps is reduced substantially and will prevent taps 6, 7 and 8 from being overused in this example. This could have a large impact on the lifetime of a VR if the use of overused taps is reduced.

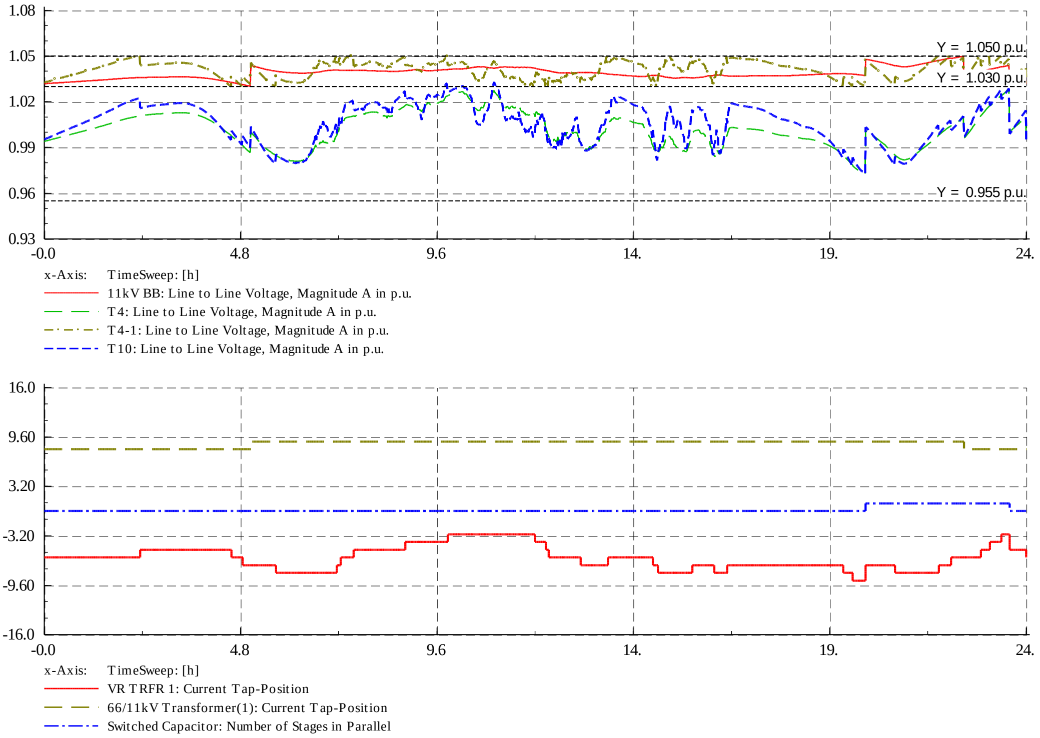

Figure 5.21: Voltages and tap positions for 1374 kW of DG operated with constant power factor control at a power factor of 0.975 on a cloudy day

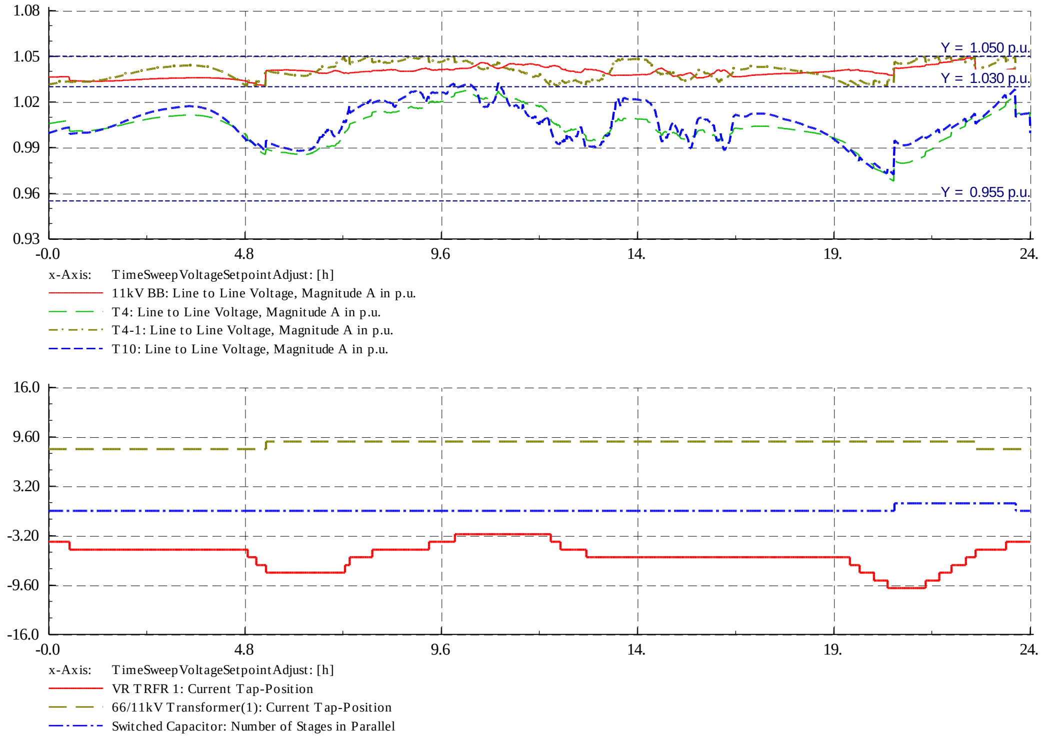

Figure 5.22: Voltages and tap positions for 1374 kW of DG operated with an adaptive voltage setpoint, at a power factor of 0.9875 and droop of 1.1% on a cloudy day

The various methods of reactive power control can be compared by plotting the voltage sensitivity to a change in power at a particular bus. An example is shown in Figure 5.23 for a change in power of a 100 kW plant at T5.

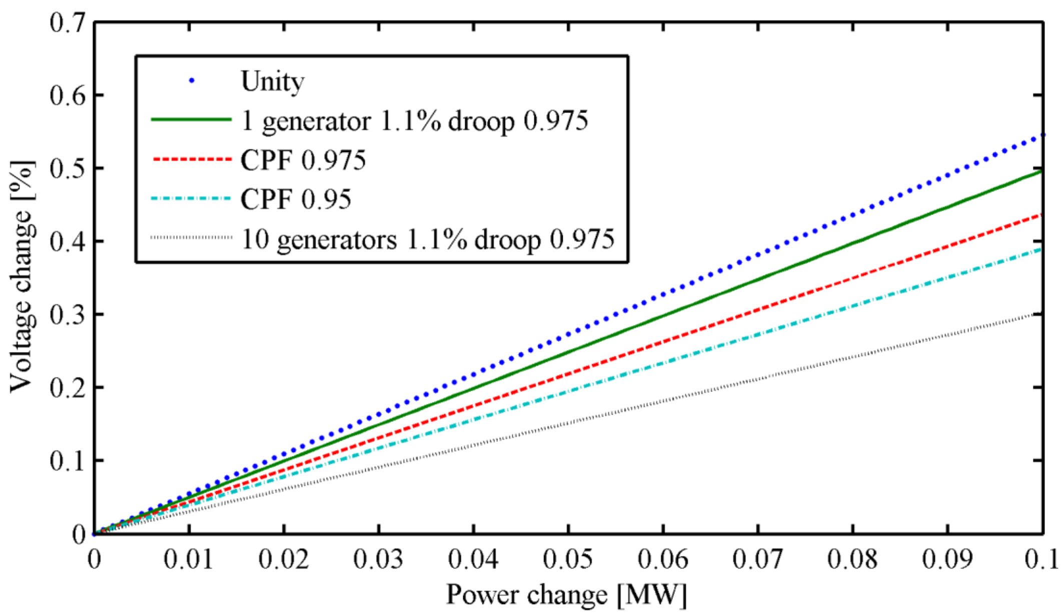

Figure 5.23: Voltage sensitivities for a change in power at PV-15 km with the various methods of reactive power control

The graph is plotted using the voltage sensitivity equations that were developed for unity, constant power factor and droop control. It can be seen that the reactive power support provided by multiple generators, configured with droop control, reduces the voltage variations the most. With a single generator, constant power factor control reduces the voltage change the most, when compared to a 1.1% droop for a generator size of 100 kW.

5.2.5 Reactive power control with a series inductance

The reactance of a feeder can be increased by installing a fixed inductor, variable inductor or thyristor controlled series compensator along it. A fixed inductor has the benefit of being cheap and easy to install, but at the cost of reduced controllability. A greater X/R ratio can cause increased voltage drop under high load and increased voltage rise during low load, especially if a fixed capacitor causes the feeder to operate at a leading power factor.

A thyristor controlled series compensator consists of a controllable inductor and capacitor, but a series capacitor is not needed on distribution feeders, because the reactance is already very low. A variable inductor can be installed in series along a distribution line to increase the X/R ratio of the line as seen by the generator [5], [23]. The inductor can be installed between the substation busbar and the feeder, as a solution to prevent violation of voltage limits during periods of minimum load and high generation. By installing an inductor to increase reactance of a particular feeder, the feeder's voltage can be better controlled when modifying the busbar voltage is not a practical solution. The inductance should only be connected when necessary, because it is undesirable in normal operation and causes a greater voltage drop during high load [23].

a) b)

Figure 5.24: a) Fixed inductor or b) variable inductor

The variable inductor was proposed in [23] as a solution to prevent violation of voltage limits during periods of low load and high generation. A variable inductor can be controlled and therefore help maintain adequate voltage levels during all loading conditions. It was proposed that an inductor is connected in parallel with two anti-parallel thyristors. In this configuration the reactance can be removed during normal operation and added when needed.

Increasing the reactance of the feeder provides maximum benefit when the DG actively controls the voltage. If fixed power factor operation of the DG's is used, then the inductor will be detrimental to the voltage variations experienced on the feeder. The variation of reactive power by the loads has a greater effect on the voltage if there is added inductance. The RVC level of the generator will be lower with the inductor installed, but the increased voltage variations will cause an increase in the number of tap changes on the feeder.

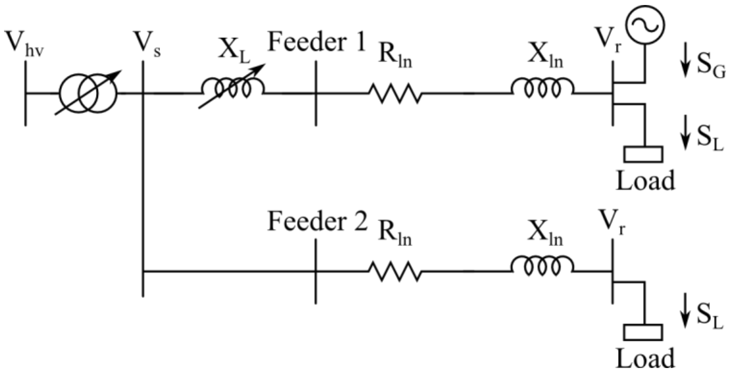

Figure 5.25: Installation of variable inductor

To test the effect of adding an inductor in series with the line, an inductor is placed at the beginning of the feeder as shown in Figure 5.25. The inductor size is selected as 10 mH or approximately equivalent to the reactance of 11 km of Hare line.

The penetration limit is assessed for the DG operating at a power factor of 0.975 and 0.95. Figure 5.26 and Figure 5.27 show the effect of installing a series inductor at the beginning of the feeder.

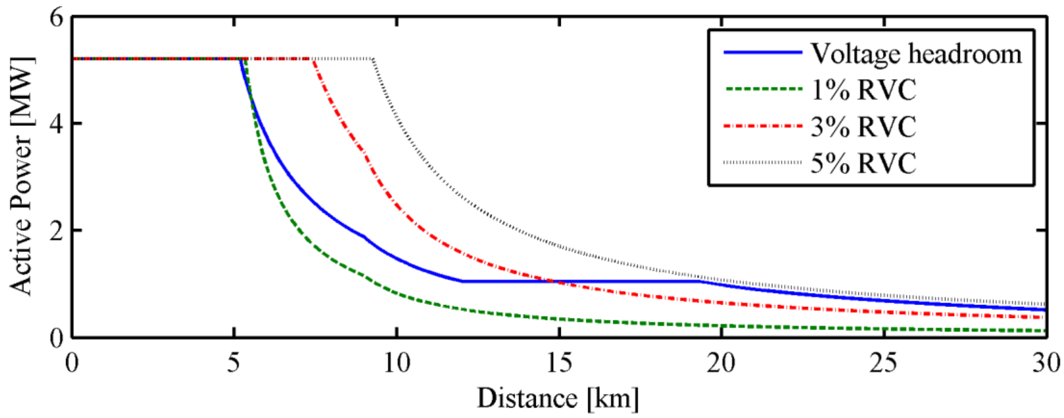

Figure 5.26: Maximum DG penetration when making use of reactive power control and a 10 mH series inductor at a power factor of 0.975

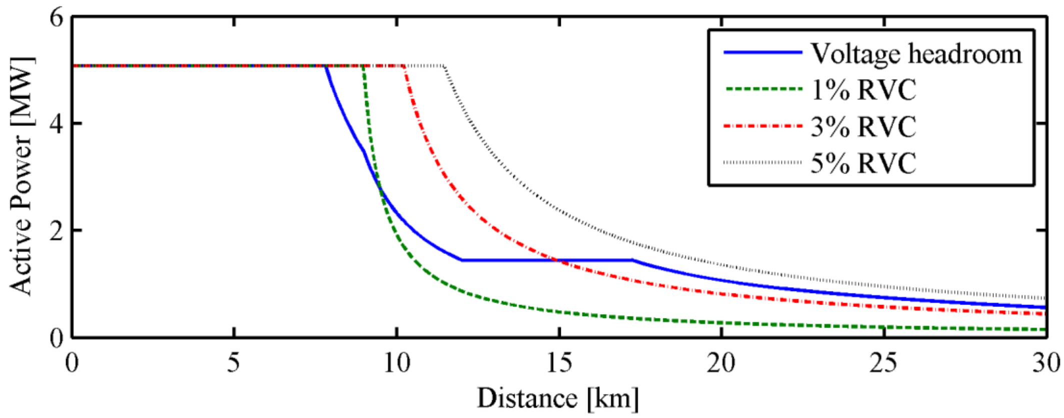

Figure 5.27: Maximum DG penetration when making use of reactive power control and a 10 mH series inductor at a power factor of 0.95

The RVC of the generators is reduced substantially and the voltage headroom is increased during minimum load, providing that the generator absorbs more reactive power than the excess reactive power generated by the overrated fixed capacitor.

It was found that for case 1 the addition of an inductor did not provide substantial benefits, as very little reactive power is needed for the generator to cause a zero RVC. Therefore, only cases 2-5 are tested. To calculate the losses and daily number of tap changes, the inductor is switched in during the day between 08:00 and 17:00. This minimised the impact of the inductor when it is not needed and provides improved voltage regulation during the evening periods when there is a large reactive power draw and no generation.

Table 5.8: DG penetration level with the DG operating at a power factor of 0.975 with a series inductor installed at the beginning of a feeder

Case	P_{DG} [kW]	Limiting factor	V_{max} Terminal	V_{max} [p.u.]	ΔV_{tot} [%]	E_{loss} [kWh]	TT	PL_{DG} [%]	Increase DG [%]
2	1100	RVC	T4	1.07	3	1671	30	44	60
3	400	RVC	T10	1.06	3	1905	28	16	33
4	1560	OV	T4	1.07	4.34	1699	34	62	43
5	6320	OC	T4	1.07	-4.5	5473	52	252	302

The series inductor increased penetration levels slightly more when compared to standard reactive power control at a power factor of 0.975. To determine the effect of allowing DG to operate at different power factors the DG is set to operate at a fixed power factor of 0.95 in Table 5.5. Case 1 and 5 were excluded because the power factor is too low for generators connected close to the substation with the series inductance.

Table 5.9: DG penetration level with the DG operating at a power factor of 0.95 with a series inductor installed at the beginning of a feeder

Case	P_{DG} [kW]	Limiting factor	V_{max} Terminal	V_{max} [p.u.]	ΔV_{tot} [%]	E_{loss} [kWh]	TT	PL_{DG} [%]	Increase DG [%]
2	1860	OV&RVC	T4	1.07	3	2064	40	74	171
3	509	RVC	T10	1.06	3	1881	28	20	70
4	1850	OV	T4	1.07	3.2	1897	46	74	70

If the DG’s are allowed to operate at a power factor of 0.95 there is a large increase in penetration when compared to standard reactive power control. DG’s up to 12 km from the substation raised the voltage when they were disconnected and operated at a power factor of 0.95.

The addition of a series inductor makes it evident that during periods of low load the feeder should always be operated with lagging reactive power to maximise DG penetration. The inductor is most useful at increasing penetration levels of DG connected towards the end of the feeder, by reducing the RVC level. Some simulations are performed to determine if the series inductor increases the controllability of the feeder. The results are shown in Table 5.10. The simulations were performed for case 4 with 1374 kW of installed DG so that the results are easy to compare to Table 5.7.

Table 5.10: Voltage fluctuation percentage and number of tap changes on a cloudy day with a series inductor

Total generation configuration	**Average voltage fluctuation [%]**				***TT***			***E*$_{loss}$ [kWh]**	**Q-gen [kVAr]**
	MV BB	**T4**	**T4-1**	**T10**	**OLTC**	**VR**	**Cap**		
CPF 0.975	0.12	0.71	0.8	1.35	2	34	2	1861	-2748
CPF 0.95	0.15	0.60	0.67	1.23	2	28	2	1932	-3978
0.975 5% droop	0.1	0.7	0.74	1.23	2	32	2	1701	1304
0.95 5% droop	0.1	0.62	0.67	1.14	2	30	2	1691	1732
AS 1.1% droop CPF 0.9875	0.14	0.37	0.39	0.75	2	20	2	1802	-1623

These results show that the addition of a 10 mH inductor at the beginning of a feeder does not increase the reactive power controllability of the feeder dramatically. It reduces the magnitude of the voltage change due to the tripping of the DG but, for voltage variations throughout the day, the average voltage variation is only reduced by 0.05% when the adaptive droop control is used. The addition of a fixed series inductor during the day does not improve the voltage controllability of the feeder enough to justify the additional investment and increased complexity.

5.2.6 Central reactive power controller

The previous reactive power control strategies used local controllers to control each of the DG's local busbar voltage. A local controller can compensate for voltage fluctuations at the generators' location but does not allow for the total feeder reactive power flow to be minimised or a single bus voltage to be optimised. A central controller is implemented that controls the reactive power through the substation transformer. The reactive power setpoint is 0 kVAr. The results are shown in Table 5.11.

Table 5.11: Voltage fluctuation percentage and number of tap changes on a cloudy day with a central reactive power controller

Total generation configuration	**Average voltage fluctuation [%]**				***TT***			***E*$_{loss}$ [kWh]**	**Q-gen [kVAr]**
	MV BB	**T4**	**T4-1**	**T10**	**OLTC**	**VR**	**Cap**		
1374 kW zero Q setpoint	0.05	0.65	0.77	1.25	0	32	2	1619	5814

The central controller reduces the voltage fluctuations when compared to constant power factor control but requires a large amount of reactive power from the generators to do so. The OLTC does not tap change because MV bus bar voltage varies slightly with no change in reactive power. The losses are the lowest for any of the reactive power control solutions because there is zero reactive power flow in the feeder. This simplified approach to a central controller does not provide enough benefits to justify the cost of installing adequate communication between all generators.

5.2.7 Reactive power sources

Reactive power used by DGs, to regulate the voltage, must be supplied by a device or machine somewhere on the network. As has been seen from the previous simulations, the reactive power requirement can vary dramatically when there are sudden changes in active power generation. There are a few possibilities that are investigated for the supply of reactive power to the DG.

1) Switched capacitors
2) Static VAr compensator (SVC)
3) STATCOM

For each additional MW of generation connected to the feeder either 222 kVAr or 328 kVAr of reactive compensation will need to be added to the feeder. For switched compensation, such as capacitors, they should be placed as close to the generator as possible. They should be configured with reactive power controllers so that they can supply the reactive power directly to the generator as previously discussed.

It is recommended that any dynamic reactive power compensation devices are added to the HV side of the substation. The reactive power control capability of the DG is maximised, as they can use the transformer as a form of added reactance to decrease the RVC. The SVC and DSTATCOMS have the advantage that they can compensate the reactive power drawn by the substation completely and can therefore keep the reactive power flow from the transmission grid to a minimum. It would appear that for cases with a single large DG, the reactive power requirement of the generator could vary substantially. Dynamic compensation might be beneficial to supply the reactive power in these cases. When many DGs are connected to the feeder and each is operated in droop control mode, there is a more constant draw of reactive power as shown in Figure 5.18. The constant draw of reactive power could be supplied by a switched capacitor and the small variations could be absorbed by the transmission system.

5.3 Electronic voltage regulator

It is apparent from the simulations presented in the previous sections that the RVC level and voltage variations, caused by PV generation, becomes the main limiting factor when attempting to connect more generation to the network. In this section it is proposed that the standard voltage regulator is replaced with an electronic voltage regulator (EVR). The EVR reduces the RVC level of generators installed on the network and therefore allows for increased DG penetration. There are two methods of regulating the voltage with an EVR. The first is a discrete method that utilises transformer taps exactly like a normal VR. The second is a continuously regulating method that utilises an AC/AC converter and provides a constant output voltage. The discrete EVR will be referred to as a DEVR and a continuously regulating EVR will be referred to as a CEVR.

5.3.1 Theory

The basic theory of the DEVR and CEVR will be covered here. The layout of a DEVR is shown in Figure 5.28 and is very similar to that of a normal VR, except the mechanical taps have been replaced by thyristors. The number of thyristors can be limited by using bucking or boosting switch thyristors that effectively allow the same taps to be used to buck or boost the voltage. The advantage of using thyristors, instead of a mechanical tap changer, is that any tap can be switched to instantaneously. Similarly to a VR, the DEVR has 16 taps that gives +-10% regulation with a step size of 0.625%. The DEVR could be expensive to manufacture due to the large amount of thyristors that will be required to build it.

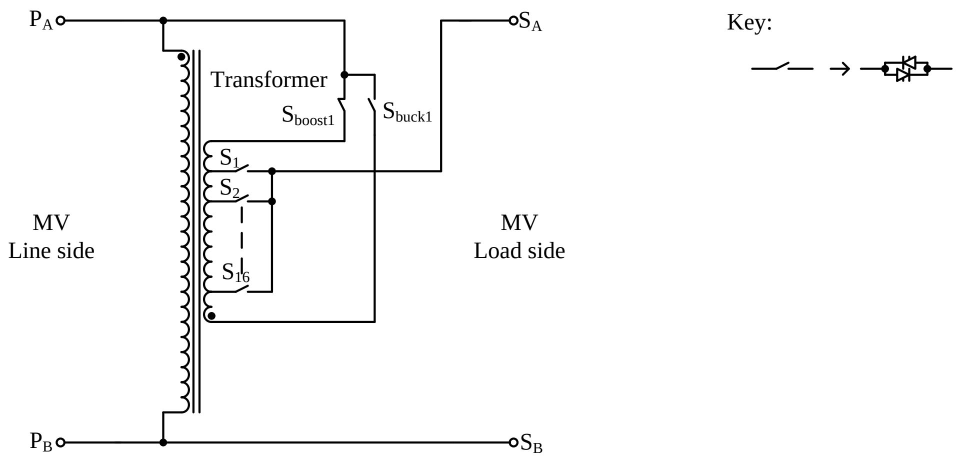

Figure 5.28: Schematic diagram of the DEVR showing the autotransformer and thyristor switch modules

The CEVR is under development and discussed in [61], [62]. A basic overview is shown in Figure 5.29. The CEVR uses an AC/AC converter connected to an autotransformer. The CEVR effectively provides an infinite number of taps within the 10% regulation range. The CEVR's topology ensures that control is only applied to 10% of the line voltage and therefore the converter's power requirement is only 10% of the transmitted power.

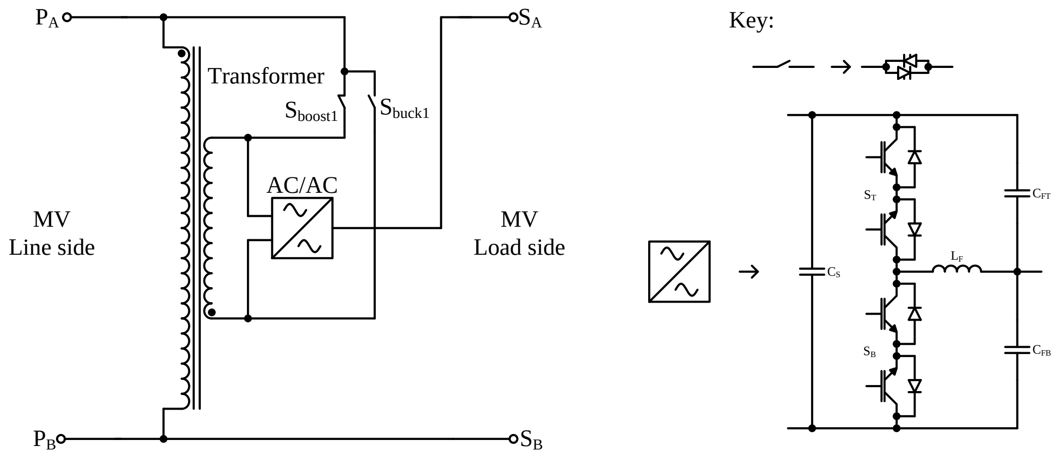

Figure 5.29: Schematic diagram of the CEVR showing the autotransformer and AC/AC converter module

The EVR can be designed to include various protection devices to ensure that the reliability, of the electricity supply to customers beyond the device, is unaffected. Overvoltage and overcurrent protection should be included in the device. Thyristors can be used as a crowbar to bypass the EVR during periods of overvoltage and short circuited faults. The bypass should be configured to be failsafe to ensure that customers are not without power if the device fails. It would be possible for an EVR to perform additional functions including: correcting voltage imbalance, harmonic compensation and limited waveform correction [62]. These characteristics, along with the reduction of the RVC level, beyond the regulator connection point, are the main reasons why the EVR is ideally suited for use on networks with variable generation. Both of the EVRs do not rely on a mechanical tap changer to regulate the voltage and therefore voltage variations that would accelerate the wear of a regular VR can be handled without further reducing the life of the device.

A constant output voltage is maintained for any input voltage variations that fall within 10% of the setpoint voltage. This means that for an output voltage of 1 p.u., the input voltage can vary between 0.9 p.u. and 1.1 p.u. This section aims to show how an EVR is ideal for use on networks with a high penetration of DG and how they can contribute to improving the power quality of the network.

A comparison of the output voltages is shown in Figure 5.30 for a step change in load on the secondary terminal of a VR, CEVR and DEVR. The CEVR's output remains constant and the DEVR's output varies within its bandwidth. The VR takes multiple periods of its time delay to bring the voltage back within acceptable levels.

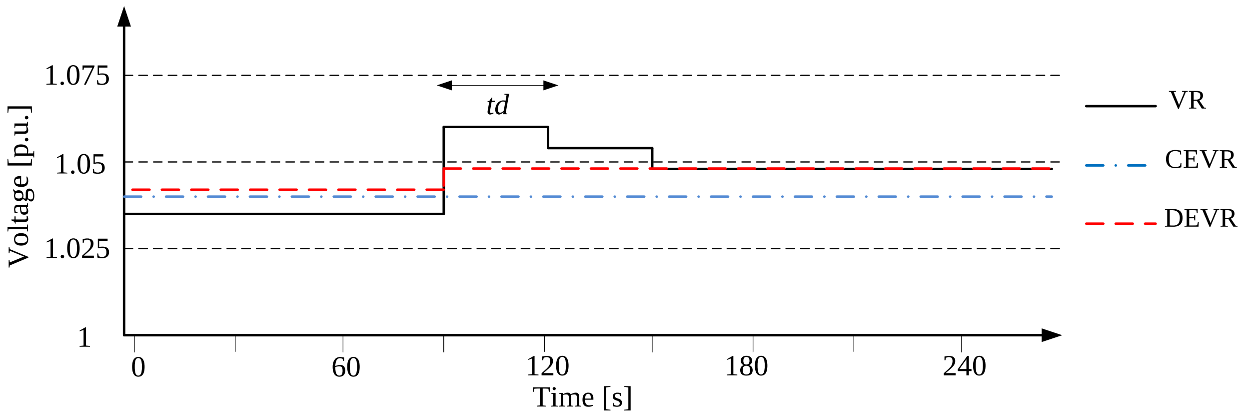

Figure 5.30: Response to a step change in load for a VR, CEVR and DEVR

When using the EVR to reduce the RVC on networks, the amount of DG that can be connected to the network is increased. It should be noted that the RVC level at the primary side of the regulator will remain the same. Therefore, DG size nearby to the EVR is limited by the both the RVC experienced at the primary side of the regulator and the RVC experienced at the DG location. The RVC at each point can be calculated using (5.25).

$$\begin{aligned} \Delta V_{RVC.DG} &\approx \frac{R_{\ln.\lambda_{DG}} P_{DG} + X_{\ln.\lambda_{DG}} Q_{DG}}{V_{\text{nom}}} - \frac{R_{\ln.\lambda_{EVR}} P_{DG} + X_{\ln.\lambda_{EVR}} Q_{DG}}{V_{\text{nom}}} \\ \Delta V_{RVC.EVR} &\approx \frac{R_{\ln.\lambda_{EVR}} P_{DG} + X_{\ln.\lambda_{EVR}} Q_{DG}}{V_{\text{nom}}} \end{aligned} \tag{5.25}$$

Figure 5.31 shows the maximum DG size limited by RVC levels for the test network if an EVR replaces the VR at 12 km.

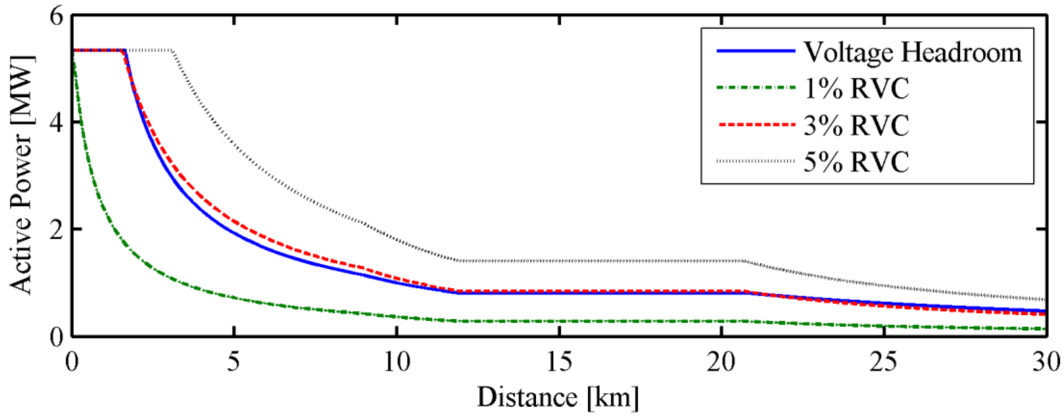

Figure 5.31: Maximum DG size for different RVC levels if an EVR is installed at 12 km

Multiple EVRs can be connected in series to increase the DG penetration level of the entire feeder. Figure 5.32 illustrates how the RVC penetration limit can be increased if two EVRs are connected in series. It should be noted that the penetration limit imposed by the voltage headroom might be restricting unless suitable control actions are performed on the OLTC and EVR setpoints. Any generation connected before the EVR will have no effect on the voltage profile of the feeder after the EVR; because any voltage fluctuations will be smoothed out. Therefore, an EVR can be installed on feeders that historically suffer from poor voltage quality.

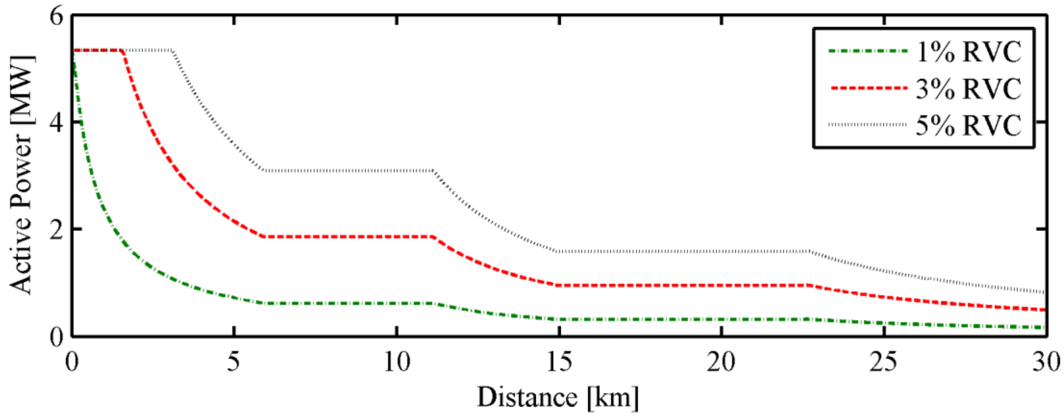

Figure 5.32: Maximum DG size for different RVC levels if an EVR is installed at 6 km and 15 km

For the purposes of this study, the CEVR is modelled as a three phase autotransformer with a continuous tap changer that provides a constant output voltage. The DEVR is modelled as a discrete tap changer with the bandwidth of the controller set to 0.008p.u. The number of 'tap changes' the device makes is not a concern but more the effect on the voltage regulation and voltage fluctuations on the feeder.

5.3.2 Simulations

The installation of the EVR requires that the control settings of any capacitors downstream of the regulator be updated. The voltage at the secondary terminals of the regulator is now held within a narrower band than the 0.02 p.u. of standard voltage regulator. Therefore the bandwidth of the capacitor voltage controller does not include the bandwidth of the voltage regulator controller. The voltage drop between the regulator and the capacitor during low and high load should now be the turn on and off settings for the capacitor. The reduced controller bandwidth can cause problems if the capacitor size is too large and the voltage change caused by switching the capacitor is greater than the bandwidth of the controller. An alternative would be to control the capacitor using the reactive power control method.

Simulations are done to investigate the difference in DG penetration levels if the VR is upgraded to one of the EVRs. The results are shown in Table 5.12 to Table 5.15. The first simulations are performed using a DEVR to determine whether the simpler EVR adequately compensates the voltage variations and increases installable DG capacity. The results for the DEVR are shown in Table 5.12 and Table 5.13.

Table 5.12: DG penetration level with the VR replaced by a DEVR

Case	P_{DG} [kW]	Limiting factor	V_{max} Terminal	V_{max} [p.u.]	ΔV_{tot} [%]	E_{loss} [kWh]	*TT*	PL_{DG} [%]	Increase DG [%]
1	3476	OV	T1	1.07	2.6	2472	4	139	1.4
2	910	OV	T4	1.07	0.9	1571	4	36	33
3	440	RVC	T4	1.06	3	1742	4	18	47
4	1115	OV	T4	1.07	2.75	1614	4	45	2.3
5	1550	OV	T4	1.07	3	1725	4	62	-1.3

Table 5.13: Voltage fluctuation percentage and number of tap changes on a cloudy day with a DEVR

Case	Average voltage fluctuation [%]				*DT*			E_{loss} [kWh]
	MV BB	T4	T4-1	T10	OLTC	DEVR	Cap	
1	0.27	11.22	0.94	1.06	4	170	2	2323
2	0.19	1.38	0.96	1.24	2	186	2	1747
3	0.15	0.85	0.83	1.7	2	116	2	1899
4	0.15	0.79	1.04	1.45	2	96	2	1818
5	0.15	0.8	1.05	1.27	4	98	2	1907

The results in Table 5.12 illustrate that the DEVR can increase DG penetration with a single generator substantially. It should be noted that the DEVR does not reduce the RVC for small generators. If the RVC caused by a generator is less than the bandwidth of the controller, the voltage change is not great enough for the DEVR to change taps. The DEVR does correct for a large RVC, caused by a single or multiple generators, if their output power suddenly changes.

The voltage fluctuations with a DEVR are substantially reduced when compared to the base values with a normal VR. However, the DEVR can actually increase the frequency of minor voltage fluctuations because of the increased number tap changes of the regulator. The number of tap changes for the EVR is shown to illustrate how many tap changes would be required by a standard VR to regulate the voltage in a similar manner.

The next simulations use the CEVR to show the improvements that are made if the voltage is continuously regulated. The results for the CEVR are shown in Table 5.14 and Table 5.15.

Table 5.14: DG penetration level with the VR replaced by a CEVR

Case	***P_{DG}* [kW]**	**Limiting factor**	***V_{max}* Terminal**	***V_{max}* [p.u.]**	**ΔV_{tot} [%]**	***E_{loss}* [kWh]**	***TT***	***PL_{DG}* [%]**	**Increase DG [%]**
1	3476	OV	T1	1.07	2.6	2472	4	139	1.4
2	910	OV	T4	1.07	1.16	1549	4	36	33
3	445	RVC	T4	1.06	3	1710	4	18	47
4	1115	OV	T4	1.07	3.16	1589	4	45	2.3
5	1460	OV	T4	1.07	2.6	1661	4	58	-7

Table 5.15: Voltage fluctuation percentage and number of tap changes on a cloudy day with a CEVR

Case	**Average voltage fluctuation [%]**				***DT***			***E_{loss}* [kWh]**
	MV BB	T4	T4-1	T10	OLTC	EVR	Cap	
1	0.3	1.2	0.22	0.35	4	178	2	2295
2	0.2	1.4	0.25	0.66	2	206	2	1698
3	0.17	0.85	0.2	1.24	2	128	2	1866
4	0.16	0.79	0.2	0.74	2	118	2	1792
5	0.18	0.8	0.2	0.55	2	122	2	1852

The CEVR increases penetration levels similarly to the DEVR and the voltage fluctuations are reduced further. Even with the increased penetration levels, the voltage fluctuations are reduced when compared to the results for the VR, in Table 4.3 and the DEVR in Table 5.13. For case 3 the DG penetration level is increased substantially because of the reduction of RVC. The average voltage fluctuation at bus 10 in case 3 is reduced from 1.56% to 1.24% even with 47% more DG installed at the bus.

The results in Table 5.12 and Table 5.14 show that the DEVR and CEVR would be a good option to improve the voltage variations, while increasing penetration levels. The EVR changes the main limiting factor for DG penetration from RVC to voltage rise. DG penetration is actually decreased in case 5 because there is a lower RVC level after the EVR. The increased generation connected after the EVR causes a greater voltage rise along the feeder. Additional measures will need to be taken to increase DG penetration further such that the over voltage is no longer a constraint.

The improved voltage along the feeder with an EVR is highlighted in Figure 5.35 and Figure 5.34, when compared to Figure 5.33. In the figures, a standard voltage regulator is compared to the two EVRs for case 2 during a cloudy day. It can be seen that the EVR visibly reduces the voltage fluctuations along the feeder, even though 33% more DG is installed at the location. The voltage at T-10 is controlled within a very narrow band and voltage variations at the end of the feeder should not affect customers at all. The voltage at T4 varies slightly more with the increased generation because the EVR has no effect on the RVC level on its source side.

The tap position of the EVR is given in Figure 5.35 and Figure 5.34, for illustrative purposes, to show how the EVR responds in real time to any voltage changes.

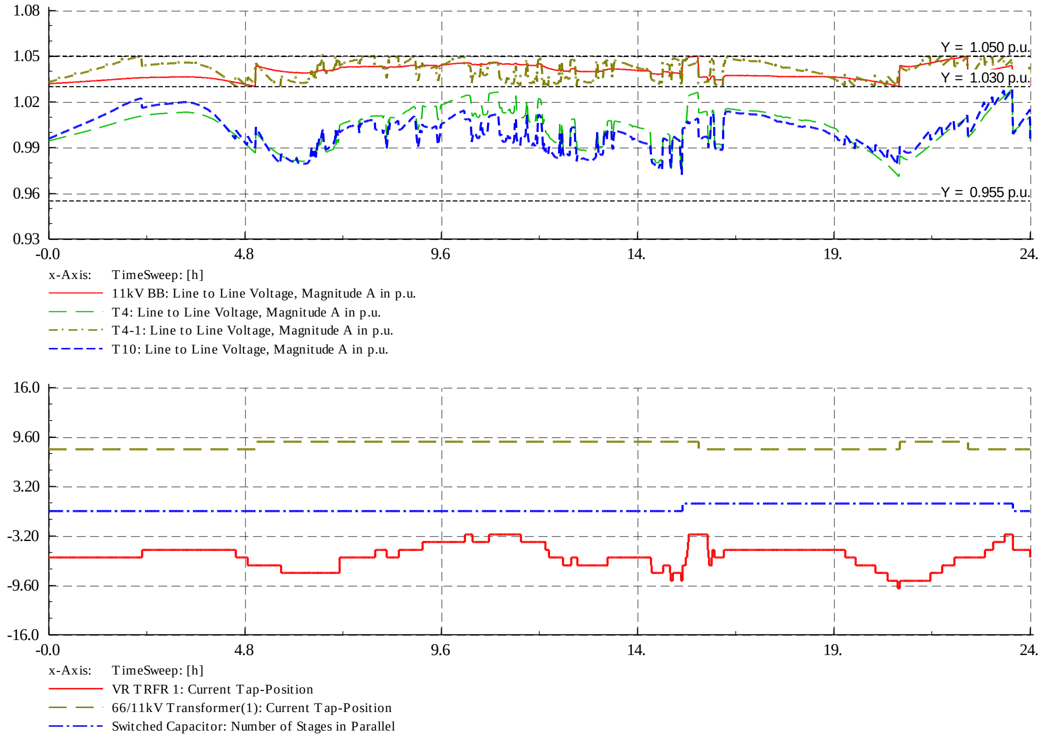

Figure 5.33: Voltage and the tap positions for case 2 (686 kW DG) using a standard VR

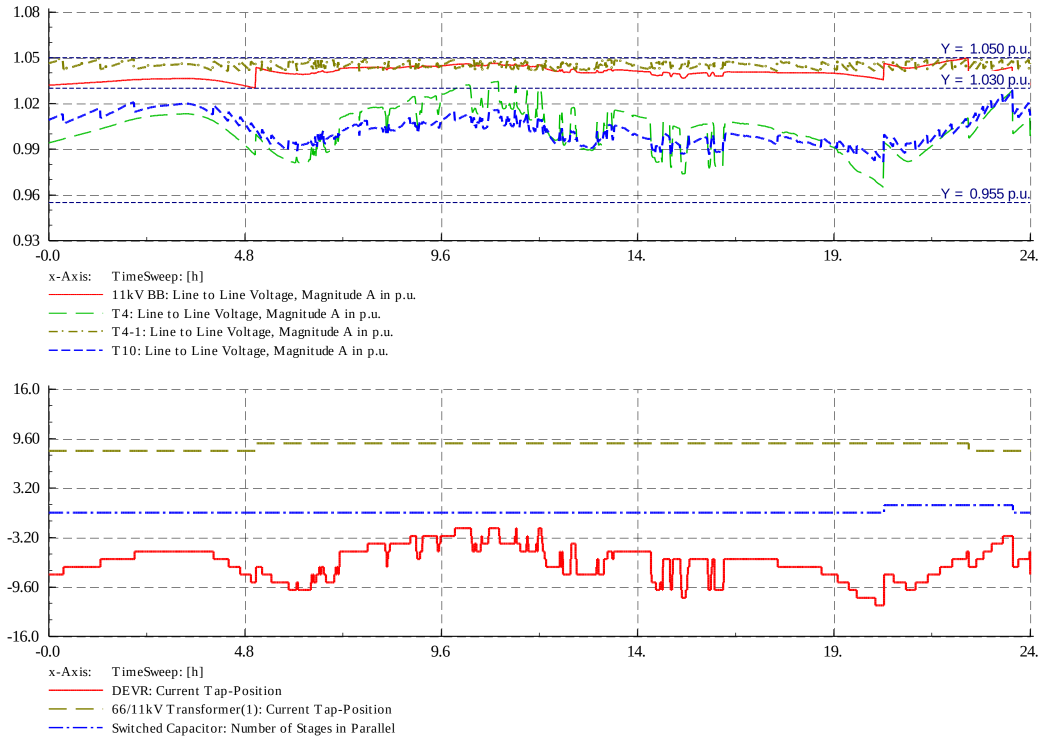

Figure 5.34: Voltage and the tap positions for case 2 (910 kW DG) using a DEVR

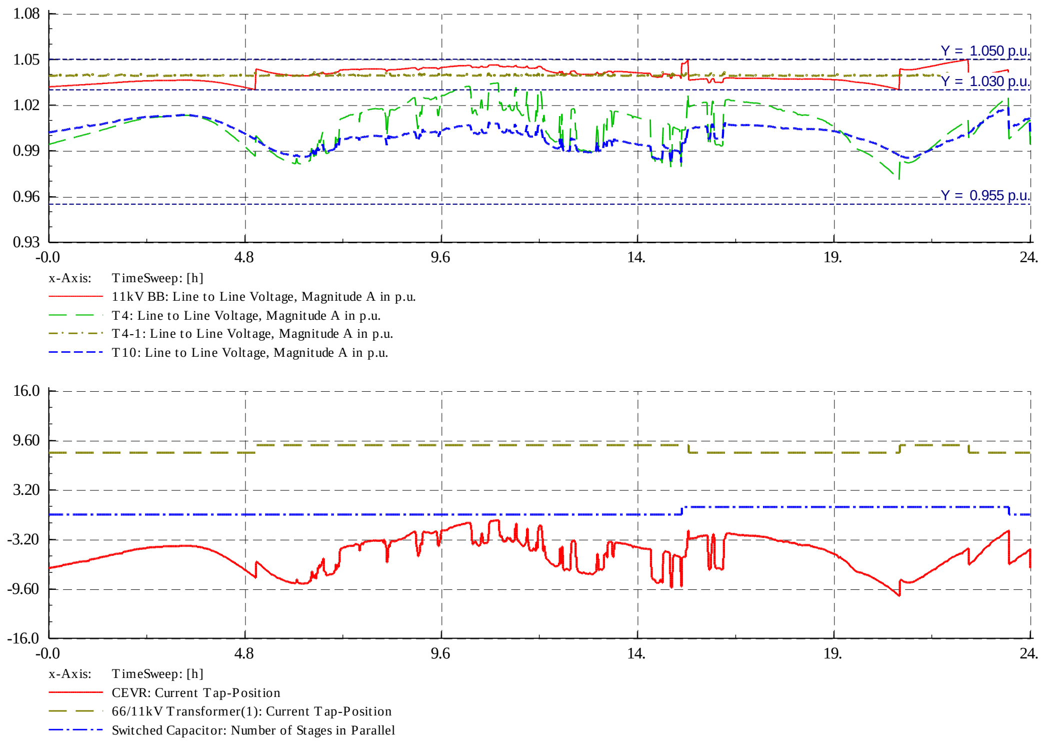

Figure 5.35: Voltage and the tap positions for case 2 (910 kW DG) using a CEVR

5.4 Network upgrade

Upgrading the network or a portion of it can be a viable option to increase the DG penetration level in certain circumstances. There are a few options to consider if a voltage regulator cannot solve the voltage regulation issues or if the line exceeds its current rating. These options are highlighted as possible solutions, but are not the focus of this thesis and in many cases will not be economically justifiable.

5.4.1 Voltage upgrade

A possibility to increase the amount of power that can be transferred by a power line is to upgrade the feeder voltage. The upgraded voltage effectively leads to a doubling of network capacity; however it comes at a considerable cost, because all of the transformers need to be replaced. Additionally the insulators along the line might need to be upgraded. In cases where a voltage upgrade is the only solution that allows for a particular DG application to be considered, a cost analysis should be done to determine whether the increased revenue will offset the cost of upgrading the line. It could be possible that the voltage upgrade is justifiable if the load forecast for the feeder would demand a voltage upgrade in the future. Figure 5.36 shows the DG penetration for a 3% voltage change if the line is upgraded to 22 kV. As can be seen in the figure, the installable DG at the same location doubles when compared to the base 11 kV network in Figure 4.8.

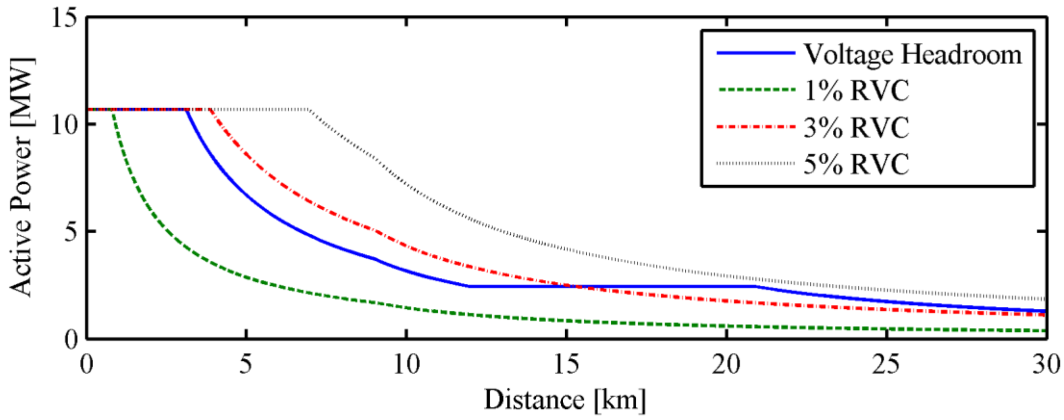

Figure 5.36: Maximum DG size for a particular change in voltage and voltage headroom, as a function of distance for varying power factors, if the voltage is upgraded to 22 kV

5.4.2 Conductor Upgrade

A more economical option than a voltage upgrade might be to upgrade the conductor along certain sections of the feeder. The increased conductor size will provide improved voltage regulation and therefore improve power quality. If the distance to the DG is small, the conductor between the substation and DG could be upgraded to allow for increased current carrying capacity. The increased conductor thickness would allow greater voltage controllability using reactive power, relative to the voltage drop/rise caused by the active power flow. Upgrading the conductor comes at considerable cost; however all of the existing transformers and equipment can still be used after the upgrade, unlike a voltage upgrade. The new conductor should be chosen to meet the economic loading limits as shown in Figure 3.15. This would ensure that the conductor is economical to operate at the required loading for the remaining lifetime of the feeder.

Figure 5.37 shows the DG penetration if the conductor of the test network is upgraded to Chicadee for the first 9 km and Hare for the remaining 21 km.

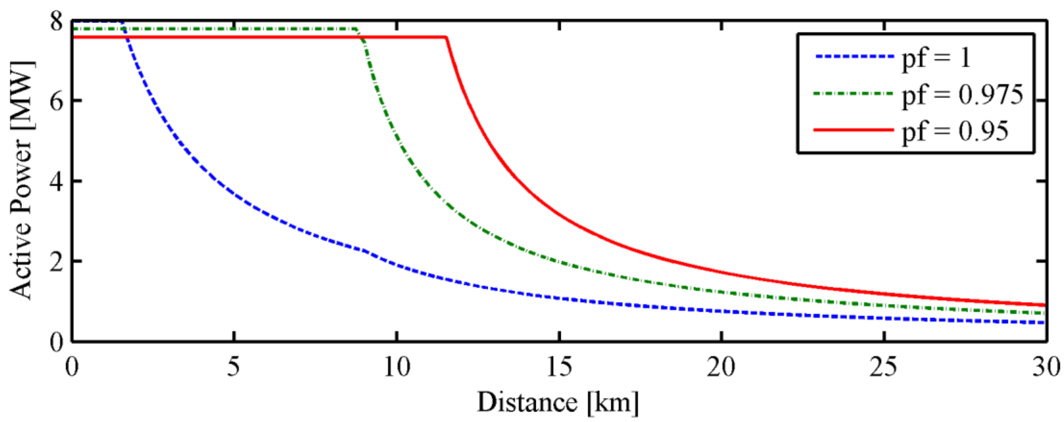

Figure 5.37: Maximum DG size for a 3% change in voltage as a function of distance for varying power factors if the Hare conductor is upgraded to Chicadee and the Mink to Hare.

The increased X/R ratio of the Chicadee conductor greatly increases the reactive power controllability of the line. Operating a DG plant at a power factor of 0.975 almost quadruples the installable capacity at 9 km when compared to operating at unity power factor.

To show the effect that upgrading the conductor has on the voltage at a bus and hence reactive power controllability, a simulation is performed. A range of power factors and three conductors with different X/R ratios are used. The basic line with load and generation model of Figure 4.5 is used. The line reactance is set at 1 Ohm and X/R ratio is varied to 1/3, 1 and 3. A real power current of 100 A is used and the apparent power is varied based upon the generators power factor. The result is shown in Figure 5.38. As can be seen, the upgraded line provides reduced voltage rise and maintains the same amount of voltage controllability per unit of reactive power.

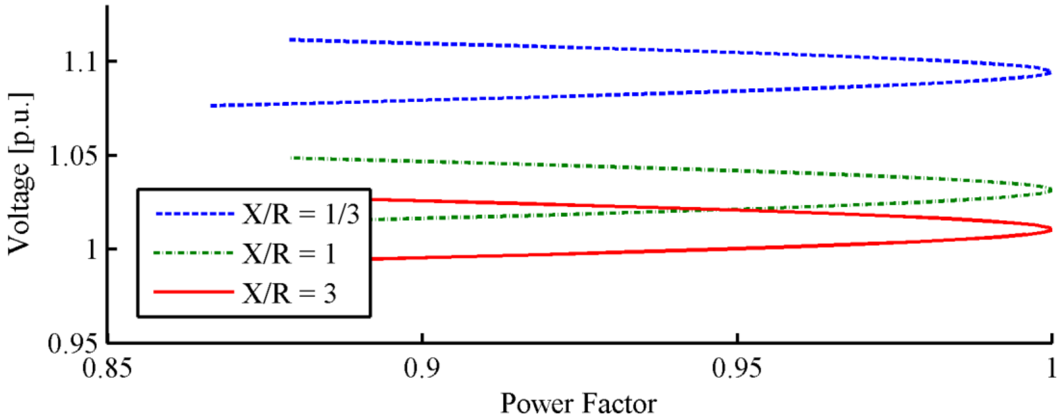

Figure 5.38: The receiving end voltage as a function of the power factor for different X/R line ratios

5.4.3 Dedicated line

A dedicated line is an expensive option to connect DG to a substation if it is more than a few kilometres away. A dedicated line provides the best integration capacity as the line is purpose built to carry the required generation to the substation busbar. In some cases with large DG, building a dedicated line might be the only solution. This method is Eskom’s preferred way of connecting DG to the grid as it does not impact existing customers and requires minimal change to the existing network. This method of connecting DG to the network will not be investigated further, as the aim of this work is to provide alternatives to building a dedicated line.

5.4.4 Increasing the minimum load

If voltage headroom during minimum load is limits DG penetration, a simple solution would be to increase the minimum load of a feeder. This can be achieved by encouraging people to use electricity during these time periods. Higher use during low load hours can be encouraged by using various forms of demand side management. For example Eskom could lower tariffs at these times. The maximum generator size for a doubling of the minimum load is shown in Figure 5.39.

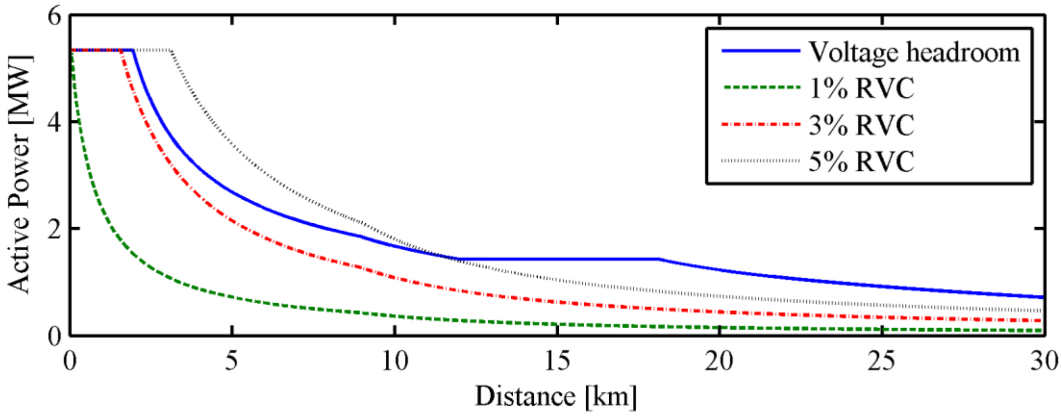

Figure 5.39: Maximum DG size for a particular change in voltage and voltage headroom, as a function of distance for varying power factors, if the minimum load is doubled

5.5 Active power curtailment

Active power curtailment (APC) is one of the easiest and most commonly implemented ways to ensure there are no over-voltages on a feeder. APC is proposed by various authors in literature [5], [19], [20], [22]. APC prevents over-voltages by limiting the active power generated by the generator during periods that over voltages occur. When renewable power generation is used, power curtailment should be treated as a worst case scenario for limiting voltage rise. APC of a renewable resource, with no energy storage, effectively wastes the available energy and therefore reduces the income of the plant.

Typically APC is used by generation to control the frequency, but it can be used to control the voltage on MV feeders. APC can be used when the maximum voltage along a feeder is exceeded during periods of low load and maximum generation. If voltage rise during periods of low demand is the main limitation for DG to be connected to a feeder (2% voltage rise during this scenario) then APC can be used to increase the installable capacity. With APC, increased generation can be installed and operated during periods of medium to high load. APC allows for more generation when it is needed as long as the voltage change limitations are not exceeded.

APC can be implemented using a variety of methods, with two of the more common methods discussed here. The first method immediately cuts a large percentage of the power generation until the network operator allows for the generation to be increased. The second and preferred method is to use droop control. The use of droop control allows the maximum amount of power to be generated for particular network conditions and keeps the voltage below the maximum feeder voltage.

There are various strategies to implement droop control and [20] compares two. The two methods of power curtailment are compared on a low voltage feeder with 12 power neutral homes. The first method uses a droop controller that calculates the droop percentage using the local bus voltage. This method of droop control resulted in an unequal sharing of the power reduction and the houses towards the end of the feeder would have a reduced income. To solve this issue, the second droop method attempts to share the power curtailment among each of the houses to achieve the same voltage regulation. Each method of droop control had its own advantages and disadvantages. For example the second method enabled each house to have the same return on investment but resulted in more energy losses overall, when compared to the first droop control method.

5.6 Control Strategies

5.6.1 Introduction

Voltage regulation devices and the DG control methods need to be co-ordinated so that they can operate effectively together. The system can be configured to be locally controlled with suitable local setpoint adjustment or a central controller can be used to co-ordinate the system. The two types of control are often referred to as centralised or decentralised control respectively. The method of control needs to be carefully selected as it could have an impact on the stability of the network.

The control strategies used will typically combine two or more of the voltage control techniques. The most commonly used methods are active and reactive power control using various different methods of centralised and decentralised control [22], [24], [63], [64].

References [22], [34], [64] show that a decentralised voltage regulation scheme can be effective in distribution networks. DG units can be configured to vary between voltage and power factor control and in worst cases curtail active power. An intelligent decentralised control strategy can improve the voltage profile, increase DG penetration and reduce losses [64]. Voltage stability can be increased during periods with rapid power swings by using decentralised generation if an intelligent controller is used [63].

In [65] a voltage regulation scheme was proposed that co-ordinates the OLTC and reactive power generation of the DG. The scheme takes the power flow and reactive power requirements of all the branches in a feeder into account when calculating the amount of reactive power that each DG should supply. Using the method in [65], the regulation scheme has the capability of satisfying the diverse regulation requirements of different feeders connected to the primary substation.

A local voltage control method, based on sensitivity analysis, was developed in [66] that made use of the capability curve of connected DG units. Sensitivity analysis is used to determine the amount of voltage variations due to a change in active or reactive power injected. The method provided good performance on the local voltage control and had minimal impact on the other parts of the network. This was due to the local effect of voltage control on the distribution network. To maximise DG penetration an improved co-ordination scheme should be investigated between the local DG controllers, capacitors and the OLTC controllers of the substation transformers [66].

5.6.2 Proposed control strategy

Two proposed decentralised control strategies will be covered here. The first makes use of standard control techniques and network equipment that can easily be implemented today. The second uses the same modifications as the first, but adds some of the new technologies discussed in this chapter. The two techniques will be compared to each other to show how the new technologies can improve the voltage regulation and DG penetration. The two strategies are compared for case 4.

In the first control strategy, the OLTC and VR are configured with a LDC. In an effort to reduce the number of tap changes by the VR, its bandwidth is increased from 0.02 p.u. to 0.03 p.u. The switched capacitor is controlled using a reactive power controller that aims to minimise reactive power flow though the substation transformer. The DGs are controlled using CPF control at a power factor of 0.975.

The second control strategy utilises the CEVR and adaptive droop control, in addition to the first control modifications. The DGs have a rated reactive power of 0.975 and a reactive power setpoint of unity power factor to minimise the losses. The CEVR has a setpoint voltage of 1.03 p.u. and the LDC is set to regulate T5.

The results for DG penetration and voltage variations are shown in Table 5.16 and Table 5.17.

Table 5.16: DG penetration level with the two proposed control strategies

Strategy	P_{DG} **[kW]**	**Limiting factor**	$V_{\max}$ **Terminal**	$V_{\max}$ **[p.u.]**	ΔV_{tot} **[%]**	E_{loss} **[kWh]**	***TT***	PL_{DG} **[%]**	**Increase DG [%]**
1	1700	RVC	T4	1.06	5.76	1417	36	68	56
2	2020	OV	T4	1.07	2.28	1444	8	81	85

Table 5.17: Voltage fluctuation percentage and number of tap changes on a cloudy day for the two proposed control strategies

Strategy	**Average voltage fluctuation [%]**				***DT***			E_{loss} **[kWh]**
	MV BB	T4	T4-1	T10	OLTC	VR/EVR	Cap	
1	0.17	0.85	1.03	1.64	8	38	2	1583
2	0.25	0.93	0.4	0.65	8	184	2	1535

The first strategy's penetration was limited to 1700 kW to ensure that the total feeders RVC fell within an acceptable level. The second strategy has 320 kW more generation connected, but the RVC is only 40% of the first, because of the combination of the CEVR and droop control.

The voltage variations of the first strategy are quite high on a cloudy day. The LDC at the OLTC and VR ensure that the number of tap changes by the VR does not increase from the base levels in Table 4.3. In both strategies the LDC of the OLTC increases the number of tap changes from 2 to 8.

The second strategy's voltage variations are kept low and are below the variations experienced with combined CPF and adaptive droop control, at a penetration level of 1374 kW. The losses for both control strategies are lower than the minimum losses calculated in Table 4.4, because of the improved reactive power control of the feeder.

The bus voltages and tap positions are shown for the first strategy in Figure 5.40. The voltages vary by 3 to 5% during the day because of the power fluctuations. The power through the substation transformer is shown in Figure 5.41 and the reactive power is controlled to be close to zero for most of the day. The reactive power control of the feeder is improved when the feeder is controlled with a reactive power controller. It can be seen that the capacitor's control functions as expected and is not influenced by the DG like the voltage controlled capacitors were.

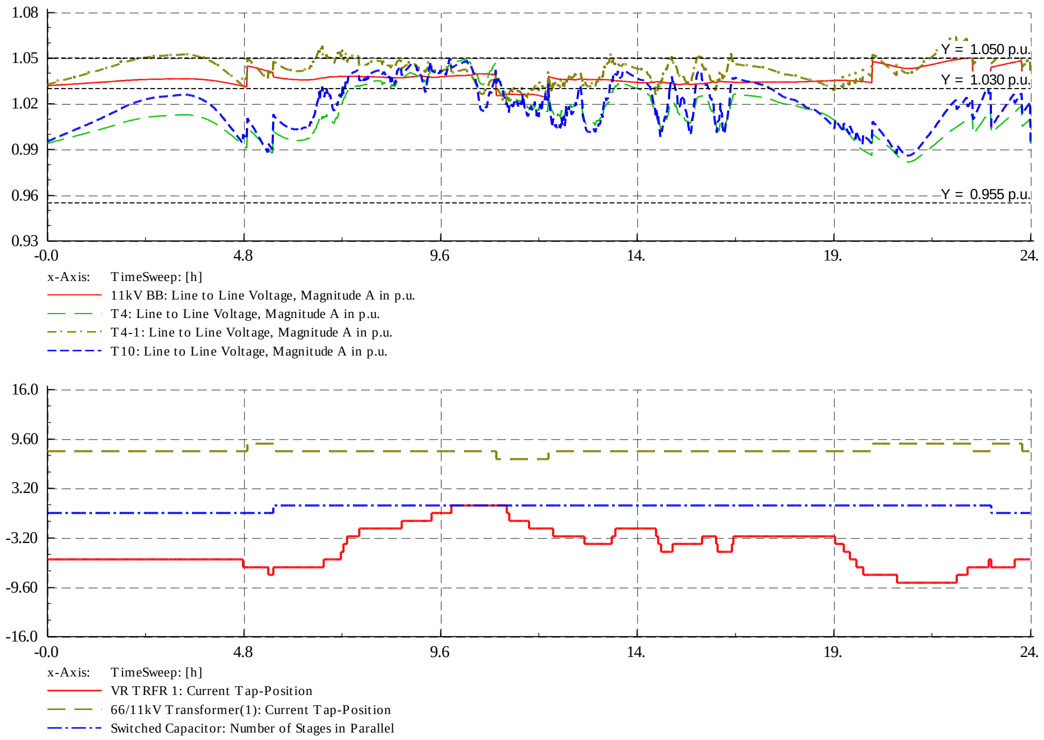

Figure 5.40: First proposed control strategy's bus voltages and tap positions

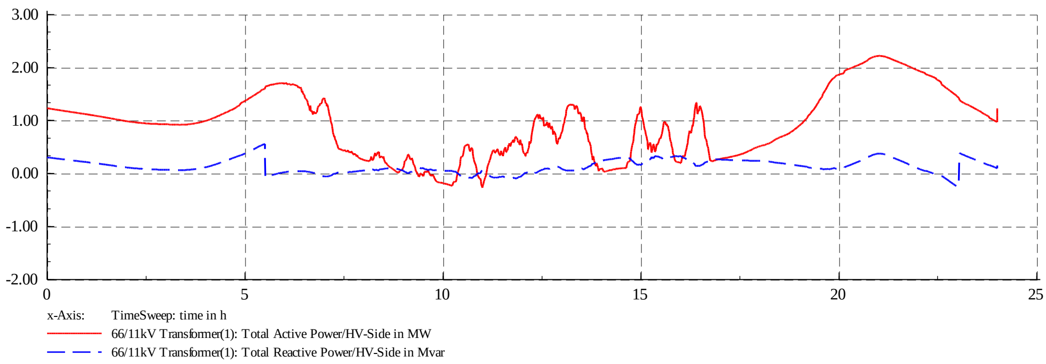

Figure 5.41: First proposed control strategy's transformer power

The bus voltages and tap positions are shown for the second strategy in Figure 5.42. The voltages are controlled within a very narrow band for most of the day, even with the highly variable generation. The voltage profile is relatively flat and the voltages only vary by 1-2% with the large variations in power. The power flow through the substation transformer is shown in Figure 5.43. There are periods during the day where power flows back into the transmission grid. The reactive power, similarly to the first strategy, is controlled to be close to zero for most of the day. The reactive power does have a slight ripple because of the increased reactive power demand caused by the droop controllers, but it is very small and could easily be absorbed by the transmission grid.

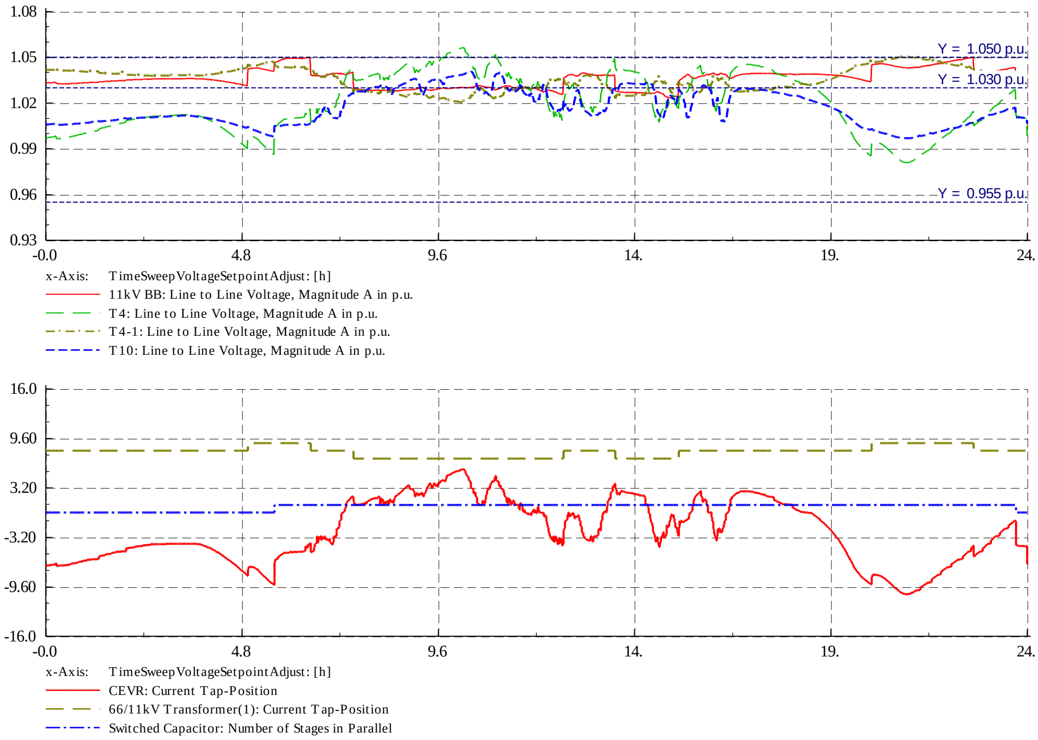

Figure 5.42: Second proposed control strategy's bus voltages and tap positions

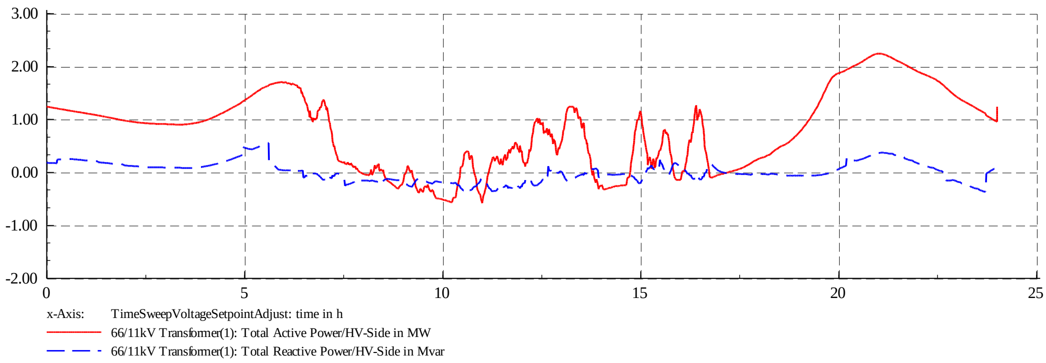

Figure 5.43: Second proposed control strategy's transformer power

5.7 Conclusions

In this chapter, various technologies that can be used to increase the DG penetration levels on a feeder have been investigated. Each technology was shown to be beneficial, depending on the circumstance.

OLTC and VR setpoint reduction was shown to increase the penetration level when over voltage limited the DG size. Depending on the generators' location and number of generators, the penetration level was increased between 18% and 36%. The reduced setpoints could cause low voltages on certain feeders, if their minimum voltage is below 0.965 p.u. during periods of high load. The LDC was shown to compensate for this at the cost of increased configuration complexity. The LDC was shown to cause an increased number of tap changes of the OLTC from 2 to 8 tap changes per day. The LDC could increase the penetration level by up to 100% but the penetration level was shown to be too high because of the increased number of tap changes by the voltage regulator on a cloudy day. The LDC could result in both under and over voltage, if there is a large load factor difference, for the feeders under its control.

Reactive power control addressed both the issue of voltage rise and RVC. The penetration level was increased by up to 66% at a power factor of 0.95. The voltage variations with the increased penetration levels were reduced when compared to the base penetration levels. The reduced voltage variations causes on average 10 fewer tap changes per day, or a reduction of 25%. Droop control provided similar reduction in tap changes to CPF control, but reduced the losses by 150 kWh per day. It was shown that if the feeder power factor is high or reactive power is compensated for at the generator, reactive power absorption can be used to reduce the losses of a feeder. It allows for more generation to be connected and the increased generation reduces the net current flow on the feeder.

Various droop modifications were proposed that reduced voltage variations further. The modifications reduced the number of tap changes to the same level as if no generation were connected to the feeder. The losses were reduced by 150 kWh per day from the base penetration levels and were similar to standard droop control.

It was suggested that reactive power control can be enhanced by installing an inductor at the beginning of the feeder. The inductor was shown to reduce the RVC level of a generator and could increase the penetration level by up to 170%. However, it only has a slight improvement on the voltage controllability of the feeder, when used with droop control and did not reduce the number of tap changes.

The EVRs were shown to reduce the RVC level and reduce the voltage variations on the feeder during periods of highly variable generation. A DEVR was shown to provide similar benefits to the more complex CEVR. Both devices increased DG penetration on remote parts of the feeder by up to 50%, when the size was limited by RVC. The voltage variations on the feeder were reduced by 50% and the large changes in voltage are smoothed out.

Finally two proposed control strategies were compared to each other that combined the technologies discussed in this chapter. It was shown that when combining some of the modifications, the penetration level can be increased by up to 85% and the voltage variations were reduced by up to 50%. The optimal control strategy made use of: adaptive droop control, a CEVR, reactive power control of the capacitor and a LDC at the OLTC and VR.

6 Conclusions and Recommendations

6.1 Conclusions

There will be a large amount of generation connected to the distribution network over the next few years. It is necessary to determine how adding generation to the distribution network affects the voltage profile and voltage regulation of a feeder. The connection of distributed generation (DG) to a typical rural distribution feeder was investigated.

There are certain constraints that cannot be exceeded when connecting generation to a network. These constraints were investigated in chapter two. South Africa has a grid code for the connection of renewable power plants to the grid. The grid code specifies the minimum technical requirements that each category of generation must meet. The grid code specifies that a generator can cause a maximum rapid voltage change (RVC) of 3%. The 3% RVC level is one of the constraints when connecting generation to the network. DG can cause voltage rise from the substation, depending on the size of generation connected relative to the load. The voltage apportionment standard specifies the maximum voltage that can be experienced at a point of the network. It specifies the maximum voltage rise that generation can cause during minimum load. It is not expected for PV generation to generate power during periods of minimum load and therefore, the voltage headroom during minimum load is limited to 2% above the maximum tap zone voltage. The voltage rise and RVC are the two main constraints when assessing the maximum amount of generation that can be connected to a feeder.

In chapter three the network equipment that is typically used to control the voltage, on a feeder without generation, was discussed. Methods that can be used to calculate the voltage profile of a feeder were discussed. It was shown that a simple approximate method, to calculate the voltage profile and voltage change, provided suitable results for analytical studies, when compared to more complicated methods. It was shown that by using a combination of an OLTC, VR and capacitors; that the network voltage can be adequately controlled under high and low load conditions. A test feeder was developed that was used for the simulations in the later chapters.

A method to calculate the maximum generator size and penetration level of a feeder was developed in chapter four. The voltage headroom was found to limit the DG penetration up until about 12 km from the substation and that RVC limits the DG penetration beyond that. It was shown that if multiple generators are connected to a network, the total RVC level of all of the generators should be used to limit the connection of additional generation. A recommended total RVC level, for ten generators connected to a feeder, of 4-5% was suggested due to the power change reduction caused by geographical dispersion of the plants. The calculated maximum power change over 10 minutes for the 10 plants was 34% of the total installed capacity.

Flicker was shown not to be an issue when connecting PV generation to the network. It was suggested that the 3% RVC level can be adjusted on networks with no VRs or capacitors connected to the feeders. The time taken for clouds to pass over an entire PV plant sufficiently reduces the magnitude of voltage change per second for flicker not to be a problem. It was shown that as long as the maximum expected voltage change level, at the primary side of any VRs, is less than the bandwidth of the controller, the number of times a VR has to tap change does not increase substantially when DG is added. Typically the addition of generation to a feeder increased the number of tap changes by the VR by 10 per day.

The losses of the feeder were typically reduced by 20% or 500 kWh with the added generation. The amount of generation that causes the lowest losses on a feeder is often above the amount of generation that can be installed, when limited by the voltage headroom and RVC constraints. The typical increase needed to reduce losses to a minimum is between 100 and 200% of the base penetration values. It was therefore determined that it would be beneficial to find ways to increase penetration levels without violating the existing constraints of the grid code and voltage apportionment standard.

Various technologies or control modifications were investigated in chapter five that can be used to increase DG penetration on distribution feeders. It was shown that each modification or technology would only be of benefit if it addressed the constraint that limited DG penetration. OLTC and VR setpoint adjustment were shown to increase DG penetration if the voltage headroom was the limiting constraint. Depending on the generators' location and number of generators, the penetration level was increased between 18% and 36%. Reactive power control can be used to increase DG penetration if the voltage headroom or the RVC are the constraints. It was shown that even on weak feeders with a low X/R ratio, that reactive power control within the limits of the grid code can increase DG penetration by 20% to 80%.

It is typically assumed that using reactive power control, to increase penetration, automatically increases the losses experienced by a network. It was shown that this is not true and that the increased generation, which can be connected to the network when using reactive power control, can actually reduce the losses. The losses are reduced providing that the feeder is operating at a high power factor or any reactive power that is absorbed is compensated for by a capacitor. A script to find the ideal operating power factor of a generator was developed. The recommended operating power factor, that would maximise generation and give the lowest losses, could be found.

An improved method of reactive power control that can be used to reduce voltage variations on the network was suggested in chapter five. It was suggested that droop control and constant power factor control could be combined into a single control strategy called combined reactive power droop control. Generators, with the improved control and are connected to strong parts of the network, can offset more of their voltage change than with standard droop control. It was also proposed that the voltage setpoint for droop control is dynamically adjusted to the average voltage of the network, over a rolling time period, so that the reactive power demand by the generators is minimised. Droop control also allows any future generation to help support the network voltage, without having to reconfigure the other generators connected to the network. The droop control modifications reduced the number of tap changes to the levels before generation was connected to the feeder.

A new technology was introduced that can replace the standard VR. Electronic voltage regulators (EVRs) were shown to have many benefits over the standard VR. EVRs address many of the concerns that arise when large amounts of generation are connected to remote parts of the network. An EVR compensates for short term voltage variations, unlike a standard VR, and was shown to substantially reduce the voltage variations experienced on a cloudy day. EVRs were shown to increase penetration levels, by reducing the RVC of generators connected beyond it. The size of a generator connected to the end of the feeder could be increased by 50% and the voltage variations of the feeder were reduced by 50%.

Two proposed control strategies were compared to each other that combined the technologies that were discussed in chapter 5. It was shown that when combining some of the modifications, the penetration level can be increased by up to 85% while the voltage variations were reduced by up to 50%. The optimal control strategy made use of: adaptive droop control, a CEVR, reactive power control of the capacitor and a LDC at the OLTC and VR.

6.2 Recommendations for future work

This work has investigated various methods that can be used to increase penetration levels from a voltage control perspective. The simulations were performed using steady state analysis and do not consider the system dynamics, various feeder configurations or protection modifications that would need to be made. There are a few directions that this research could lead to and they will be discussed here.

Simulation of a real network with generator applications

The technologies discussed in this document should be simulated on a real network, with actual generation applications. Many applications have to be turned down or their capacity limited, due to the limitations imposed by RVC and OV. The principles discussed in this document should be applied to these applications and the effect on long term voltage control of these feeders should be investigated.

Practical implementation

Following on from simulations on a real network, the technologies discussed in this document should be implemented on a real network. The impact on the control of the network and the network operation can then be compared to the simulated results. Any differences can be used to update the simulation model, to improve the accuracy for future studies.

Install irradiance sensors and power sensors with a fast sample rate at PV plants

The work on geographical dispersion and the low pass filter effect should be extended to practical results obtained in South Africa. The maximum recorded power changes, for various PV plants at different locations, should be determined. The results could be used in future planning and power quality studies. It would be necessary to record data with a sample rate of at least 1 Hz.

Dynamic studies

Islanding operation and dynamic stability of various DG technologies should be investigated. The problems that might arise, when there is a large amount of generation with low inertia on the system, during a large grid disturbance should be determined before the situation arises. The frequency stability of a system could be compromised, as most of the DG could be lost during a large disturbance [31].

Protection coordination

Protection co-ordination would need to be investigated, especially on networks with multiple autoreclosers and high DG penetration [11]. In this document it was assumed that voltage control issues would pose more of a problem than protection co-ordination. The increased penetration levels that could arise, if the improved voltage control discussed in this document is implemented, will start to make the protection coordination more difficult. New protection philosophies would need to be determined and additional protection equipment might be required.

Investigation of more advanced control methods

More advanced control methods that use model predictive control, tabu search, genetic algorithms, neural networks and other advanced methods could be investigated [67]–[69]. These methods make it easier to determine the optimal network operating condition based upon various cost functions and weightings that cannot easily be evaluated using traditional methods. The viability of using these methods in real time, to co-ordinate voltage control devices and place network components, would need to be determined.

Investigate other renewable energy technologies

It should be investigated how this research can be applied to other renewable energy technologies. It would be expected that the same constraints and limitations will be applicable for the other technologies. The diversification of energy sources could benefit the network further and allow for a greater percentage of power to come from renewable resources.

Bibliography

[1] T. E. Kim and J. Kim, “Voltage regulation coordination of distributed generation system in distribution system,” in *2001 Power Engineering Society Summer Meeting. Conference Proceedings (Cat. No.01CH37262)*, 2001, vol. 1, no. C, pp. 480–484.

[2] S. J. van Zyl and C. Gaunt, “Control strategies for distributed generators operating on weak distribution networks,” in *2003 IEEE Bologna Power Tech Conference Proceedings,*, 2003, vol. 3, pp. 252–258.

[3] D. Peters, “Integrated Resource Plan 2010-2030.” 2011.

[4] P. Barker and R. W. De Mello, “Determining the impact of distributed generation on power systems. I. Radial distribution systems,” in *2000 Power Engineering Society Summer Meeting (Cat. No.00CH37134)*, 2000, vol. 3, no. c, pp. 1645–1656.

[5] J. Morren, “Grid Support by power electronic converters of Distributed Generation units,” Delft University of Technology, Netherlands, 2006.

[6] F. Viawan, “Steady state operation and control of power distribution systems in the presence of distributed generation,” Chlamers University of Technology, 2006.

[7] M. Klopper, M. Bello, and C. Carter-Brown, “Voltage Control Strategies for Synchronous Generators operating as Distributed Generation on a weak Distribution Network,” *bits.eskom.co.za*, 2009.

[8] E. J. Coster, J. M. a Myrzik, B. Kruimer, and W. L. Kling, “Integration Issues of Distributed Generation in Distribution Grids,” *Proceedings of the IEEE*, vol. 99, no. 1, pp. 28–39, Jan. 2011.

[9] J. a. P. Lopes, N. Hatziargyriou, J. Mutale, P. Djapic, and N. Jenkins, “Integrating distributed generation into electric power systems: A review of drivers, challenges and opportunities,” *Electric Power Systems Research*, vol. 77, no. 9, pp. 1189–1203, Jul. 2007.

[10] EPRI, “Planning Methodology to Determine Practical Circuit Limits for Distributed Generation,” Palo Alto, 2010.

[11] M. Bollen and F. Hassan, *Distributed Generation in the Power System*, 1st ed. IEEE press, 2011.

[12] J. Marcos, L. Marroyo, E. Lorenzo, and M. García, “Power output fluctuations in large PV plants,” in *icrepq.com*, 2012.

[13] N. Jenkins, R. Allan, P. Crossley, D. Kirschen, and G. Strbac, *Embedded Generation*. The Institution of Engineering and Technology, Michael Faraday House, Six Hills Way, Stevenage SG1 2AY, UK: IET, 2000.

[14] NRS, *NRS 048-2-2008 Electricity supply - Quality of supply*, Edition 3. 2008.

[15] SAGC Std., “Grid connection code requirements for renewable power plants (RPPS) connected to the transmission system (TS) or the distribution system (DS) in South Africa,” 2012.

[16] M. M. Bello and C. G. Carter-brown, “Network planning guideline for MV step voltage regulators,” *DST 34-539*. Eskom controlled document, 2011.

[17] C. G. Carter-brown, “Network planning guideline for MV shunt capacitors,” *DST 34-598*. Eskom controlled document, 2010.

[18] F. a. Viawan, A. Sannino, and J. Daalder, “Voltage control with on-load tap changers in medium voltage feeders in presence of distributed generation,” *Electric Power Systems Research*, vol. 77, no. 10, pp. 1314–1322, Aug. 2007.

[19] M. Jacxsens, B. Meersman, T. L. Vandoorn, J. D. M. De Kooning, and L. Vandevelde, “Overview of voltage control strategies in medium voltage networks with implementation of distributed generation,” *IET Conference on Renewable Power Generation (RPG 2011)*, pp. 232–232, 2011.

[20] R. Tonkoski, L. A. C. Lopes, and T. H. M. El-Fouly, “Coordinated Active Power Curtailment of Grid Connected PV Inverters for Overvoltage Prevention,” *IEEE Transactions on Sustainable Energy*, vol. 2, no. 2, pp. 139–147, Apr. 2011.

[21] M. Lees, A. Collinson, and M. Barlow, “Practical measures to accommodate increased levels of distributed generation in existing distribution networks,” *Proceedings 17th International Conference on Electricity Distribution*, no. 32, pp. 12–15, 2003.

[22] T. Sansawatt, L. F. Ochoa, and G. P. Harrison, “Integrating distributed generation using decentralised voltage regulation,” in *IEEE PES General Meeting*, 2010, pp. 1–6.

[23] M. Tonso, J. Moren, S. W. H. de Haan, and J. A. Ferreira, “Variable inductor for voltage control in distribution networks,” in *2005 European Conference on Power Electronics and Applications*, 2005, p. 10 pp.–P.10.

[24] H. Hatta and H. Kobayashi, “A study of centralized voltage control method for distribution system with distributed generation,” in *19th International Conference on Electricity Distribution (CIRED)*, 2007, no. 0330, pp. 21–24.

[25] M. Bollen and A. Sannino, “Voltage Control With Inverter-Based Distributed Generation,” *IEEE Transactions on Power Delivery*, vol. 20, no. 1, pp. 519–520, Jan. 2005.

[26] L. B. Perera, G. Ledwich, and A. Ghosh, “Distribution feeder voltage support and power factor control by distributed multiple inverters,” in *2011 IEEE Electrical Power and Energy Conference*, 2011, pp. 116–121.

[27] C. G. Carter-brown, “Distribution volatge regulation and apportionment limits,” *DST 34-542*. Eskom controlled document, 2012.

[28] M. W. Davis, R. Broadwater, and J. Hambrick, “Modeling and Testing of Unbalanced Loading and Voltage Regulation,” 2007.

[29] M. M. Bello and C. G. Carter-brown, “Network planning guidelines for lines and cables,” *DST 34-619*. Eskom controlled document, 2010.

[30] J. D. Glover and M. S. Sarma, *Power System Analysis and Design: With Personal Computer Applications*. Books, Cole, 2002, p. 656.

[31] F. Viawan, “Voltage control and voltage stability of power distribution systems in the presence of distributed generation,” Chlamers University of Technology, 2008.

[32] T. Areva, *Network protection & automation guide*. 2002.

[33] T. Lund, “Analysis of Distribution Systems with High Penetration of Distributed Generation,” Technical University of Denmark, 2007.

[34] E. Mogos and X. Guillaud, “A voltage regulation system for distributed generation,” in *IEEE PES Power Systems Conference and Exposition, 2004.*, 2004, pp. 30–37.

[35] C. Brice, “Comparison of Approximate and Exact Voltage Drop Calculations for Distribution Lines,” *IEEE Transactions on Power Apparatus and Systems*, vol. PAS-101, no. 11, pp. 4428–4431, Nov. 1982.

[36] N. Meyer and C. Carter-Brown, “Network Planning guidelines for transformers.” Eskom controlled document, 2010.

[37] C. P. Systems, “McGraw-Edison VR-32 Regulator and CL-5 series control installation, operation and maintenance instructions and parts replacement information,” 2001.

[38] J. Black, “Impact of Embedded Generation on Voltage Regulation and Transformer Tap Changer Lifetime and Operation,” 2012.

[39] G. Ari and Y. Baghzouz, “Impact of high PV penetration on voltage regulation in electrical distribution systems,” in *2011 International Conference on Clean Electrical Power (ICCEP)*, 2011, pp. 744–748.

[40] K. Turitsyn, P. Sulc, S. Backhaus, and M. Chertkov, “Options for Control of Reactive Power by Distributed Photovoltaic Generators,” *Proceedings of the IEEE*, vol. 99, no. 6, pp. 1063–1073, Jun. 2011.

[41] Y. Yang and M. Bollen, “Power quality and reliability in distribution networks with increased levels of distributed generation,” 2008.

[42] J. Marcos, L. Marroyo, E. Lorenzo, D. Alvira, and E. Izco, “From irradiance to output power fluctuations: the PV plant as a low pass filter,” *Progress in Photovoltaics: Research and Applications*, vol. 19, no. 5, pp. 505–510, Aug. 2011.

[43] J. Marcos, L. Marroyo, E. Lorenzo, and M. García, “Smoothing of PV power fluctuations by geographical dispersion,” *Progress in Photovoltaics: Research and Applications*, vol. 20, no. 2, pp. 226–237, Mar. 2012.

[44] H. Mousazadeh, A. Keyhani, A. Javadi, H. Mobli, K. Abrinia, and A. Sharifi, “A review of principle and sun-tracking methods for maximizing solar systems output,” *Renewable and Sustainable Energy Reviews*, vol. 13, no. 8, pp. 1800–1818, Oct. 2009.

[45] J. Marcos, L. Marroyo, E. Lorenzo, D. Alvira, and E. Izco, “Power output fluctuations in large scale pv plants: One year observations with one second resolution and a derived analytic model,” *Progress in Photovoltaics: Research and Applications*, vol. 19, no. 2, pp. 218–227, Mar. 2011.

[46] P. Beaucage, “Development of a Stochastic-Kinematic Cloud Model to Generate High-Frequency Solar Irradiance and Power Data,” *American Solar Energy Society*, pp. 1–8, 2012.

[47] M. M. Bello, “Network and grid planning standard for generation grid connection - Application for planning studies,” *DST 34-1946*. Eskom controlled document, 2013.

[48] M. Kashem, A. Le, M. Negnevitsky, and G. Ledwich, “Distributed generation for minimization of power losses in distribution systems,” in *2006 IEEE Power Engineering Society General Meeting*, 2006, p. 8 pp.

[49] J. C. Hernández, M. J. Ortega, J. De la Cruz, and D. Vera, “Guidelines for the technical assessment of harmonic, flicker and unbalance emission limits for PV-distributed generation,” *Electric Power Systems Research*, vol. 81, no. 7, pp. 1247–1257, Jul. 2011.

[50] R. Tzartzev, W. Mack Grady, and J. Patel, “Impact of high-penetration PV on distribution feeders,” in *2012 3rd IEEE PES Innovative Smart Grid Technologies Europe (ISGT Europe)*, 2012, pp. 1–6.

[51] E. M. Stewart, S. D. J. MacPherson, and R. Davis, “A realistic irradiance-based voltage flicker analysis of PV applied to Hawaii distribution feeders,” *2012 IEEE Power and Energy Society General Meeting*, pp. 1–7, Jul. 2012.

[52] M. J. Ortega, J. C. Hernández, and O. G. García, “Measurement and assessment of power quality characteristics for photovoltaic systems: Harmonics, flicker, unbalance, and slow voltage variations,” *Electric Power Systems Research*, vol. 96, pp. 23–35, Mar. 2013.

[53] S. Halpin, R. Bergeron, T. M. Blooming, R. F. Burch, L. E. Conrad, and T. S. Key, “Voltage and lamp flicker issues: should the IEEE adopt the IEC approach?,” *IEEE Transactions on Power Delivery*, vol. 18, no. 3, pp. 1088–1097, Jul. 2003.

[54] L. P. Frater and N. R. Watson, “Light flicker sensitivity of high efficiency compact fluorescent lamps,” in *2007 Australasian Universities Power Engineering Conference*, 2007, pp. 1–6.

[55] T. Kim, M. Rylander, E. J. Powers, W. M. Grady, and A. Arapostathis, “LED Lamp Flicker Caused by Interharmonics,” *2008 IEEE Instrumentation and Measurement Technology Conference*, pp. 1920–1925, May 2008.

[56] IEC, “IEC 1000-4-15 Electromagnetic Compatibility (EMC) - Part 4: Testing and measurement techniques - Section 15: Flickemeter - Functional and desing specifications,” 2003.

[57] IEC, “IEC/TR 61000-3-7 EMC: Low frequency phenomena,” *Draft*, 2006.

[58] L. Kojovic, “Impact of DG and voltage regulator interaction on distribution system voltage regulation,” in *CIRED, Barcellona*, 2003, no. 31, pp. 12–15.

[59] CIGRE, “Capacity of distribution feeders for hosting DER,” *WG C6.24*, 2013.

[60] C. W. Taylor, *Power system voltage stability*. 1994.

[61] M. Tomlinson, D. Abrie, and T. Mouton, “Series-stacked medium voltage electronic voltage regulator,” *2011 IEEE Energy Conversion Congress and Exposition*, vol. 3, pp. 1087–1093, Sep. 2011.

[62] M. Tomlinson, D. Abrie, H. Fuchs, and T. Mouton, “MV Voltage regulator technology development,” *Eskom report*, 2012.

[63] F. Baalbergen, M. Gibescu, and L. van der Sluis, “Voltage stability consequences of decentralized generation and possibilities for intelligent control,” in *2010 IEEE PES Innovative Smart Grid Technologies Conference Europe (ISGT Europe)*, 2010, pp. 1–8.

[64] D. N. Gaonkar, P. C. Rao, and R. N. Patel, “Hybrid Method for Voltage Regulation of Distribution System with Maximum Utilization of Connected Distributed Generation Source,” *2006 IEEE Power India Conference*, pp. 261–265, 2006.

[65] R. Caldon and S. Spelta, “Co-ordinated voltage regulation in distribution networks with embedded generation,” *18th International Conference and Exhibition on Electricity Distribution*, no. June, 2005.

[66] V. Calderaro, V. Galdi, G. Massa, and A. Piccolo, “Distributed Generation and local voltage regulation: An approach based on sensitivity analysis,” in *2011 2nd IEEE PES International Conference and Exhibition on Innovative Smart Grid Technologies*, 2011, pp. 1–8.

[67] O. Ausavanop and S. Chaitusaney, “Coordination of dispatchable distributed generation and voltage control devices for improving voltage profile by Tabu Search,” in *The 8th Electrical Engineering/ Electronics, Computer, Telecommunications and Information Technology (ECTI) Association of Thailand - Conference 2011*, 2011, pp. 869–872.

[68] D. K. Singh and S. Gupta, “Optimal coordination of directional overcurrent relays: A genetic algorithm approach,” *2012 IEEE Students’ Conference on Electrical, Electronics and Computer Science*, pp. 1–4, Mar. 2012.

[69] F. Ugranli, C. Ersavas, and E. Karatepe, “Neural network based distributed generation allocation for minimizing voltage fluctuation due to uncertainty of the output power,” in *2011 International Symposium on Innovations in Intelligent Systems and Applications*, 2011, pp. 415–419.

Appendix A - Power flow conventions

When referring to the power factor of a load or generator, as either leading or lagging, one is referring to the current lagging or leading the voltage. Figure A 1 shows the convention for loads and generators.

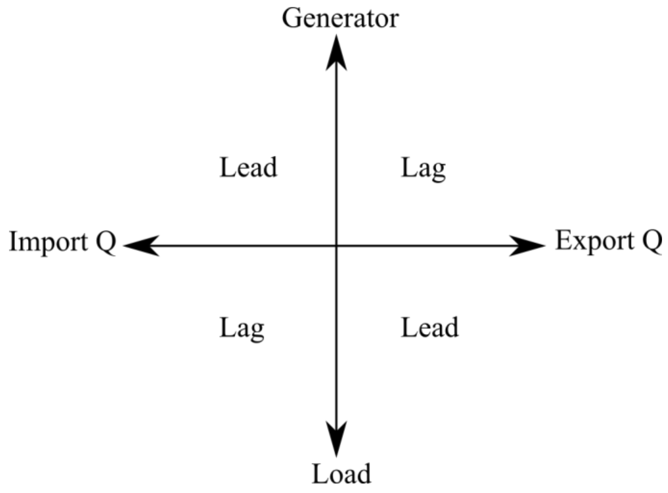

Figure A 1: Power factor convention

As Figure A 1 shows, a generator that is operating at a leading power factor is absorbing reactive power, while a load is exporting reactive power to the grid. When a generator operates at a lagging power factor, it is supplying reactive power to the grid while a load is absorbing reactive power from the grid. This is the reason why most loads are ’lagging’ and most distributed generators are ’leading’, as they are both absorbing reactive power.

When referring to a positive load power, it is assumed that power is being absorbed from the grid. Likewise when referring to a generator, a positive power refers to the generator supplying power to the grid. Figure A 2 shows the orientation of power and reactive power flow when referring to a load and generator.

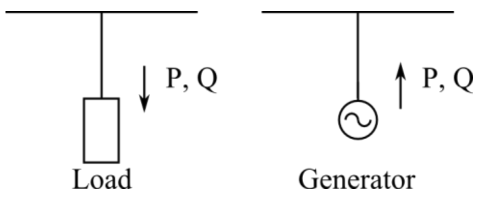

Figure A 2: Power flow convention

Appendix B - Implementation of the developed tools and methods

B1. Matlab Scripts

Three main Matlab scripts were developed to obtain the results used for this work and will be discussed here.

Voltage profile, headroom and RVC

This Matlab script calculates the voltage profile, the DG size limited by the voltage headroom and RVC. It was used to calculate any of the voltage profiles and the RVC, voltage headroom graphs.

The inputs to the script require:

- The feeder length
- Uncompensated feeder load and power factor
- Conductors and lengths of each conductor
- OLTC and VR setpoints
- Impedance of the source network
- Location of any VRs and their maximum buck/boost percentage
- Location and size of any capacitors
- Location and size of any currently installed DGs
- Whether the LDCs are used and their R_{set} and X_{set}

The script requires that any switched capacitors are manually included or excluded depending on the loading. For example at minimum load, the switched capacitor should be removed from the simulation. The maximum OLTC and VR setpoint voltages should be used for the minimum loading test and the minimum OLTC and VR setpoint voltages should be used for the maximum loading tests.

Sensitivities

The voltage sensitivities are calculated depending on the type of voltage or reactive power control employed. The voltage sensitivity is calculated for a change in power of a single DG at a specific location, but the voltage support of multiple DGs can be included. It requires the following inputs:

- The feeder impedance
- Range of DG powers to test
- Location of the DG under test
- Location of any other DGs if droop control is used
- Impedance of the source network
- Power factor rating/setting of the DGs

- Droop coefficient if droop control is used

The output is the voltage sensitivity graph. The various control methods can be compared by calculating the voltage sensitivity for each individually and displaying them on the same graph.

Losses and RVC

The losses and RVC curves are calculated for a feeder. The losses and RVC are calculated for particular power factor and DG powers. The results are in the form of a three dimensional curve, with the RVC and losses being the z-value. The 3 dimensional curves are difficult to read so the contours of the three dimensional curves are plotted. These contours give the constant loss and constant RVC curves that are used in this document. The script requires the following information about the feeder.

- The feeder impedance
- Impedance of the source network
- Average compensated feeder load and power factor
- Location of the DG under test

B2. PowerFactory scripts

This section will provide an explanation of the PowerFactory scripts that were developed to provide the results in this document. The programs are called PMaxDG, TimeSweep and PMinLoss.

PMaxDG

The program PMaxDG calculates the maximum power for specific generators connected to the network under study. The script increases the power of the generators until one of the constraints has been exceeded. The constraints that are considered are the RVC level, the maximum/minimum feeder voltage and the maximum current carrying capacity of the lines. The method of executing the script can be customised through initial settings as shown in Figure B 1.

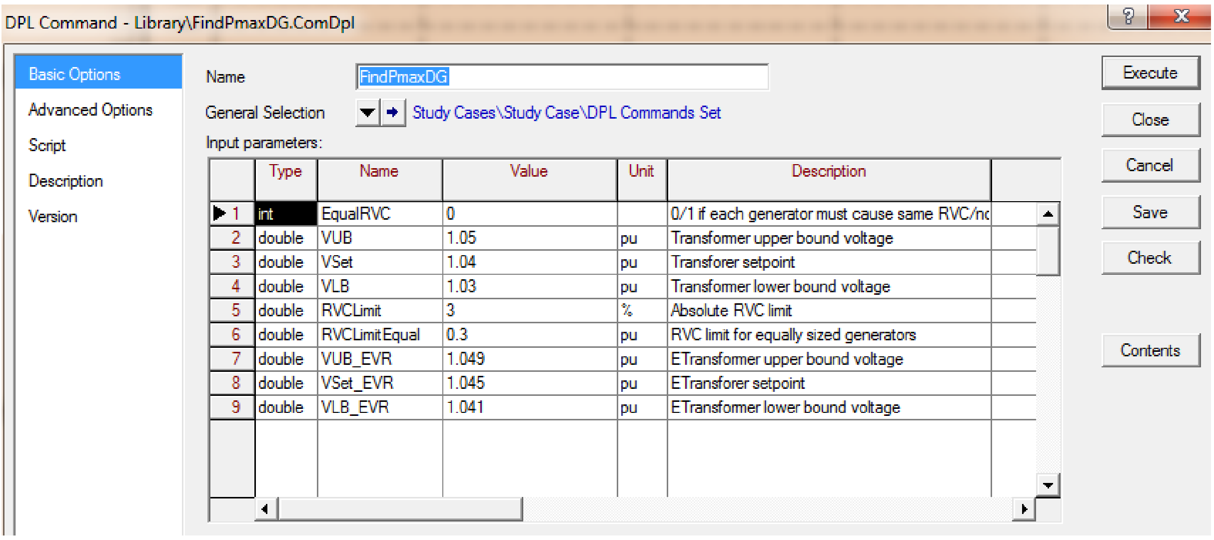

Figure B 1: Script user settings

EqualRVC

This setting specifies whether the script will increase the generators power such that the RVC level of each generator is the same.

VUB, VSet and VLB (Including EVR)

These are the settings for the upper and lower bound voltage of the tap changing transformers. This option was added so that the effect of reducing the OLTC and VR setpoint could be observed.

RVCLimit and RVCLimitEqual

The RVCLimit is the maximum RVC limit for an individual generator. It is used as a limitation in all simulations. The RVCLimitEqual is used when the EqualRVC limit is enabled. The program will increase each generators output so that the RVC for each generator is equal to this value, and if no other constraint has been breached will slowly increase all generators RVC until either the RVCLimit, maximum voltage or over current condition has been breached.

The program requires that the generators are configured in their required operating mode. For example, the generator must be enabled to operate at a certain power factor, if power factor control of the generators is being tested.

The program differentiates between a normal VR and an EVR by using the construction date field in the transformer settings page. For a CEVR the setting should be set to 2015, for a standard tap changing transformer the setting should be 2016 and for the DEVR the setting should be 2017. The program uses this setting to determine whether it must calculate the RVC level at the primary side of the EVR.

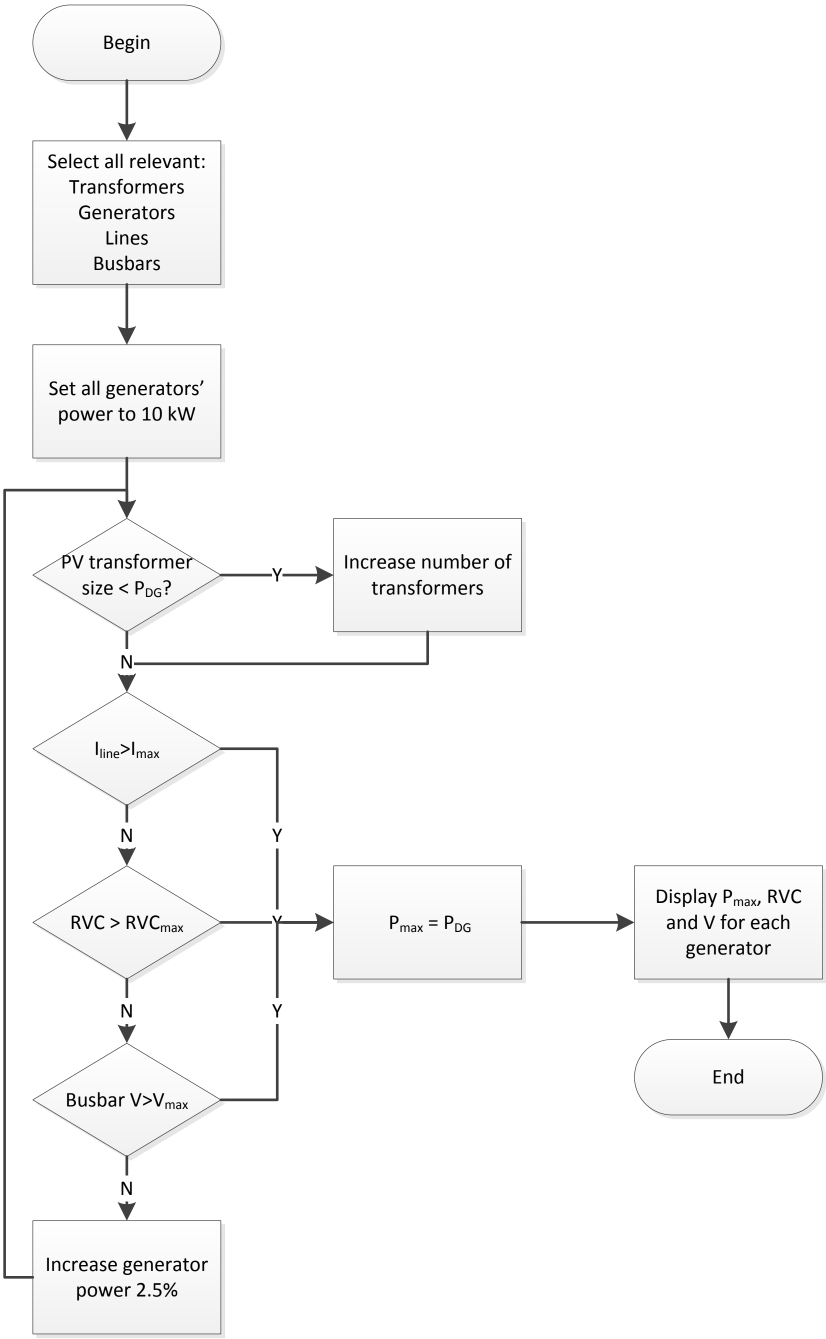

Figure B 2: Algorithm to calculate maximum DG penetration for a feeder

The different sections of the program are described below:

Initialisation (Figure B 4**)**

1) Initialise script by selecting all of the relevant busbars, transformers, generators and lines
2) Remove all irrelevant objects such as those that aren't energised or are not needed for the calculations
3) Determine if regulators are standard VRs or EVRs, and enable continuous mode for VR
4) Set initial power values for generators under study.
5) Calculate the number of generators, transformers and lines in the study case
6) Resize temporary array for generator voltages

Main Loop

This loop is the main body of the program that executes until one of the constraints is breached

1) Execute load flow
2) Adjust the number of parallel PV transformers so that the total rating is greater than the PV plants
3) Check if any lines currents exceed the thermal rating
4) Set discrete transformers back to discrete mode
5) Check RVC level at generator MV terminal and primary side of EVR if it is in use (Figure B 5)
6) Re enable continuous tap changing on discrete transformers
7) Execute load flow
8) Check if any busbars are over or under voltage
9) Calculate the point on the feeder with the highest voltage
10) Increase generator power levels if maximum power is not found and repeat loop

The main algorithm includes a function to keep RVC of each generator the same if the option is enabled.

Program end

This part of the program calculates and displays the total installed generation and total feeder RVC. It displays all of the information required on the screen.

1) Display each generators individual power and RVC
2) Calculate total feeder RVC
3) Calculate total amount of generation
4) Display total RVC level
5) Display total generation
6) Reset transformer setpoint values to their default and enable discrete tap changing

The sample output of the script is shown in Figure B 3.

```
Number of Generators 1
RVC limit exceeded at T5
Generator PV 15k, Power 0.686047 MW, Rapid Voltage change level 2.989341 percent, Maximum Voltage 1.055951 p.u.
Total RVC level for all generators 2.989341 percent
Total installed generation 0.686047 MW
The maximum feeder voltage is at T4 of 1.063753 p.u.
DIgSI/info - DPL program 'FindPmaxDG' successfully executed
```

Figure B 3: PMaxDG script sample output

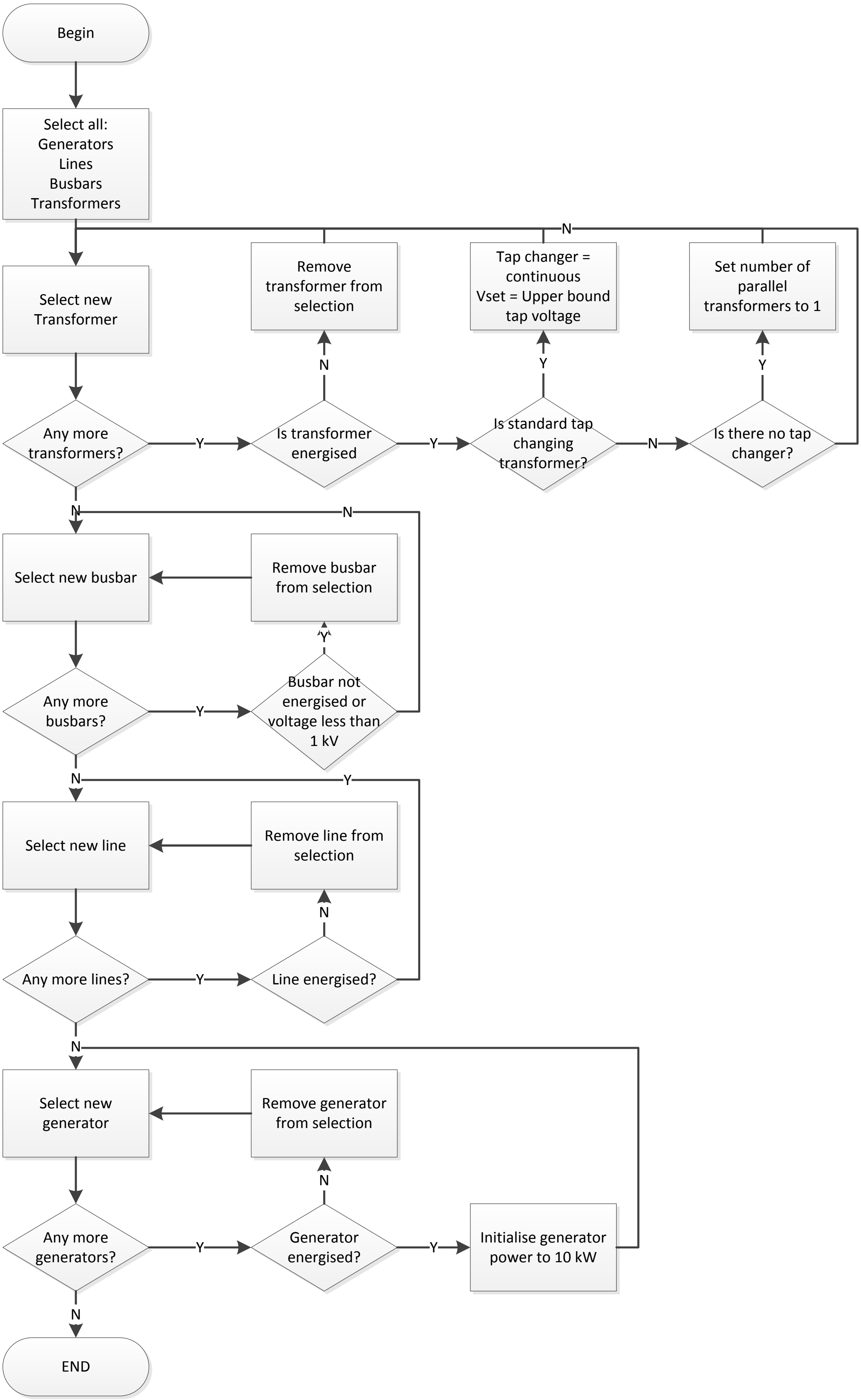

Figure B 4: Initialisation flow diagram

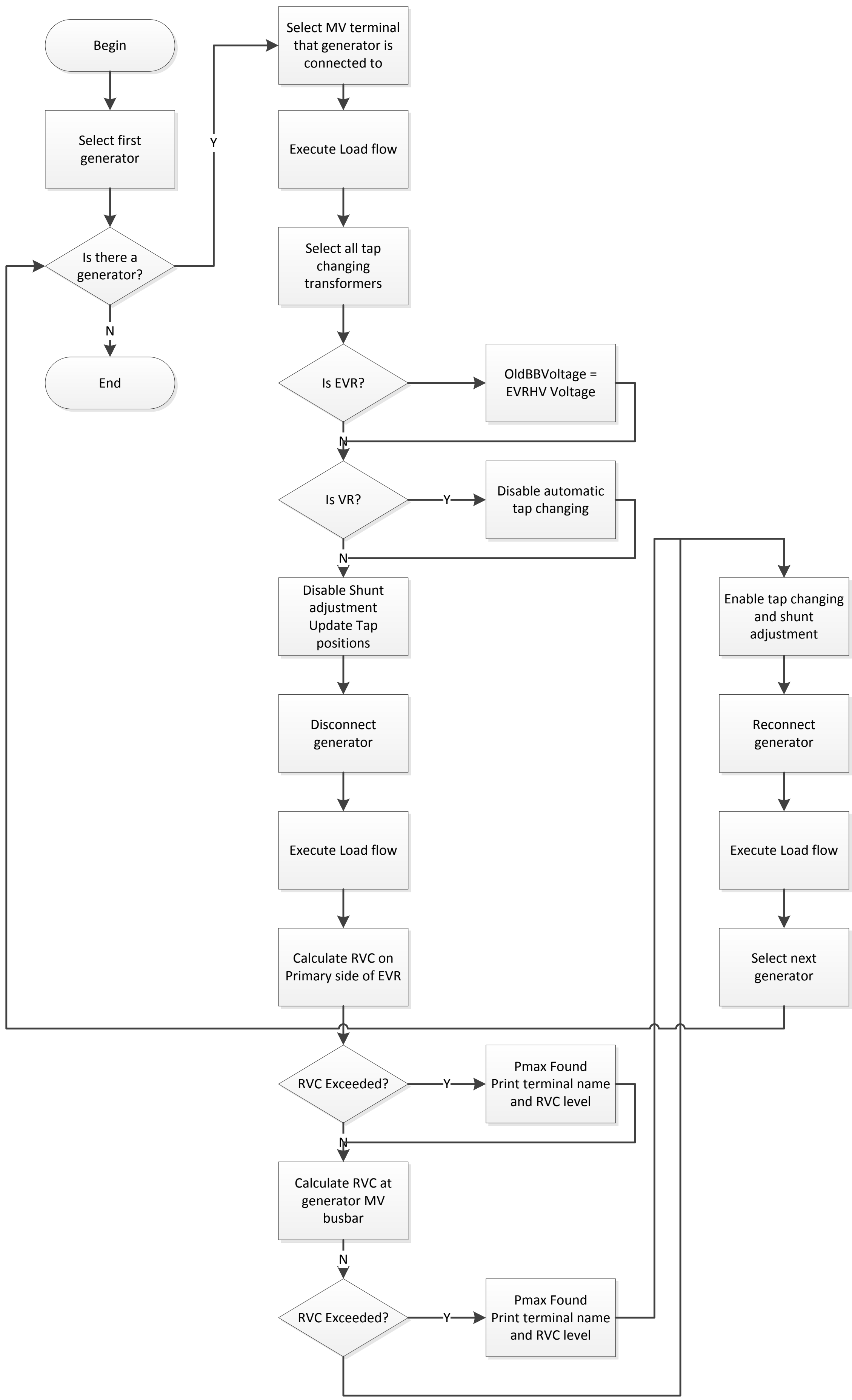

Figure B 5: RVC calculation flow diagram

TimeSweep

TimeSweep makes use of the load and solar profile, and performs multiple load flows over a specified time period. The script was set up to calculate the daily load, losses, generation, number of tap changes by voltage regulation devices and voltage fluctuations at specified busses. The information is displayed on graphs, so that the individual bus voltages can be monitored over a particular time period. The program is a modified version of the TimeSweep DPL script found within the PowerFactory DPL scripts. A basic overview of the script is shown in Figure B 6.

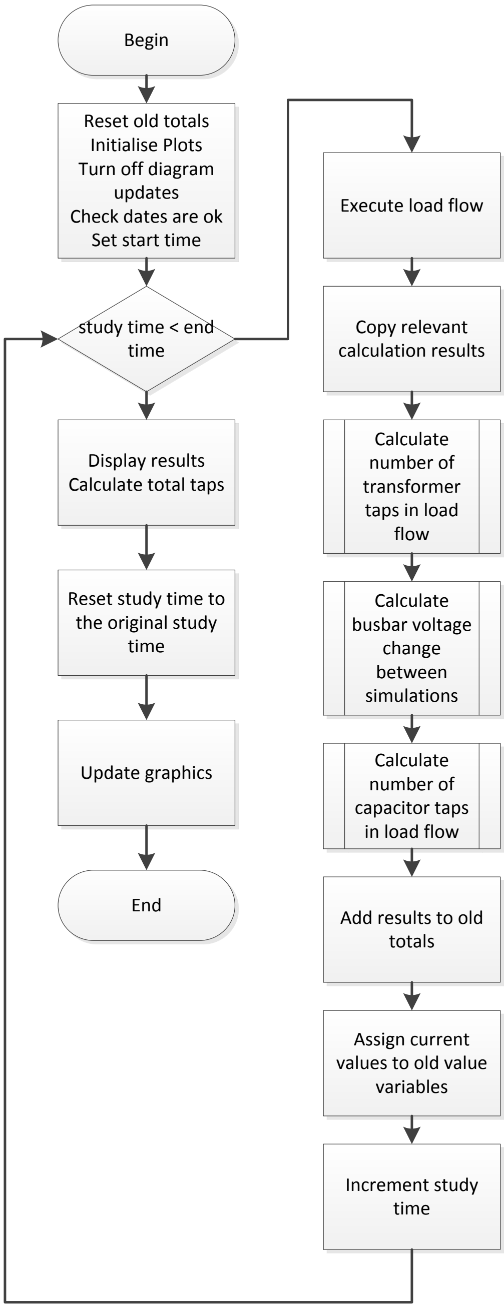

Figure B 6: TimeSweep process diagram

Voltage setpoint adjustment

The voltage setpoint adjustment is added to this base TimeSweep script. The period that the voltage must be averaged over is specified in the script's settings. The script then calculates the average voltage at each generator. The setpoint voltage is updated every iteration with the new average value. The setpoint can be adjusted between 1 p.u. and 1.04 p.u.

A sample output for the TimeSweep script is shown in Figure B 7.

```
Summary:
Total External Infeed =    30.915 MWh     6.430 MVArh
Total Generation      =     6.045 MWh     0.002 MVArh
Total Load            =    35.099 MWh    21.355 MVArh
Total Losses          =     1.860 MWh
Loss Load Ratio       =     5.301 percent
VR TRFR 1 Total number of taps =        56
66/11kV Transformer(1) Total number of taps =         4
CEVR Total number of taps =         0
DEVR Total number of taps =         0
Switched Capacitor Total number of taps =         2
Total number of taps =        62
T1 Average voltage fluctuation =  0.419729 [percent]
11kV BB Average voltage fluctuation =  0.207601 [percent]
T10 Average voltage fluctuation =  1.491494 [percent]
T4 Average voltage fluctuation =  1.147279 [percent]
T4-1 Average voltage fluctuation =  1.136059 [percent]
T7 Average voltage fluctuation =  1.463876 [percent]
DIgSI/info - DPL program 'TimeSweep' successfully executed
```

Figure B 7: TimeSweep script sample output

PMinLoss

PMinLoss calculate the DG peak power that results in the minimum losses or minimum number of tap changes over a day, while abiding to predefined constraints. It makes use of both the PMaxDG and TimeSweep programs. The program can be configured to optimise four different objectives:

Minimum losses with constraints

1) Execute PMaxDG to find the absolute maximum size of DG that can be installed on the feeder.
2) Execute TimeSweep command to calculate the daily losses for this penetration level.
3) Reduce DG size by 5%
4) Loop to 2 until the losses start to increase

Minimum number of tap changes

1) Execute PMaxDG to find the absolute maximum size of DG that can be installed on the feeder.
2) Execute TimeSweep command to calculate the daily number of tap changes for this penetration level
3) Decrease DG size 5%
4) Loop to 2 until the number of tap changes start to increase

Minimum losses without constraints

1) Execute PMaxDG to find the absolute maximum size of DG that can be installed on the feeder.
2) Execute TimeSweep command to calculate the daily losses for this penetration level.
3) Increase DG size by 5%
4) Loop to 2 until the losses start to increase

Minimum losses with constraints, power factor optimisation

1) Execute PMaxDG to find the absolute maximum size of DG that can be installed on the feeder.
2) Execute TimeSweep command to calculate the daily losses for this penetration level.
3) Decrease power factor by 0.005
4) Loop to 1 until the losses start to increase

It should be noted that in many cases, the point of minimum losses will often be greater than the maximum penetration limits imposed by the constraints. If this is the case then the program should be configured to calculate the minimum losses without constraints.